Understanding the Critical Quality Attributes Influencing Doxil® Performance *In Vitro* and *In Vivo*

by

Adaeze U. Eneli

A dissertation submitted in partial fulfillment
of the requirements for the degree of
Doctor of Philosophy
(Pharmaceutical Sciences)
in The University of Michigan
2025

Doctoral Committee:

Professor Anna S. Schwendeman, Chair
Clinical Associate Professor David Frame
Professor Steven Schwendeman
Professor Duxin Sun

Adaeze U. Eneli

enelia@umich.edu

ORCID iD: 0000-0003-1008-0473

© Adaeze U. Eneli 2025

Dedication

I dedicate this dissertation to my late maternal grandfather, Benson Emelike Ukpabi, whom we lost to multiple myeloma and prostate cancer on July 4th, 2008. Nearly 20 years ago, I still remember the day he looked deeply into my eyes as a young, impressionable 13-year-old and told me I could do anything that I wanted to in this world. As he lay on his hospice bed, he made me repeat it until he believed that I believed it too. I pursued this path because of you, and I will leave this university in honor of you, the work I've accomplished and those in our family who paved the way before me.

To my parents – Okey and Ihuoma Eneli – and my brothers, Obi and Emeka, thank you for always believing in me.
I love you all.

Acknowledgements

It is often said, “It takes a village to raise a child”, but even the child needs the right environment to thrive and blossom into the kind of person they are destined to be. I want to begin by extending my deepest gratitude to my immediate family for all the love, *extensive* patience, guidance and support they’ve shown over the years in my academic journey. Mom, Dad, Obi and Emeka – you teach me something new every day, not only in the work and path that I have chosen to pursue, but also about myself. There is something unique about journeying the road to a Ph.D. that makes you confront yourself daily and rediscover yourself, and you have been with me every step of the way. Thank you for pouring into me and lifting me up in your own unique way no matter what I faced throughout this journey. I love you so much.

To my paternal grandma Edna and my late grandparents, thank you for paving the way before me and laying the strong foundation for my parents to blossom independently and then together to provide for me and my brothers. I like to believe that I’m living my ancestors’ wildest dreams, and my heart is warm thinking about how you are always watching over me in heaven. Grandma – I promise now that I have time after defending that I will learn more Igbo and become fluent in our native tongue. I can’t wait to share the news of my graduation with you and visit you soon indeed. To my cousin Ruth – thank you for being the big sister I never had. Your heart extends far and wide, and I am blessed God gave me you in my board of directors throughout this journey. To my extended family, thank you for always believing in me and supporting me in various ways, whether through a word of encouragement, a listening ear or a personal visit.

To my advisor Anna, thank you for your support all these years and giving me a chance to pursue my dreams. I remember writing my statement of intent about how my grandfather inspired me to pursue this path, and it took me about a year into my thesis work to realize that you gave me this project, not only because it suited my engineering background, but because it was a regular reminder of who I was doing it for – thank you. To my committee, thank you for continually pushing me to expand my understanding and knowledge of my topic to pursue the

highest forms of excellence in my field of expertise. Thank you for encouraging me, for being an advocate and believing in my capabilities. To my support network in Michigan, Ohio, Indiana and beyond – I'm beyond floored. The outpouring of love and support from friends I've made across the country from undergrad at Ohio State until now at the University of Michigan feels endless.

To the NightWriters community at U-M, I am so grateful for all of the moments spent laughing, crying and supporting each other while working tirelessly overnight in the pursuit of this degree that made it all make sense somehow. Thank you for your advice, for pouring into me, for lifting me up when I was low and keeping me rooted in community filled with brilliant scholars across countless disciplines who also share my love of dance and enjoyment. A very special shout out to Dr. Dominic Bednar, Dr. Paulina Fraser, Dr. Desnor Chigumba, Dr. Chiamaka Ukachukwu, Dr. Nathalie Momplaisir, Dr. Christine Quince and Dr. Richard Smith.

To my dance community at Detroit Dance Loft, my words feel few, but my emotions run very deep for all of you. Thank you for finding me at a time when I needed it; when my love for dance started evolving, and the demands of the Ph.D. began to necessitate a new normal for me. "Dance lessons are life lessons" is a saying I will always stand by, but I would also add that the exploration of dance facilitates the exploration of self and is analogous to my experience along my Ph.D. journey. The woman that stands before you today is not the woman who came to U-M five years ago. As I continued to progress in my Ph.D. intellectually, I found parallels in my growth emotionally and relationally through dance. You guys have been like a second family to me, and I love you all very deeply. Marc and Rose, thank you for cultivating such a beautiful community for us to grow and connect through your love of dance. Neika, Egla and Sandra – thank you for your beautiful presence, for being such a soft landing for me to experience and to know what true friendship feels like.

To my Ohio State family, although you lost me to that state up north, you will always have a special place in my heart. To the friends and sisters I made at OSU, thank you for always rooting for me and supporting my growth. To the friends I made in Indianapolis, California, and beyond who saw my potential before I did, thank you.

Table of Contents

Dedication ii

Acknowledgements iii

List of Tables x

List of Figures xii

Abstract xviii

Chapter 1 Challenges and Opportunities in Establishing Bioequivalence for Generic Development of Complex Liposomal Drug Products: A Review 1

1.1 Introduction 1

1.1.1 Regulatory landscape for liposome generic development 1

1.1.2 Challenges in generic development 3

1.2 Case Studies 4

1.2.1 FDA-approved products with approved generics 5

1.2.2 FDA-approved products with no approved generics 26

1.2.3 Research Scope and Chapter Overviews 35

Chapter 2 A Comparative Study on Physicochemical and Analytical Characterizations of Doxil® and its Generic Drug Products 38

2.1 Abstract 38

2.2 Introduction 39

2.3 Materials 42

2.4 Methods 43

2.4.1 Particle Size 43

2.4.2 Zeta Potential 43

2.4.3 Doxorubicin Content 43
2.4.4 Lipid Content 44
2.4.5 Doxorubicin Purity 44
2.4.6 Lipid Purity 45
2.4.7 Free, Non-Encapsulated Doxorubicin in Liposomal Formulations 45
2.4.8 Cryogenic Transmission Electron Microscopy (Cryo-TEM) 46
2.4.9 Small Angle X-Ray Scattering (SAXS) 46
2.4.10 In Vitro Dissolution 47
2.5 Results 48
2.5.1 Size Characterization 48
2.5.2 Zeta Potential 49
2.5.3 Doxorubicin & Lipid Content 50
2.5.4 Doxorubicin Purity 51
2.5.5 Lipid Purity 52
2.5.6 Free, Non-Encapsulated Doxorubicin in Liposomal Formulations 53
2.5.7 Cryo-TEM 54
2.5.8 SAXS 55
2.5.9 In Vitro Dissolution 56
2.6 Discussion 56
2.7 Conclusion 59
2.8 Author Contributions & Acknowledgements 60
2.8.1 Author Contributions 60
2.8.2 Funding & Acknowledgements 60
Chapter 3 Development of an *In Vitro* Drug Release Assay Utilizing Bio-Beads SM-2 Resin to Evaluate Doxorubicin Liposomes 62
3.1 Abstract 62

3.2 Introduction 63

3.3 Materials 66

3.4 Methods 67

3.4.1 Pretreatment for Bio-Bead SM-2 resin material 67

3.4.2 Solubility determination of doxorubicin hydrochloride in various solvents 67

3.4.3 Spectrofluorometric analysis method for quantifying DOX release/adsorption under assay development conditions 68

3.4.4 Determining the optimal Bio-bead amount for complete DOX release and adsorption in aqueous release media 69

3.4.5 Determining the optimum testing concentration for encapsulated doxorubicin release and free doxorubicin adsorption by Bio-beads SM-2 resin in aqueous release media 69

3.4.6 Requirement and validation of sink condition using Bio-bead SM-2 resin in aqueous release media 70

3.4.7 Validating rapid absorbance of free DOX to Bio-bead SM-2 resin in aqueous release media 71

3.4.8 Assay optimization to retain empty liposome structural quality and facilitate DOX release 71

3.4.9 Discriminative capability of developed assay 73

3.5 Results & Discussion 75

3.5.1 Solubility determination of doxorubicin (DOX) hydrochloride in various solvents 75

3.5.2 Determining the optimal Bio-bead amount for complete DOX release and adsorption in aqueous release media 76

3.5.3 Determining the optimum testing concentration for encapsulated DOX release and free DOX adsorption by Bio-beads SM-2 resin in aqueous release media 77

3.5.4 Requirement and validation of sink condition using Bio-bead SM-2 resin in aqueous release media 79

3.5.5 Validating rapid absorbance of free DOX to Bio-bead SM-2 resin in aqueous release media 80

3.5.6 Assay optimization to retain liposome structural quality during dissolution 82

3.5.7 Cyclodextrin addition to release media 86
3.5.8 Discriminative capability of developed assay 88
3.6 Conclusion 90
Chapter 4 Drug Adsorption to Microtubes Impacting the Reliability of *In Vitro* Dissolution Testing: A Case Study on *Doxorubicin Hydrochloride* 92
4.1 Abstract 92
4.2 Introduction 93
4.3 Materials 96
4.4 Methods 96
4.4.1 Solubility determination for DOX in various solvents and dissolution media 96
4.4.2 Selecting a model microtube for investigations of DOX adsorption 97
4.4.3 Concentration dependent DOX adsorption analysis 98
4.4.4 Temperature dependent DOX adsorption analysis 98
4.4.5 Speed dependent DOX adsorption analysis 99
4.4.6 Effect of inner surface area per volume ratio on DOX adsorption 99
4.4.7 Effect of microtube material on DOX adsorption 100
4.4.8 Effect of media composition on DOX adsorption 101
4.4.9 Adsorption Kinetics of DOX 102
4.5 Results 102
4.5.1 Solubility determination for DOX in various solvents and dissolution media 102
4.5.2 Selecting a model microtube for investigations of DOX adsorption 103
4.5.3 Effect of doxorubicin concentration on adsorption 104
4.5.4 Effect of temperature on doxorubicin adsorption 105
4.5.5 Effect of agitation speed on doxorubicin adsorption 106
4.5.6 Effect of inner surface area per unit volume ratio on doxorubicin adsorption 107
4.5.7 Effect of microtube material on DOX adsorption 109

4.5.8 Effect of media composition on DOX adsorption 110
4.5.9 Adsorption Kinetics of DOX 112
4.6 Conclusion 113
Chapter 5 Conclusions and Future Directions 114
Appendix 117
Bibliography 129

List of Tables

Table 1. FDA-approved, prescription-based liposomal drug products and their generics currently available in the United States. 2

Table 2. FDA-approved, liposomal drug products discontinued currently in the United States. ... 9

Table 3. Clinical pharmacokinetic parameters of encapsulated doxorubicin from Libaoduo compared with Caelyx® in an *in vivo* bioequivalence study; adapted from source [43]. 12

Table 4. Results of preclinical studies comparing AmBisome with Anfogen or Lambin [51]. ... 18

Table 5. Size distribution, pH value, and free drug contents of intact, expired and compromised Exparel. All values are presented as mean ± SD (n=3) [69]. 22

Table 6. Pharmacokinetic parameters for Ak-lip and Pure amikacin following i.v. injection [84]. 33

Table 7. Stability study for optimized Ak-lip. 34

Table 8. Sample inventory. 41

Table 9. Physicochemical properties of Bio-beads SM-2 resin. 65

Table 10. Solubility of DOX in various solvents. 76

Table 11. Sample solution volumes added to Eppendorf Natural microtubes with varied surface areas ranging from 0.1 – 1.0. 100

Table 12. Specifications of microtubes with different material compositions. 100

Table 13. Sample volumes added to different sized microtubes with a fixed volume to surface area ratio of 0.67. 101

Table 14. Solubility of DOX in various solvents. 103

Appendix Table 1. ICH Q2(R1) validation results for the doxorubicin quantitation method. ... 118

Appendix Table 2. Gradient mobile phase for the UPLC-ELSD assay for lipid quantification. 119

Appendix Table 3. ICH Q2(R1) validation results for the lipid quantitation method for HSPC. 119

Appendix Table 4. ICH Q2(R1) validation results for the lipid quantitation method for cholesterol. 120

Appendix Table 5. ICH Q2(R1) validation results for the lipid quantitation method for DSPE-PEG 2000. 120

Appendix Table 6. Gradient mobile phase for the UPLC-TUV assay for DOX and impurity quantification in formulations. 121

Appendix Table 7. Size distribution, polydispersity index and zeta potential measurements of different liposomal doxorubicin formulations analyzed by DLS (n ≥ 3, mean ± SD). 122

Appendix Table 8. Quantification of doxorubicin and lipid content within liposomal doxorubicin formulations by different manufacturers (mean ± SD; n = 3). 123

Appendix Table 9. Quantification of doxorubicin purity and identification of USP impurities within liposomal doxorubicin formulations by different manufacturers (mean ± SD; n = 3). ... 124

Appendix Table 10. Quantification of free doxorubicin present in liposomal doxorubicin formulations by different manufacturers (n > 2). 125

Appendix Table 11. Measured size dimensions and membrane thickness of doxorubicin liposomes in different liposomal doxorubicin hydrochloride formulations imaged by cryo-TEM (mean ± SD, n ≥ 500). 126

List of Figures

Figure 1. Schematic representation of a PEGylated liposomal doxorubicin [23]..... 5

Figure 2. Cumulative percent of patients developing doxorubicin-associated congestive heart failure in relation to total dose of the drug. (Fractions indicate number of patients with congestive heart failure divided by number of patients who reached that dose level) [20]..... 6

Figure 3. Remote loading approach of doxorubicin (DOX) into the intraliposomal aqueous phase [24]..... 7

Figure 4. Plasma levels of doxorubicin (total or liposome-encapsulated) in Doxil and doxorubicin-treated patients. (A) 25 mg/m (n = 8 for Doxil; n = 3 for free DOX). (B) 50 mg/m (n = 14 for Doxil; n = 4 for free DOX). Adapted and reprinted by permission from the American Association for Cancer Research [23, 40]..... 10

Figure 5. (A) Plasma concentration-time curves for free doxorubicin; (B) Plasma concentration-time semi-logarithmic curves for free doxorubicin [43]..... 12

Figure 6. (A) Plasma concentration-time curves for liposomal doxorubicin; (B) Plasma concentration-time semilogarithmic curves for liposomal doxorubicin [43]. 13

Figure 7. Schematic cross-section of amphotericin B intercalated within its liposomal membrane [45]..... 14

Figure 8. Size distribution of amphotericin B formulations by DLS (A) and NTA system (B) [49]..... 16

Figure 9. DSC thermograms of liposomal amphotericin B formulations (A), amphotericin B standard and Fungizone (B), and main lipid components (C) [49]..... 16

Figure 10. Dissolution profiles of different amphotericin B formulations. Data represented as mean ± SD (n = 3) [49]..... 17

Figure 11. Schematic diagrams and electron microscopy images of A) unilamellar liposomes (ULV); B) multilamellar liposomes (MLV); C) multivesicular liposomes (MVL) using the DepoFoam® technology [64, 66]. 20

Figure 12. Scanning electron microscope image of DepoFoam® containing bupivacaine liposome resembling a honeycomb-like structure [67]..... 21

Figure 13. *In vitro* release profiles of intact, expired, and compromised Exparel formulations stressed via mechanical agitation, freeze-thawing, and high-temperature incubation. All values are presented as mean ± SD (n = 3) [69]. 22

Figure 14. Plasma concentration-time profiles of Exparel and free bupivacaine solution following subcutaneous administration at 15 mg/kg dose in Sprague-Dawley rats (n=4, mean ± SD) [69]. 23

Fig. 15. Bupivacaine plasma concentration profiles of subcutaneous injected intact, expired, and compromised Exparel stressed via freeze-thawing, mechanical agitation, and high-temperature incubation, at 15 mg/kg in SD rats (n = 5, mean ± SD) [69]. 24

Figure 16. A) Primary measure of clinical efficacy as the adjusted mean of the area under the curve (AUC) of the numeric rating scale (NRS) pain intensity scores in the DepoFoam bupivacaine 120 mg group; B) Percentage of patients who went pain-free (NRS < 1) for 120 mg DepoFoam bupivacaine compared to placebo; C) Percentage of patients who received no opioid rescue pain medication with 120 mg DepoFoam bupivacaine compared to placebo. Figures and captions adapted from [70]..... 25

Figure 17. Schematic depiction of Onivyde (irinotecan liposome injection) [75]. 27

Figure 18. Cryo-TEM images of Onivyde®. Green arrows indicate the prolate spheroid with crystal bundle inside. Yellow arrows point out round shape particles. White arrows refer to complex structures with both liposome and drug crystal inside. Red arrows indicate symmetric multilamellar vehicles. Blue arrows point out empty liposomes. A1-A2 and B1-B2 are representative cryo-TEM images of batch #120518S and batch #200048A of Onivyde® respectively. Scale bar, 100 nm. Image adapted from [74]..... 27

Figure 19. Lamira Nebulizer System and controller [83]. 29

Figure 20. Transmission Electron Microscopy (TEM) image of amikacin loaded liposomes (Ak-lip) at 100 nm scale (a) and 50 nm scale (b). DSC thermogram of Amikacin, Amikacin loaded liposomes (Ak-lip) and Blank liposomes (Blank-Lip) (c); X-ray diffraction pattern of pure Amikacin, cholesterol, Soy phospholipid S-100, stearylamine, physical mixture, Blank-Lip and Ak-lip (d). Caption adapted from [84]..... 31

Figure 21. *In vitro* cumulative % drug release of pure amikacin and Ak-lip formulation. Image adapted from Maxwell *et al* [84]. 32

Figure 22.*In vitro* drug release profile of Ak-lip over 72 h, at Day 15 and 90, following storage at room temperature (a), refrigeration (b) and at 37°C (c) [84]. 32

Figure 23. *In vivo* drug release of Ak-lip and Pure amikacin in Sprague-Dawley Rats. 33

Figure 24. Chapter 2 Graphical Abstract 39

Figure 25. Size characterization of doxorubicin liposomes in formulation developed by innovator and different generic manufacturers: Baxter Healthcare, Dr. Reddy's Laboratories,

Sun Pharmaceuticals and Zydus. a) Particle size, b) polydispersity index, and c) zeta potential was measured using the Malvern Zetasizer (mean ± SD, $n \geq 3$). 49

Figure 26. Measured doxorubicin and lipid content present in different liposomal preparations of doxorubicin hydrochloride produced by different manufacturers (mean ± SD, n = 3). a) Doxorubicin content, b) Lipid content for HSPC, DSPE-PEG (MW 2000) and cholesterol. **c**) Chromatographic separation of doxorubicin from lipid components using an UPLC-ELSD assay under a gradient mobile phase. 50

Figure 27. Purity of liposomal doxorubicin formulations quantified as a percentage of peak AUC over cumulative peak AUC in each sample using UPLC-TUV analysis. a) Doxorubicin purity (%), b) daunorubicinone impurity levels (%), c) daunorubicin impurity levels (%), d) doxorubicinone impurity levels (%), e) chromatographic separation of doxorubicin and the respective impurities (mean ± SD, $n = 3$). 52

Figure 28. Quantification of lipid impurities in liposomal doxorubicin hydrochloride formulations. a) cumulative lyso-PC (16:0) and (18:0) impurities (mean ± SD, $n \geq 2$). b) Chromatographic separation of lyso-PC (16:0) and (18:0) impurities in a representative, liposomal DOX sample manufactured by Dr. Reddy's Laboratories. 53

Figure 29. Quantification of free, non-encapsulated doxorubicin present in liposomal doxorubicin hydrochloride formulations produced by different manufacturers (mean ± SD, $n \geq 2$). 54

Figure 30. Morphology of the doxorubicin liposome from different formulations: a) Doxil® (batch no. MDZT300); b) Dr. Reddy's (batch no. 501635); c) Sun Pharmaceuticals (batch no. JX5514A); d) Zydus (batch no. P100084) 54

Figure 31. SAXS scattering profiles for a) one liposomal DOX formulation representative of each manufacturer (n = 4). b) Structural similarity between generic and reference, liposomal DOX formulations was compared and depicted using the SAXS similarity map (SSM) developed by SIBYLS at the Advanced Light Source (12.3.1), Lawrence Berkeley Laboratory. The Volatility of Ratio, V_R, correlation method was used to define similarity and dissimilarity between samples (mean ± SD, $n \geq 2$). 55

Figure 32. Characterization and comparison of *in vitro* dissolution profiles for individual batches of approved generic liposomal doxorubicin hydrochloride formulations with the reference Doxil® formulation (mean ± SD; n = 3) 56

Figure 33. Rate of DOX adsorption and release in free and liposomal formulations to determine the quantity of Biobead resin necessary for rapid, complete DOX adsorption in release media consisting of phosphate buffered saline (1X, pH 7.4) under rotational agitation at 40 RPM and incubation at 45°C using an *in vitro* release assay under development (mean ± SD, n = 3). 77

Figure 34. Evaluation of released and absorbed DOX in free and liposomal formulations by 200 mg of Biobeads at increasing concentrations in release media consisting of phosphate

buffered saline (1X, pH 7.4) under rotational agitation at 40 RPM and incubation at 45°C using an *in vitro* release assay under development (mean ± SD, n = 3). 78

Figure 35. Experimental validation for sink condition using a free DOX solution (2 mg/mL) prepared in Doxil® formulation buffer diluted to concentrations 3-10 times the target concentration of 10 μg/mL in phosphate buffered saline (1X, pH 7.4) under rotational agitation and incubation at 40 RPM and 45°C (mean ± SD, n = 3). 79

Figure 36. Validate that free DOX is rapidly absorbed by Biobeads in media and encapsulated DOX is released at a slower rate from liposomes in the same media consisting of phosphate buffered saline (1X, pH 7.4) under rotational agitation and incubation at 40 RPM and 45C using an *in vitro* release assay under development (mean ± SD, n = 3). 81

Figure 37. Particle size distribution analysis for an experimental study validating the slow-release rate of encapsulated DOX from liposomes and rapid adsorption of free, released DOX in release media consisting of phosphate buffered saline (1X, pH 7.4) under rotational agitation and incubation at 40 RPM and 45C using an *in vitro* release assay under development (mean ± SD, n = 3). 82

Figure 38. (A) Rate of DOX release from liposomes in release media consisting of phosphate buffered saline (1X, pH 7.4) under incubation at 45°C and rotational agitation at different test speeds using an *in vitro* release assay under development; (B-D) Particle size distribution analysis to evaluate the impact of agitation speed on empty liposome structural quality while facilitating DOX release (mean ± SD, n = 3). 83

Figure 39. (A) Rate of DOX release from liposomes in release media consisting of phosphate buffered saline (1X, pH 7.4) under rotational agitation at different incubation temperatures using an *in vitro* release assay under development; (B-D) Particle size distribution analysis to evaluate the impact of temperature on empty liposome structural quality while facilitating DOX release (mean ± SD, n = 3). 84

Figure 40. Rate of DOX release from liposomes at increasing concentrations using 200 mg Biobeads to absorb released DOX tested at lower agitation speed and temperature, 20 RPM and 37C, to evaluate the ability to retain the empty liposome structure upon DOX release (mean ± SD, n = 3). 85

Figure 41. Time-dependent particle size analysis for DOX release assay under development at reduced agitation speed and temperature, 20 RPM and 37°C, to improve the structural quality of the empty liposome while facilitating complete drug release from the liposome (mean ± SD, n = 3). 85

Figure 42. Effect of cyclodextrin type on DOX release from liposomes (10 μg/mL) and liposome structural quality upon DOX release in phosphate buffered saline (1X, pH 7.4) with 200 mg Biobeads at 20 RPM and 37°C (mean ± SD, n =3). 86

Figure 43. Chemical structure of doxorubicin [114]. 88

Figure 44. First evaluation for discriminatory ability of the *in vitro* release assay under development using Biobead SM-2 resin as sink agent by spiking increasing levels of free DOX (2 mg/mL) prepared in 9.4% sucrose, 1.55 mg/mL L-histidine, pH 6.5 to Doxil® (liposomal doxorubicin hydrochloride formulation) under optimized assay conditions (20 RPM, 37°C) with 200 mg Biobeads for sink condition (mean ± SD, n = 3). 89

Figure 45. Second evaluation for discriminatory ability of the *in vitro* release assay under development by applying freeze thaw stress to a commercial Doxil® formulation to introduce meaningful differences to the liposome structure and assess the capability of the assay to distinguish between these formulations under optimized assay conditions (20 RPM, 37°C) using 200 mg Biobeads for sink condition (mean ± SD, n = 3)..... 90

Figure 46. DOX adsorption to different brands of microtubes for the identification of a model tube for DOX adsorption in phosphate buffered saline (1X, pH 7.4) under mild agitation at 20 RPM and 37°C, reported as A) percentage, and B) initial and final concentration at 0 and 24 hours (mean ± SD, n = 3). 104

Figure 47. Concentration dependence of DOX adsorption to standard, natural polypropylene Eppendorf® microtubes at a fixed volume to surface area ratio of 1 mL to 1.5 mL in phosphate buffered saline (1X, pH 7.4) at 20 RPM and 37°C, reported as A) percentage, and B) initial and final concentration at 0 and 24 hours (mean ± SD, n = 3). 105

Figure 48. Temperature dependence of DOX adsorption to standard, natural polypropylene Eppendorf® microtubes at a fixed volume to surface area ratio of 1 mL to 1.5 mL in phosphate buffered saline (1X, pH 7.4) at 20 RPM, reported as A) percentage, and B) initial and final concentration at 0 and 24 hours (mean ± SD, n = 3). 106

Figure 49. Speed dependence of DOX adsorption to standard, natural polypropylene Eppendorf® microtubes at a fixed volume to surface area ratio of 1 mL to 1.5 mL in phosphate buffered saline (1X, pH 7.4) at 37°C, reported as A) percentage, and B) initial and final concentration at 0 and 24 hours (mean ± SD, n = 3). 107

Figure 50. The influence of volume to inner surface area ratio on DOX adsorption in standard, natural polypropylene Eppendorf® microtubes of varying sizes in phosphate buffered saline (1X, pH 7.4) at 20 RPM and 37ºC for 24 hours as a percentage (mean ± SD, n = 3). 108

Figure 51. Microtube material composition on the extent of DOX adsorption to 1.5 mL standard, natural polypropylene Eppendorf® microtubes in phosphate buffered saline (1X, pH 7.4) at 20 RPM and 37ºC as A) percentage, and B) initial and final concentration at 0 and 24 hours (mean ± SD, n = 3). 110

Figure 52. Effect of media composition on DOX adsorption in various solvent media conditions to standard, natural 1.5 mL polypropylene Eppendorf® microtubes under mild agitation at 20 RPM and 37ºC, as A) percentage, and B) initial and final concentration (mean ± SD, n = 3). 111

Figure 53. Rate of adsorption of doxorubicin hydrochloride to standard, polypropylene Eppendorf® microtubes in phosphate buffered saline at 20 RPM and 37C for 24 hrs (mean ± SD; n = 3). 112

Appendix Figure 1. Specificity of doxorubicin quantification assay. Blank is in black, doxorubicin in blue. 118

Appendix Figure 2. Specificity of the lipid quantification assay. Blank is in black, lipids in blue. 121

Appendix Figure 3. Chromatographic identification of doxorubicin in a Doxil® formulation using an isocratic mobile phase of deionized water and methanol with 0.1% formic acid (Baxter Healthcare, batch no. MDZT300). 126

Appendix Figure 4. Size distribution histograms for liposome length and width measured in images generated by cryo-TEM. 127

Appendix Figure 5. Calibration curves for doxorubicin quantification assay. 128

Abstract

Doxil®, a PEGylated liposomal suspension of doxorubicin (DOX) hydrochloride, was the first liposome-based drug product approved by the U.S. FDA. Although off-patent, only a limited number of generics have gained approval, largely due to manufacturing complexity and challenges in demonstrating bioequivalence. Regulatory agencies require that generic drug products exhibit physicochemical and therapeutic equivalence to the reference listed drug through bioequivalence assessment. In this regard, we developed and applied a series of analytical methods to evaluate the critical quality attributes (CQAs) of Doxil® and its generics, including size distribution, zeta potential, DOX and lipid content, purity, non-encapsulated free drug, morphology, nanostructure similarity, and *in vitro* drug release.

Cryo-TEM revealed the characteristic "coffee bean" morphology of Doxil® liposomes, while SAXS analysis highlighted subtle differences in nanostructure across batches, evident from variations in scattering intensity and radius of gyration. We also developed a non-compendial, single-vial *in vitro* release (IVR) assay using Bio-Beads SM-2 resin as a novel sink agent. Under optimized conditions—200 mg resin, 10 μg/mL DOX in 1X PBS (pH 7.4) media with α-cyclodextrin, 37°C, and 20 RPM—more than 90% drug release was achieved within 24 hours. However, structural destabilization of the liposome post-release prompted further investigation into strategies for preserving the empty liposome.

The IVR assay was optimized across parameters including resin weight, temperature, agitation, media composition, and DOX concentration in dissolution media. While limited in its ability to discriminate between formulations with varying free drug content, the assay effectively detected release differences in samples subjected to freeze-thaw stress, suggesting its ability to identify stress-induced changes during processing or storage. This assay presents a cost-effective, reproducible alternative for assessing release performance of complex liposomal generics and could be further optimized for regulatory application.

Recognizing that reliable mass balance is essential for credible *in vitro* release data, we conducted a parallel study to examine the effect of non-specific DOX adsorption to microtubes

in dissolution testing. Using a validated UPLC-TUV method, we quantified DOX recovery under several assay conditions: drug concentration, temperature, agitation speed, tube material, inner surface area-to-volume ratio, and media composition. Up to 35.5% drug loss was observed in untreated polypropylene microtubes after 24 hours at 37°C. DOX adsorption decreased with increasing concentration, saturating at 180 μg/mL in polypropylene microtubes. Higher temperatures increased adsorption, while faster agitation reduced it. The influence of surface area-to-volume ratio was most pronounced in 2.0 mL tubes. Tube material and composition, as well as media additives like cyclodextrins or organic solvents, significantly reduced DOX adsorption relative to aqueous formulation buffer.

This dissertation offers a comprehensive framework for characterizing the critical quality attributes of liposomal drug products, using Doxil® as a model drug. The findings inform best practices for assay development, contribute to the growing body of knowledge supporting regulatory evaluation of complex liposomal drugs, and offer practical solutions to overcome analytical challenges that hinder generic liposome drug development. Ultimately, this work provides valuable insights to advance formulation optimization, quality assurance, and regulatory approval of complex liposomal drug products and their follow-on versions for clinical treatment.

Chapter 1 Challenges and Opportunities in Establishing Bioequivalence for Generic Development of Complex Liposomal Drug Products: A Review

1.1 Introduction

1.1.1 Regulatory landscape for liposome generic development

Regulatory oversight in pharmaceutical drug development is of critical significance to ensure the therapeutic safety and efficacy of innovative and generic drug products. This is particularly important with lipophilic drugs due to the characteristics that define their therapeutic application. Liposomes are spherical lipid vesicles comprised of one or more lipid bilayers in structure by design due to spontaneous formation upon mixing and emulsification of lipids in an aqueous medium [1]. Liposomes were first discovered in the 1960s by Alec Bengham and are now among the most used nanocarriers for poorly soluble and cytotoxic drug substances [1, 2]. Liposomes boast several advantages for therapeutic applications including their biocompatibility, biodegradability, high drug loading efficiency, high bioavailability, and its ability to encapsulate hydrophilic drugs in its interior aqueous core or hydrophobic drugs within its lipid bilayer membrane [1–4]. Liposomes have also been employed to improve the therapeutic index of drug substances by modifying their pharmacokinetics, biodistribution, and circulation half-life in addition to altering physicochemical properties that influence *in vitro and in vivo* drug performance [5].

Several FDA-approved liposome drug products have achieved great success in the global pharmaceutical market. Doxil® (liposomal *doxorubicin hydrochloride* injection) developed by Sequus Pharmaceuticals was the first liposome drug product to be approved by the Food and Drug Administration (FDA) in the United States (U.S.), followed by market authorization in Europe as Caelyx® by the EMA in 1996 [6]. Since the approval of Doxil®/Caelyx®, several other liposome drug products have been approved (Table 1).

Table 1. FDA-approved, prescription-based liposomal drug products and their generics currently available in the United States.

Brand Name	Active Ingredient	Innovator	Indications	Approval Year	Patent Expiry	Approved Generics/ Developers
Doxil	Doxorubicin hydrochloride	Sequus Pharmaceuticals	Ovarian cancer Multiple myeloma AIDS-related Kaposi's sarcoma Metastatic breast cancer	1995	2010	Sun Pharma Industries Dr. Reddy's Laboratories Zydus Lifesciences Global FZE Ayana Pharma Ltd Lupin Inc
Ambisome	Amphotericin B	Astellas Pharma USA	Anti-fungal treatment	1997	2004	Eugia Pharma Specialties Sun Pharma Industries Avet Lifesciences Private Ltd
Exparel	Bupivicaine	Pacira Pharmaceuticals	Analgesic	2011	2021	Jiangsu Hengrui Pharma Co Ltd
Onivyde	Irinotecan	Ipsen Biopharmaceuticals	Metastatic pancreatic adenocarcinoma	2015	2025	No AB-designated generics available
Arikayce	Amikacin sulfate	Insmed Inc	*Mycobacterium avium complex* (MAC) lung disease	2018	2028	No AB-designated generics available.

The global liposome drug market was valued at 1.28 billion USD in 2024 and demand is projected to rise at a compound annual growth rate (CAGR) of 6.3% from 2024 to 2034 estimating 2.37 billion USD in 2034 [7]. Patent protections and exclusivities

have expired for several of the FDA-approved products, making them attractive candidates for generic development. Following patent expiry, the first generic company to obtain market approval receives a significant market share and profit advantage in comparison with later market entrants, which can reach up to 90% of the market share for the first three years following patent expiry [8].

Generic drug development for liposomal products is regulated by a combination of general and product-specific guidelines issued by the U.S. Food and Drug Administration (FDA). A key document is the FDA's guidance entitled *Liposome Drug Products Chemistry, Manufacturing, and Controls; Human Pharmacokinetics and Bioavailability; and Labeling Documentation Guidance for Industry* [9]. This guidance describes the technical expectations for new drug applications (NDAs) and abbreviated new drug applications (ANDAs), and includes recommendations on chemistry, manufacturing and controls (CMC), bioavailability, pharmacokinetics, and labeling considerations specific to liposomal formulations [9].

The FDA also issues product-specific guidance documents (PSGs) that provide recommendations for demonstrating bioequivalence and analytical comparability for specific drug products, including certain liposomal formulations. These PSGs describe study designs and characterization approaches needed to submit a successful ANDA application. However, it is important to note that PSGs are only available for a limited number of approved liposomal drug products, making the general liposome guidance document an important reference for products without one.

1.1.2 Challenges in generic development

Failure to meet bioequivalence results in failed attempts to garner market approval and carries an extensive resource and cost burden for generic applicants. Additionally, complexity of liposome manufacturing directly impacts the physicochemical profile of the drug product, and subsequently, its *in vitro* and *in vivo* bioequivalence. Therefore, the main purpose of these regulatory guidelines is to 1) identify the most appropriate methodologies to evaluate generic drug candidates and 2) generate sufficient bioequivalence data. According to the FDA, a generic formulation is considered bioequivalent if it is qualitatively (Q1) and quantitatively (Q2) the same in comparison with the reference listed drug (RLD) product and possesses physicochemical similarity (Q3) [10].

Q3 evaluation should demonstrate that the physical arrangement of matter in the formulation, characterized by nanostructure, is similar to that of the RLD. Q1/Q2(Q3)-compliant generics require extensive *in vitro* and *in vivo* evaluation, however, the FDA describes different types of evidence that may be used to establish or waive bioequivalence between a generic and reference product in the Code of Federal Regulations (21 CFR 320.22, 21 CFR 320.24) [11, 12]. A waiver of evidence for *in vivo* bioequivalence evaluation for generic drug candidates that meet specific criteria can be obtained using sufficient *in vitro* data [11].

Once approved, drug products undergo post-market surveillance to monitor for patient safety, efficacy concerns and adverse drug reactions. If the efficacy of the approved product is suspected to be compromised or a new adverse drug reaction is suspected after market approval, corrective actions may be taken by the regulatory agency and company to either update the label with warnings and/or contraindications, provide further advisement to patients or discontinue the product altogether [13].

1.2 Case Studies

Over the last two decades, 14 liposome drug products have been approved in the United States and European Union [14]. However, in recent years, over half of the FDA-approved liposome products have since been discontinued. **Table 2** describes the FDA-approved liposome drug products that have been withdrawn from the market due to various reasons, most notably due to manufacturing.

Liposome manufacturing complexity is compounded by the impact of their physicochemical attributes on *in vivo* drug performance and how they are influenced by minor variations in the manufacturing process [15]. Of the prescription products described in Table 1, we present drug-specific case studies to discuss the state of the generic landscape, the specific challenges limiting generic drug development for complex, liposomal drug products, and the similarity of the liposome quality characteristics for drug product.

1.2.1 FDA-approved products with approved generics

1.2.1.1 Liposomal Doxorubicin Hydrochloride

Doxil® (liposomal *doxorubicin hydrochloride* injection) was the first liposomal drug product approved by the FDA (Sequus Pharmaceuticals, 1995) indicated for treatment of recurrent ovarian cancer after failure of platinum-based chemotherapy, AIDS-related Kaposi's sarcoma after failure of prior combination chemotherapy, multiple myeloma in combination with bortezomib, and metastatic breast cancer in the European Union [6]. Doxil® is a liposomal formulation of doxorubicin hydrochloride encapsulated within a STEALTH® liposome nanocarrier [16].

The STEALTH® liposome utilizes the covalent attachment of a polyethylene glycol (MW 2000) chains to the surface of the liposome to introduce steric hindrance and minimize electrostatic interactions between opsonins and the liposome which tag and signal the liposome as a foreign pathogen for rapid uptake and clearance from the body by Kupffer macrophage cells [17]. The STEALTH® liposome technology was developed to stealthily avoid detection by the reticuloendothelial system and reduce rapid clearance of the liposomes [17–19]. Additionally, encapsulation of doxorubicin within the liposome nanocarrier also addressed the safety and cardiotoxicity concerns associated with free doxorubicin hydrochloride detailed in prior studies [20–22].

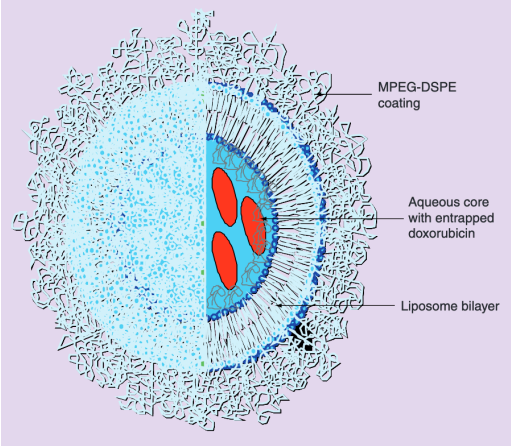

Figure 1. Schematic representation of a PEGylated liposomal doxorubicin [23].

In a study by Buzdar *et al*, early and delayed clinical cardiotoxicity of doxorubicin was investigated in 534 patients with breast cancer treated with a doxorubicin combination chemotherapy regimen with 5-fluorouracil and cyclophosphamide [20]. Fig. 2 shows the

incidence of doxorubicin-associated congestive heart failure in patients in relation to the total dose of the drug [20]. Incidence of congestive heart failure for doses of doxorubicin up to 300 mg/m^2 was $\leq$ 1% after which incidence increased [20]. The median time from the end of doxorubicin treatment to the development of congestive heart failure was approximately one month, and the longest time to the onset of heart failure was 33 months [20]. Out of the 534 patients, 326 were followed for 3 years after completion of the doxorubicin combination therapy and experienced no doxorubicin-associated cardiotoxicity. For this specific indication, doses up to 300 mg/m^2 were tolerable without significant risk of congestive heart failure but is much higher up to 450 mg/m^2. Encapsulation of doxorubicin in liposomes served to address the dose limitations due to the cardiotoxicity risk of free doxorubicin hydrochloride for cumulative doses greater than 300 mg/m^2 for different indications.

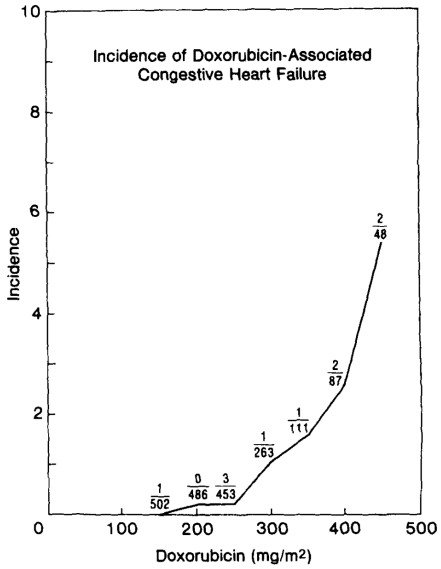

Figure 2. Cumulative percent of patients developing doxorubicin-associated congestive heart failure in relation to total dose of the drug. (Fractions indicate number of patients with congestive heart failure divided by number of patients who reached that dose level) [20].

Fig. 3 describes the remote loading approach of doxorubicin into the intraliposomal aqueous phase of the Doxil® liposome via a transmembrane ammonium ion gradient [24]. Inside the liposomes, ammonium sulfate dissociates into ammonium and sulfate ions. Ammonium ions exist in equilibrium with ammonia gas, which can permeate across the lipid bilayer membrane and diffuse out of the liposome, leaving behind protons that gradually acidify the internal environment. As ammonia diffuses out of the liposome, unionized doxorubicin is driven into the

liposome membrane where it becomes protonated and trapped inside, precipitating with sulfate ions [16, 24]. This process enables highly efficient and stable encapsulation , greater than 95% in loading efficiency [16].

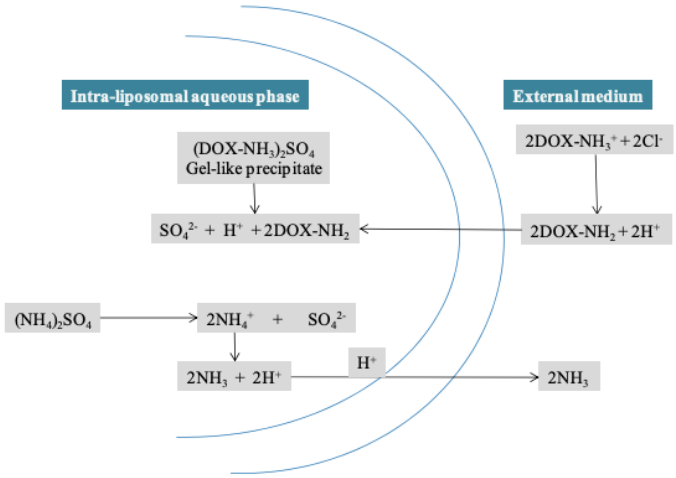

Figure 3. Remote loading approach of doxorubicin (DOX) into the intraliposomal aqueous phase [24].

Strategic lipid composition of the Doxil® liposome employed hydrogenated soy phosphatidylcholine (HSPC) and cholesterol for liposome stability and controlled release, and MPEG-DSPE for reduced clearance and extended circulation time in plasma. HSPC is a phospholipid with a high phase transition temperature of 53°C which when mixed with cholesterol was used to develop a stable liposome formulation preventing premature doxorubicin leakage from its aqueous core [25]. Cholesterol is often mixed with phospholipids due to its ability to decrease the crystalline packing order of phospholipids thus increasing the rigidity of the liposome membrane [26].

Five, generic liposomal doxorubicin hydrochloride products have been approved by the FDA since patents and exclusivities expired in 2010 [27]. Ben Venue Laboratories was the sole manufacturer of Doxil® in 2010, however, drug production halted due to problematic manufacturing and sanitation concerns that led to a global shortage of Doxil® [28]. Many patients suffered without treatment due to lack of drug availability. Lipodox® developed by Sun Pharmaceuticals (India) was the first generic doxorubicin liposome product approved to address the global shortage under FDA emergency approval in 2013 [29]. As a result, Lipodox® by Sun Pharmaceuticals was designated the reference standard for liposomal doxorubicin hydrochloride generic products [30]. Soon after patent expiry, generic development proved to be extremely

difficult due to manufacturing complexity and a need for improved bioequivalence standards for complex liposomal drug products.

Traditional bioequivalence methods for liposomal drug products yield inaccurate values for plasma concentration because they cannot reliably distinguish between free and encapsulated drug in tumor tissues and systemic circulation, and the plasma concentration profiles are not correlative of therapeutic performance [31]. Liposome biodistribution after administration is also dependent on formulation and manufacturing properties [1, 32]. Research been conducted to study the influence of manufacturing on the physicochemical profile and therapeutic performance of liposome drug products [33, 34]. It has been found that variations in manufacturing and process control strategy have a direct effect on the physicochemical profile of liposomal drug products. Therefore, complete characterization of the physicochemical properties and its relation to *in vitro* and *in vivo* drug performance through analytical techniques is necessary for the evaluation of safety, stability and efficacy of liposome drug products and their generics.

In 2010, the FDA released a draft guidance for generic development of liposomal doxorubicin hydrochloride products [10]. Per the recommendations in the guidance, generic test products for liposomal doxorubicin hydrochloride must meet the following criteria to be eligible for bioequivalence studies: 1) qualitative and quantitative sameness to the reference listed drug; 2) use of an active drug loading process via an ammonium sulfate concentration gradient in manufacture; 3) at least one batch produced using the commercial scale process to be used in subsequent bioequivalence studies; 4) equivalent physicochemical characteristics of the liposome, including particle size distribution, electrical charge, liposome composition, state of encapsulated drug and internal environment of the liposome, number of lamellar, surface-grafted PEG and *in vitro* leakage rates comparable with the reference standard [10].

Table 2. FDA-approved, liposomal drug products discontinued currently in the United States.

Brand Name	Active Ingredient	Innovator	Indications	Approval Year	Patent Expiry	Reason for Discontinuation (Year)
DaunoXome	Daunorubicin citrate	NeXstar Pharmaceuticals	Advanced HIV-associated Kaposi's sarcoma	1996	2012	Business decision to discontinue the product, not related to manufacturing, quality or safety (2016)
Depocyt	Cytarabine	Pacira Pharmaceuticals	Lymphomatous meningitis	1999	2027	Unspecified technical issues in manufacturing (2017)
DepoDur	Morphine sulfate	SkyePharma Inc	Analgesic	2004	2015	Company decision to discontinue product (2012)
Marqibo	Vincristine sulfate	Talon Therapeutics	Philadelphia chromosome-negative (Ph) acute lymphoblastic leukemia	2012	2021	Lack of clinical benefit verification in post-marketing trials (2022)

Several characterization techniques are used for analytical evaluation of Doxil® and liposomal doxorubicin hydrochloride products including HPLC methods with a UV or ELS detector for doxorubicin and lipid quantification, syringe filtration and ion chromatography to determine the internal sulfate and ammonium ion concentration, and fluorescence, cryogenic transmission electron microscopy or x-ray diffraction techniques to determine the state of encapsulated doxorubicin, liposome morphology and lamellarity [35, 36].

Differential scanning calorimetry (DSC) is used to determine the gel-liquid phase transition behavior of the lipid bilayer membrane, and particle size distribution could be measured by several techniques including dynamic light scattering, static light scattering and field-flow fractionization, size-exclusion chromatography, electron microscopy, flow cytometry and cryo-electron tomography [36–39].

Despite the multitude of analytical techniques and generic products approved, there is currently no comparative analysis available comparing the physicochemical profiles of Doxil® with every approved, liposomal doxorubicin hydrochloride generic product currently on the market to study their similarities, differences and measured specification ranges for each quality characteristic. Existing studies compare the reference product with either one or two generic products, often Lipodox® by Sun Pharmaceuticals, the reference standard, or the generic product developed by Dr. Reddy's Laboratories. In clinical studies discussed in literature, plasma levels of doxorubicin in Doxil® versus plasma levels of free doxorubicin administered to cancer patients were evaluated in Fig. 4 from a study by Gabizon and colleagues [40, 41].

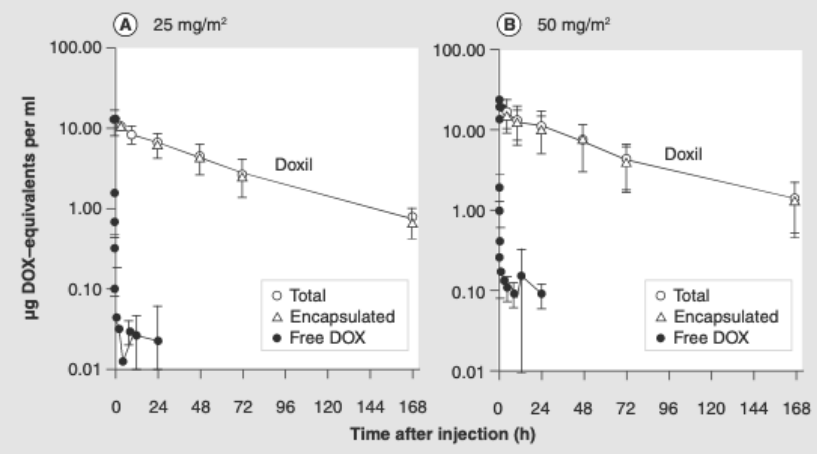

Figure 4. Plasma levels of doxorubicin (total or liposome-encapsulated) in Doxil and doxorubicin-treated patients. (A) 25 mg/m (n = 8 for Doxil; n = 3 for free DOX). (B) 50 mg/m (n = 14 for Doxil; n = 4 for free DOX). Adapted and reprinted by permission from the American Association for Cancer Research [23, 40].

For liposomal doxorubicin formulations, the AUC is significantly larger than that of the free doxorubicin formulation indicating significantly greater exposure in circulation of liposomal doxorubicin [41]. Doxil® also remains in plasma 6 days longer than free doxorubicin at a much lower clearance rate than free doxorubicin.

In the draft guidance for liposomal doxorubicin hydrochloride products, a single-dose, two-way crossover *in vivo* bioequivalence study is recommended for generic test candidate

evaluation using a 50 mg/m^2 dose in ovarian cancer patients whose disease has progressed or recurred after platinum-based chemotherapy and are scheduled to begin treatment with liposomal doxorubicin hydrochloride [10]. Determination of bioequivalence based on 90% confidence intervals (CI) for AUC and C_{max} for free and encapsulated doxorubicin [10]. A randomized, open-label, single-dose, two-preparation, two-sequence, two-cycle crossover, bioequivalence study was conducted for Lipodox® with respect to Caelyx® (50 mg/m^2 dose) in Chinese female patients with breast cancer by Shenzhen Kangzhe Pharmaceutical Co [42].

While the results of the study are not yet available, the study overview provides useful, detailed information on how *in vivo* bioequivalence is tested for generic versions in practice. Two treatment arms corresponding to the reference and generic test product at the same dose were evaluated for two cycles of this crossover study with a cleaning period of 28-42 days [42]. The dose was administered via intravenous drip on day 1 of each cycle, in which patients were given either the reference or generic test formulation. On the first day of the second cycle, the patients would crossover to the alternative reference or test formulation. The pharmacokinetic parameters of Caelyx® versus Lipodox® were measured: C_{max}, AUC_{0-t}, $AUC_{0-\infty}$ as primary outcome measures and AUC_{0-48h}, AUC_{48h-t}, T_{max}, λ_z, $t_{1/2z}$, $AUC_{\%Extrap}$, CL/F (apparent clearance), V_d/F (apparent volume of distribution) as secondary outcome measures [42].

Another clinical study compared the bioequivalence and safety of a generic doxorubicin hydrochloride liposome injection (Trade Name: Libaoduo) developed by Shanghai Fudan-Zhangjiang Biopharmaceutical Company with Caelyx® in advanced breast cancer patients under a similar study design: multicenter, single-dose, open-label, randomized, two-way crossover study [43]. Both test and reference formulations were administered via intravenous infusion at single dose of 50 mg/m^2 every 4 weeks to patients in randomized treatment groups. Blood samples were collected at predetermined time intervals from pre-dose up to 337.5 hours after the start of drug infusion for each treatment cycle [43]. Samples were centrifuged and plasma samples were separated and stored until analysis at -80°C for 24 hours. Plasma concentrations for encapsulated and free doxorubicin were quantified using two separate, validated LC-MS/MS methods [43]. Clinical pharmacokinetic results are detailed in Table 3 and Fig. 5 and 6. Bioequivalence between the generic test product and reference Caelyx® formulation was established based on the data generated [43].

Table 3. Clinical pharmacokinetic parameters of encapsulated doxorubicin from Libaoduo compared with Caelyx® in an *in vivo* bioequivalence study; adapted from source [43].

Parameters	**Mean ± SD (IIV%)**	
	Test (N=44)	**Reference (N=43)**
C_{max} (μg/mL)	34.37 ± 3.83 (11.1)	33.73 ± 3.82 (11.3)
AUC_{0-t} (h*mg/mL)	3.90 ± 0.68 (17.3)	3.70 ± 0.60 (16.2)
$AUC_{0-\infty}$ (h*mg/mL)	4.19 ± 0.82 (19.7)	3.93 ± 0.74 (18.8)
AUC_{0-48h} (h*mg/mL)	1.26 ± 0.14 (11.2)	1.22 ± 0.13 (11.0)
AUC_{48h-t} (h*mg/mL)	2.64 ± 0.58 (22.1)	2.48 ± 0.51 (20.6)
T_{max} (h)	2.06 (1.5, 9.5)	2.0 (1.5, 9.5)
$t_{1/2}$ (h)	81.31 ± 17.26 (21.2)	78.89 ± 16.57 (21.0)
λ_z ($x10^{-3}$ 1/h)	8.98 ± 2.30 (25.7)	9.20 ± 2.13 (23.1)
V_d (L/m^2)	1.41 ± 0.21 (15.1)	1.47 ± 0.30 (20.4)
CL_z ($mL/h/m^2$)	12.51 ± 3.02 (24.1)	13.16 ± 2.52 (19.2)

IIV refers to the intra-individual variation; All data are expressed as arithmetic mean ± standard deviation, except for T_{max}, which is expressed as median (min, max).

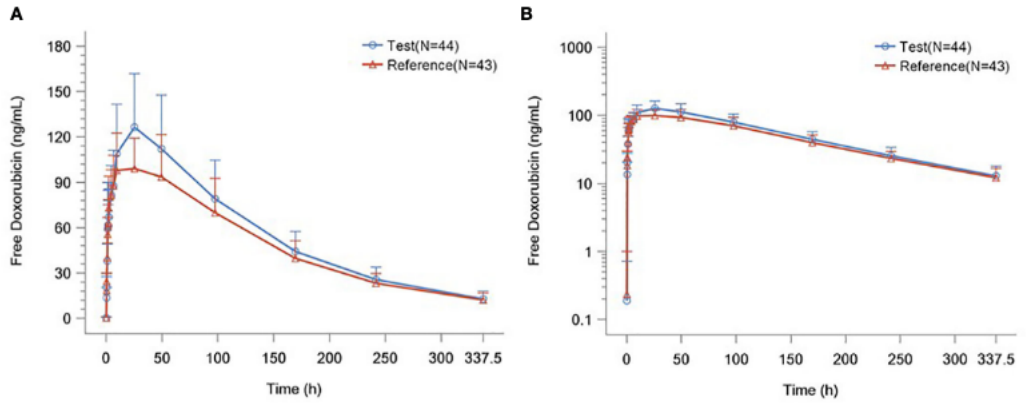

Figure 5. (A) Plasma concentration-time curves for free doxorubicin; (B) Plasma concentration-time semi-logarithmic curves for free doxorubicin [43].

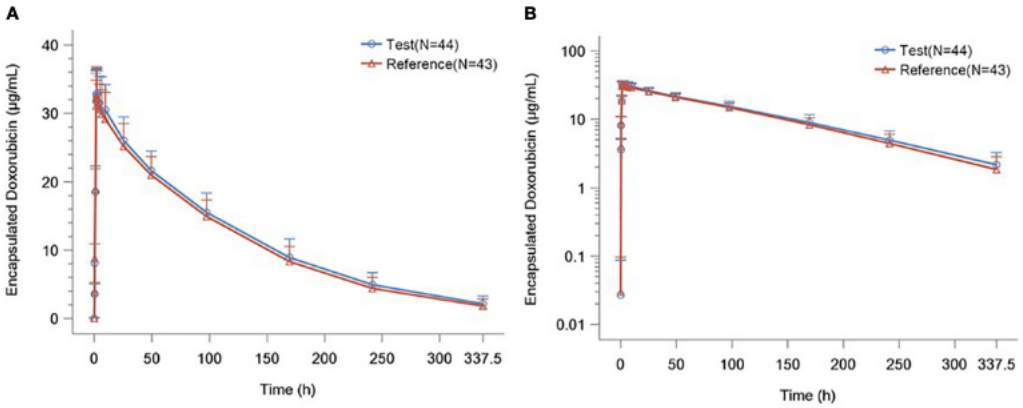

Figure 6. (A) Plasma concentration-time curves for liposomal doxorubicin; (B) Plasma concentration-time semilogarithmic curves for liposomal doxorubicin [43].

1.2.1.2 Amphotericin B Liposome for Injection

AmBisome® (*amphotericin B* liposome for injection) is a sterile, non-pyrogenic lyophilized product for intravenous infusion developed by NeXstar Pharmaceuticals and was approved by the FDA in 1997 [44]. Ambisome® is available in one dosage strength at 50 mg/vial and is indicated as an antifungal treatment for *Aspergillus, Candida* and/or *Cryptococcus* species infections, cryptococcal meningitis in HIV infected patients, and for visceral leishmaniasis – a parasitic disease transmitted by sandflies [44].

The *amphotericin B* liposome is a true single bilayer liposome (ULV) formed by micro-emulsification of multilamellar vesicles (MLV) using a homogenizer with amphotericin B intercalated within the lipid membrane [44]. Drug intercalation into the lipid membrane of a liposome product has a critical effect on the physicochemical properties of the drug relative to its free, non-encapsulated form. The liposome itself consists of 50 mg amphotericin B, 213 mg of hydrogenated soy phosphatidylcholine (HSPC), 52 mg cholesterol, 84 mg of distearoyl-phosphatidylglycerol (DSPG), 0.64 mg of α-tocopherol as preservative, 900 mg of sucrose and 27 mg of disodium succinate hexahydrate as buffer [44]. After reconstitution in Sterile Water for Injection, USP, the pH of the formulation falls between 5-6.

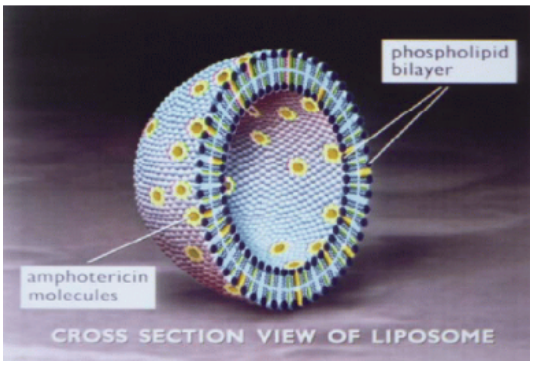

Figure 7. Schematic cross-section of amphotericin B intercalated within its liposomal membrane [45].

Crucial quality characteristics for development include liposome composition, size distribution, number of lamellae, electrical surface potential, lipid bilayer phase transition temperatures, amphotericin B aggregation state, *in vitro* hemolytic potential and antifungal activity, and *in vitro* release rates comparable to the reference standard [46]. The design characteristics used for amphotericin B liposome product development were strategic due to the need to reduce the nephrotoxicity associated with the free amphotericin B form – amphotericin B deoxycholate – while maintaining its antifungal efficacy. Liposome characteristics were specifically selected with the intent to improve its biodistribution, reduce toxicity, and provide a means for targeted drug delivery of amphotericin B.

Phospholipids comprising the lipid bilayer membrane of Ambisome® possessed characteristics suitable for liposome stability and reduced leakage of its drug contents. HSPC and DSPG have high phase transition temperatures at 55°C which were used to make a stable liposome formulation above physiological temperature at 37°C [47]. Cholesterol is also often mixed with phospholipids as it is known for its properties for decreasing membrane fluidity and increasing the rigidity of liposome membrane to make liposome structure less prone to leaking their internal contents [26, 47]. Additionally, it has been suggested that electrostatic interactions between the negative charge from the DSPG molecule and the positive amine group of amphotericin B form the stable ionic complex for drug intercalation within the lipid membrane, and cholesterol increases the stability of this complex as amphotericin B also has binding affinity to cholesterol [47]. Size distribution for Ambisome® was similar to Doxil® designed to be less than 100 nm for passive targeting to sites of infection [48]. Challenges in developing bioequivalent, liposomal amphotericin B generic products are due to difficulty in replicating the precise structure of the AmBisome® liposome in manufacturing [49]. Structural variations of the

amphotericin B liposome often result in faster drug release and increased toxicity *in vitro* and *in vivo* and has been the cause for product discontinuation and market withdrawals [49, 50].

To overcome these challenges, analytical characterization of approved, amphotericin B liposome products can provide useful insights into the critical quality attributes for *in vitro* and *in vivo* performance. Analytical techniques for the comparison of generic liposomal formulations of amphotericin B for manufacturing quality control include HPLC analysis for amphotericin B and lipid quantification, particle size analysis, measurement of the absence of flocculation and aggregation over time, stability testing at different temperatures, *in vitro* activity tests against different fungi and *in vivo* toxicity studies at increasing doses [49, 51]. Differential scanning calorimetry (DSC) is also used to evaluate lipid thermal behavior and phase transition temperatures, amphotericin B aggregation state can be determined by measuring the UV adsorption spectra of amphotericin B using circular dichroism (CD), and a flow-through USP-4 dissolution method has also been developed to evaluate the *in vitro* release profile of amphotericin B liposomes [49, 52, 53]. *In vitro* toxicity was evaluated by measuring the red blood cell hemolysis ratio, and antifungal activity was evaluated by determining the minimum inhibitory concentration of different amphotericin B formulations in *Candida albicans* fungal cells [49].

Characterization of Ambisome® and two generic amphotericin B liposome products approved in India (Phosome® and Amphonex®) were reported in a publication by Liu and colleagues [49]. Physicochemical data from their study revealed similarities in particle size for reference Ambisome®, and Phosome® and Amphonex® generics (Fig. 8) [49]. Quantification of amphotericin B concentration in reference batches of Ambisome® and generic Phosome® and Amphonex® revealed measured concentrations that were 3-10% higher in all Ambisome® batches while they were 10% lower in the generic batches from both manufacturers [49]. Lipid quantification in Ambisome® revealed higher HSPC concentrations 5-10% greater than label claim whereas all lipids in the Phosome® formulation were lower than label claim and Amphonex® lipid concentration met label claim values [49].

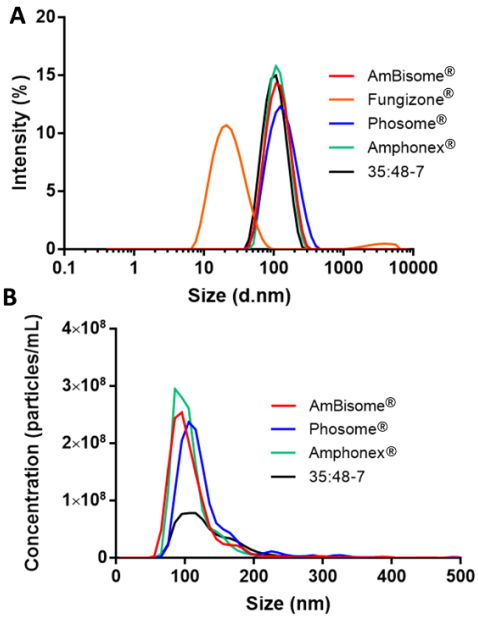

Figure 8. Size distribution of amphotericin B formulations by DLS (A) and NTA system (B) [49].

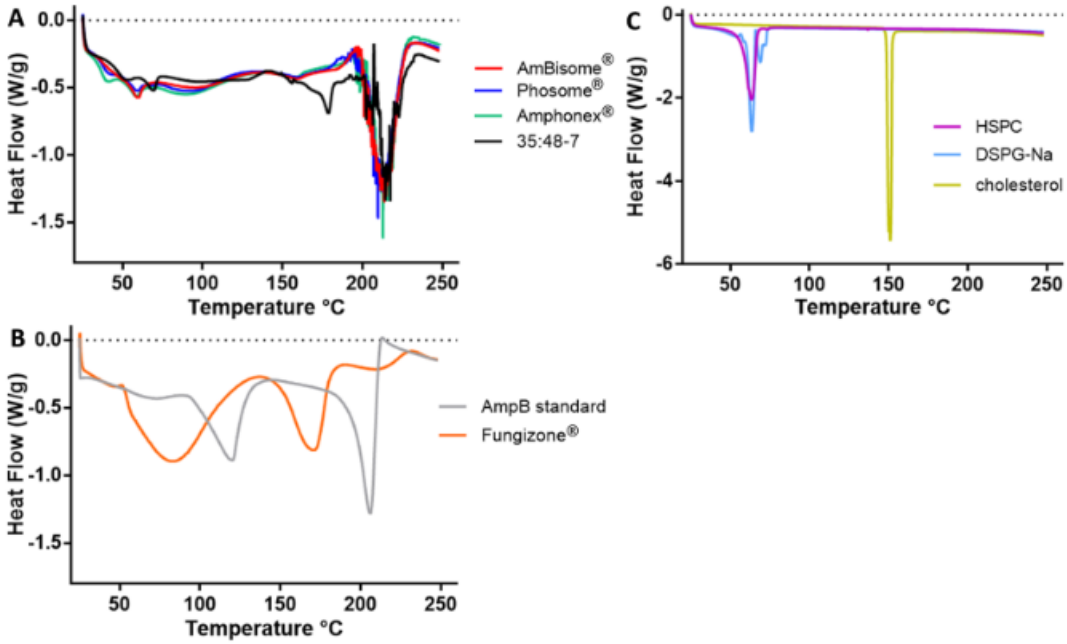

Figure 9. DSC thermograms of liposomal amphotericin B formulations (A), amphotericin B standard and Fungizone (B), and main lipid components (C) [49].

The thermal behavior of Ambisome® and generic products, Phosome® and Amphonex® in Fig. 9 are highly similar as evidenced by only one endothermic peak at 210°C correlating with the endothermic peak of the amphotericin B standard confirming the thermal presence of amphotericin B loaded liposomes. Dissolution profiles of the reference and generic amphotericin B liposome formulations revealed a high degree of similarity achieving a slower rate of

cumulative release within 24 hours when compared with the micellar formulation and the in-house developed formulation, 35:48-7 (Fig. 10).

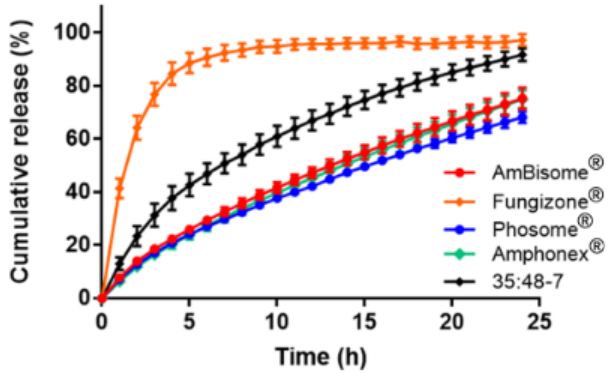

Figure 10. Dissolution profiles of different amphotericin B formulations. Data represented as mean ± SD (n = 3) [49].

In an article by Adler-Moore *et al*, a comparison of lipid/liposomal formulations of amphotericin B was discussed to assess the clinical advantages for treatment of invasive fungal infections over amphotericin B deoxycholate in reference to their physicochemical properties, mechanisms for reduced host toxicities, manufacturing processes, quality control assays, and preclinical/clinical assessments [50, 51, 54].

Adler-Moore *et al* discusses preclinical data comparing Ambisome with generic Anfogen and Lambin, and its impact on the critical importance of controlling the way the product is manufactured in Table 3 [51]. Anfogen® was liposomal amphotericin B product previously marketed in Argentina by Genpharma, S.A. that was discontinued and withdrawn due to toxicity. In Table 3, preclinical results show particle size for Ambisome to be significantly smaller than both generic products, and the dose of liposomal amphotericin B required to induce RBC toxicity to be much greater for Ambisome than for Anfogen or Lambin [51, 55, 56]. The maximum tolerated single intravenous dose of Anfogen (10 mg/kg) was at least 10-fold lower than that of AmBisome (>100 mg/kg) suggesting that the toxicity claims attributed to discontinuing Anfogen were substantiated [50, 51, 54]. The maximum tolerated single intravenous dose of Lambin (20 mg/kg) was also 2.5-fold lower than AmBisome (>50 mg/kg) [50, 51]. Moreover, upon *A. fumigatus* challenge and drug treatment with either A) 7.5 mg/kg, 4X AmBisome versus 7.5 mg/kg, 4X generic Anfogen, or B) 10 mg/kg, 6X AmBisome versus 10 mg/kg, 6X Lambin, survival rates for A) AmBisome vs Anfogen and B) Ambisome vs Lambin were 100% to 70% and 60% to 30%, respectively [50, 51].

Table 4. Results of preclinical studies comparing AmBisome with Anfogen or Lambin [51].

	AmBisome *vs* Anfogen [1]		AmBisome *vs* Lambin [2]	
	AmBisome	Anfogen	AmBisome	Lambin
Median diameter of liposomes (nm)	77.8	111.5	77.8	122.2
RBC toxicity (K_{50} μg/ml)	20	0.9	7.4	1.4
Maximum tolerated single iv dose (mg/kg)	>100	10	>50	20
BUN at 7.5 mg/kg	12 (normal)	78	NL	NL
Renal tubular necrosis with daily 5 mg/kg dosing in uninfected mice	Normal renal tubules	Renal tubular dilation	Normal renal tubules	Renal tubular dilation
Survival following *A. fumigatus* challenge and drug treatment	7.5 mg/kg,4X: 100%	7.5 mg/kg, 4X: 70%	10 mg/kg, 6X: 60%	10 mg/kg, 6X: 30%

Abbreviations: RBC: red blood cell, iv: intraveneous, BUN: blood urea nitrogen, NL: within normal limits.

Several, randomized clinical trials of Ambisome® were discussed in an article by Stone *et al* including select studies, such as a dose-ranging study for liposomal amphotericin B treating invasive aspergillosis (2007), Ambisome (5 mg/kg) versus amphotericin B deoxycholate (1 mg/kg) to treat invasive aspergillosis (1998), and 50 mg of liposomal amphotericin B on alternate days vs a negative control group to treat antifungal prophylaxis in neutropenia (2006) [57].

In the 1998 invasive aspergillosis study, 14 of the 32 patients treated with Ambisome experienced a complete response compared with only 6 out of 34 patients treated with amphotericin B deoxycholate [57, 58]. In the 2006 antifungal prophylaxis study, only 5% of patients with neutropenia treated with liposomal amphotericin B experienced invasive fungal infections following treatment compared to 35% of patients with neutropenia in the control group [57, 59]. In the 2007 dose-ranging study, the treatment arms were 3 mg/kg versus 10 mg/kg of liposomal amphotericin B for 14 days followed by a 3 mg/kg dose. The study findings revealed 72% of the 3 mg/kg group and 59% of the 10 mg/kg group experienced 12 weeks of survival when administered each treatment arm against invasive aspergillosis, although greater toxicity was experienced with the 10 mg/kg group [57, 60].

Ultimately, in the clinical comparison of Ambisome® and few generic amphotericin B liposome products, it can be observed that despite physicochemical similarity and qualitative and quantitative sameness of bioequivalent generics *in vitro*, relevant differences do exist upon clinical evaluation for formulations of the same composition developed by different processes.

Further investigations into the critical quality attributes influencing *in vitro in vivo* drug performance for complex liposomal drug products is needed to resolve the gaps in performance and safety to support the development of high-quality, complex liposomal generic drug products.

1.2.1.3 Exparel®

Exparel® (*bupivacaine* liposome injectable suspension) is a sterile, aqueous suspension of *bupivacaine* multivesicular liposomes using the DepoFoam® technology developed by Pacira Pharmaceuticals approved by the U.S. FDA in 2011 [61]. Exparel® is indicated as a post-surgical local analgesic and as an interscalene brachial plexus nerve block to produce post-surgical regional analgesia for single-dose administration only. Two dosage strengths are available: 266 mg/20 mL (13.3 mg/mL) and 133 mg/10 mL (13.3 mg/mL) in single-dose vials [61].

According to the 2018 draft product specific guidance for liposomal bupivacaine generics, generic bupivacaine liposomes should have the same drug product composition and equivalent liposome characteristics to the RLD, including liposome composition, amount of free and encapsulated drug, internal environment of liposome, liposome particle structure, morphology, size distribution, electrical surface potential and *in vitro* release rates [62]. Strategic design characteristics were employed to develop Exparel® particularly upon the use of the DepoFoam technology, in which bupivacaine is encapsulated in multivesicular liposomes (MVLs) presenting an inner particle structure resembling that of a honeycomb with several non-concentric aqueous chambers separated by lipid membranes [63–65]. Particle size is on the order of magnitude from 1 – 100 microns, significantly larger than that of small ULV and MLV like Doxil® or Ambisome®. DepoFoam encapsulation of bupivacaine is shown to result in sustained release lasting over multiple days to weeks following non-vascular routes of administration [63].

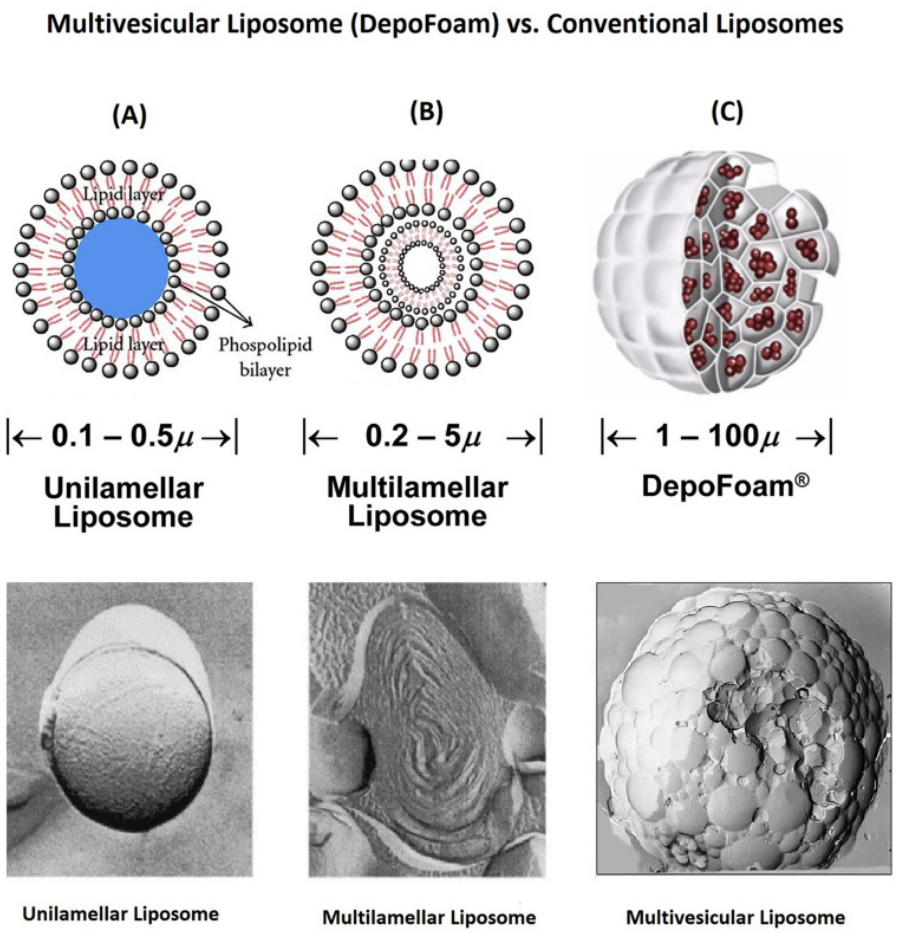

Figure 11. Schematic diagrams and electron microscopy images of A) unilamellar liposomes (ULV); B) multilamellar liposomes (MLV); C) multivesicular liposomes (MVL) using the DepoFoam® technology [64, 66].

Yu *et al* developed a series of analytical methods characterizing Exparel® products in respect to particle size, inner particle structure, drug and lipid concentration, residual solvents, pH and developed an accelerated *in vitro* drug release assay to characterize dissolution profiles for formulation evaluation and quality control for liposomal bupivacaine formulations [65]. Four different batches of Exparel® were analyzed for batch-to-batch variability and the methods developed were to support subsequent development of generic bupivacaine MVLs and other similar MVL-based products.

Briefly, particle size was determined using a Malvern Mastersizer 2000. Electron microscopy (cryo-SEM) and confocal microscopy techniques were employed to visualize the internal honeycomb-like structure of the bupivacaine MVLs [65, 67, 68]. Bupivacaine drug concentration was quantified using an ultra-performance liquid chromatography (UPLC) system assay with UV detection at 265 nm and lipid concentrations for DEPC, DPPG-Na and tricaprylin

were determined using UPLC mass spectrometry (MS) equipped with a QdaTM detector [65]. Cholesterol was quantified using a free cholesterol detection kit.

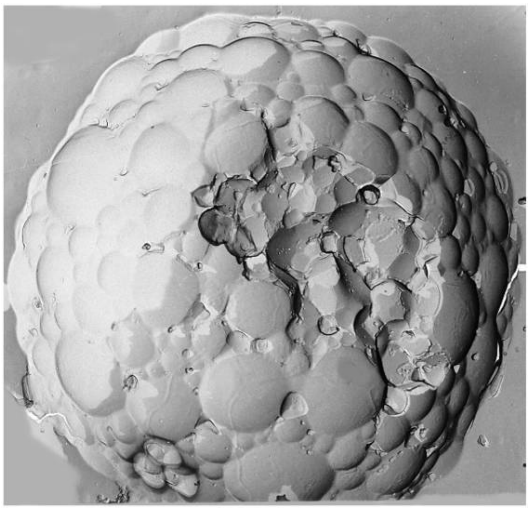

Figure 12. Scanning electron microscope image of DepoFoam® containing bupivacaine liposome resembling a honeycomb-like structure [67].

Residual solvents present in the formulation were quantified using gas chromatography. The pH of the internal and external aqueous environment was determined using pH measurement with probe sonication. Lastly, Yu *et al* developed a novel *in vitro* release assay using a rotator-based, sample-and-separate release method to characterize the accelerated release kinetics for bupivacaine MVLs at 37°C. In this work, a thorough evaluation of bupivacaine liposomal characteristics and their relevant characterization methods may be used for subsequent development efforts and investigations [65].

In a separate study by Xia *et* al, the impact of product quality on the *in vivo* performance of bupivacaine MLV liposomes was assessed using several of these analytical methods for physicochemical characterization to complement *in vivo* pharmacokinetic analysis in Sprague-Dawley rats [69]. Commercial bupivacaine MVLs were deliberately compromised in product quality using, either: 1) freeze-thawing; 2) mechanical agitation; 3) high temperature stress; or 4) expired formulations. Table 5 shows data for liposome size, pH and amount of free bupivacaine (%) in compromised bupivacaine liposome formulations [69]. Fig. 13 reveals the differences in the *in vitro* dissolution profiles for compromised Exparel® formulations in comparison with the intact and expired formulations [69].

Table 5. Size distribution, pH value, and free drug contents of intact, expired and compromised Exparel. All values are presented as mean ± SD (n=3) [69].

Formulation	d0.1 (μm)	d0.5 (μm)	d0.9 (μm)	pH	Free drug %
[a]Intact	13.2 ± 0.2	26.0 ± 0.3	53.5 ± 0.1	6.3	5.26
Freeze-thawed	3.1 ± 0.1	13.0 ± 0.5	30.6 ± 1.7	5.5	80.04
High-temp incubated	16.6 ± 1.1	49.7 ± 1.7	95.1 ± 5.0	6.1	12.07
Mechanical agitated	13.3 ± 0.3	25.7 ± 0.3	50.6 ± 0.1	6.5	28.49
[b]Expired	13.5 ± 0.2	26.5 ± 0.2	54.0 ± 0.1	6.0	5.83

[a]Intact Exparel batch# 20-P097, with the expiration in July 2022

[b]Expired Exparel batch# 17-4046, with the expiration in April 2018

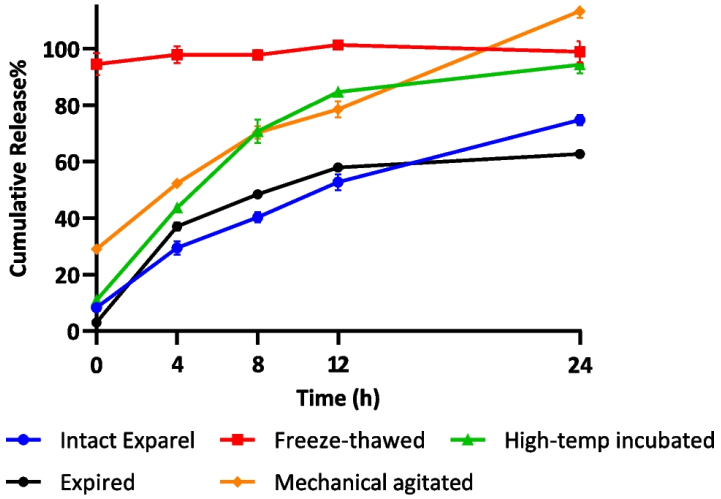

Figure 13. *In vitro* release profiles of intact, expired, and compromised Exparel formulations stressed via mechanical agitation, freeze-thawing, and high-temperature incubation. All values are presented as mean ± SD (n = 3) [69].

Product expiration has an insignificant effect on particle size, pH, and free bupivacaine in the liposomal formulation when compared to the intact, commercial Exparel® formulation. The dissolution profile of the expired Exparel® batch is also most similar to the intact commercial batch when compared with the other quality-compromised formulations despite having low cumulative release (~60%) within 24 hours [69]. Physicochemical data for the freeze-thaw formulation suggest that the structural quality of the MVL has been significantly compromised, which is indicated by a significant decrease in particle size for d0.1, 0.5 and 0.9 (μm) and pH when compared with the intact formulation. The drop in pH for this form of stress falls outside of the reported pH range for the reference product (pH 5.8-7.4) which Xia *et al* suggests is due to

leaking of internal contents [69]. This is also confirmed in Fig. 13 with initial burst release showing nearly complete release at 0 hour. All other forms of stress compromising the quality of Exparel® formulations achieve complete release within 24 hours which show statistical significance from the intact and expired formulations.

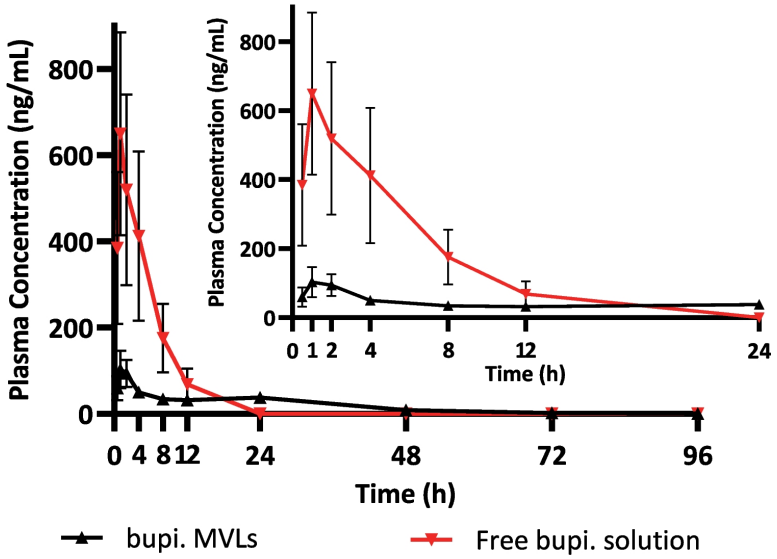

Figure 14. Plasma concentration-time profiles of Exparel and free bupivacaine solution following subcutaneous administration at 15 mg/kg dose in Sprague-Dawley rats (n=4, mean ± SD) [69].

In an attempt to draw a correlation with the *in vitro* physicochemical data, *in vivo* pharmacokinetic studies comparing the commercial Exparel® formulation to free bupivacaine solutions at a subcutaneous dose of 15 mg/kg in Sprague-Dawley rats revealed C_{max} values 6-fold lower than the free drug evidenced in Fig. 14, an AUC value 2-fold lower than the free drug and a significant difference in mean residence time (MRT) in rat plasma nearly 5 times that of the free bupivacaine formulation [69]. Bupivacaine plasma concentration profiles after a 15 mg/kg subcutaneous injection of intact, expired, freeze-thawed, high temperature incubation and mechanically agitated Exparel® formulations to Sprague-Dawley rats are shown in Fig. 15.

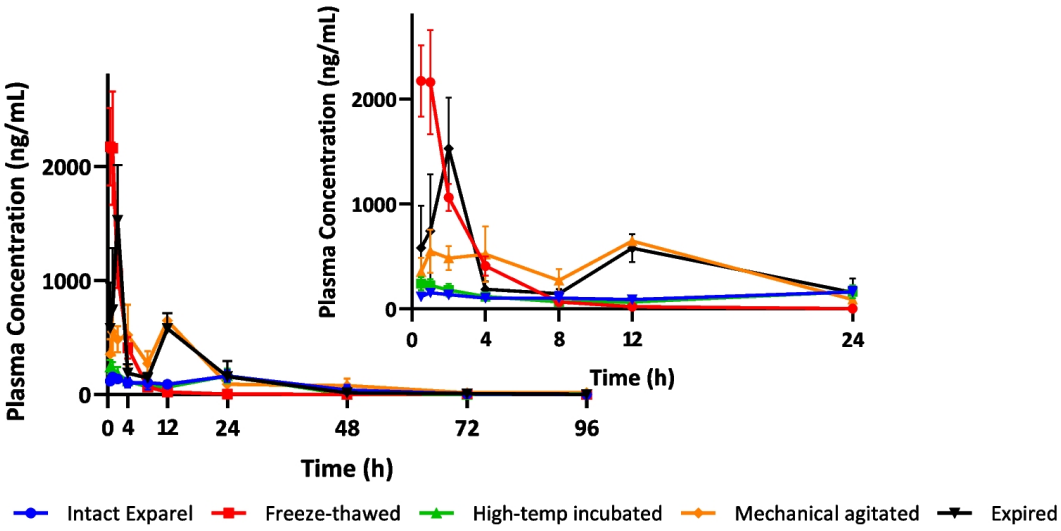

Fig. 15. Bupivacaine plasma concentration profiles of subcutaneous injected intact, expired, and compromised Exparel stressed via freeze-thawing, mechanical agitation, and high-temperature incubation, at 15 mg/kg in SD rats (n = 5, mean ± SD) [69].

Significant differences in pharmacokinetic profiles for freeze-thawed, mechanically agitated and expired Exparel® formulations exist when compared with the intact, commercial formulation. The pharmacokinetic profile for the compromised formulation by high temperature incubation is most similar, however, to the commercial formulation. Overall, freeze thaw stress reveals the most significant effect on product quality [69].

In reference to preliminary clinical data for Exparel®, a phase III, multicenter, randomized, double-blind, parallel-group, placebo-controlled study evaluating the safety and efficacy of a single administration of test drug candidate, SKY0402 (Exparel®), for prolonged postoperative analgesia in subjects undergoing a bunionectomy was conducted from April 2009 to November 2009.

A statistically significant difference exists for the mean-adjusted AUC of the numeric rating scale (NRS) for pain intensity scores using the bupivacaine liposome treatment group in comparison with the placebo shown in Fig. 16A. At a 120 mg dose, the liposomal drug treatment group exhibited lower AUC scores than the placebo group (123.9 vs. 146.2; p=0.0005) [70]. Patients who were pain-free after administration of bupivacaine liposomes when compared to placebo treatment over 72 hours in Fig. 16B [70]. Interestingly, placebo treatment in comparison to the study drug treatment followed a similar trend in patient-reported outcomes using the bupivacaine DepoFoam liposomes.

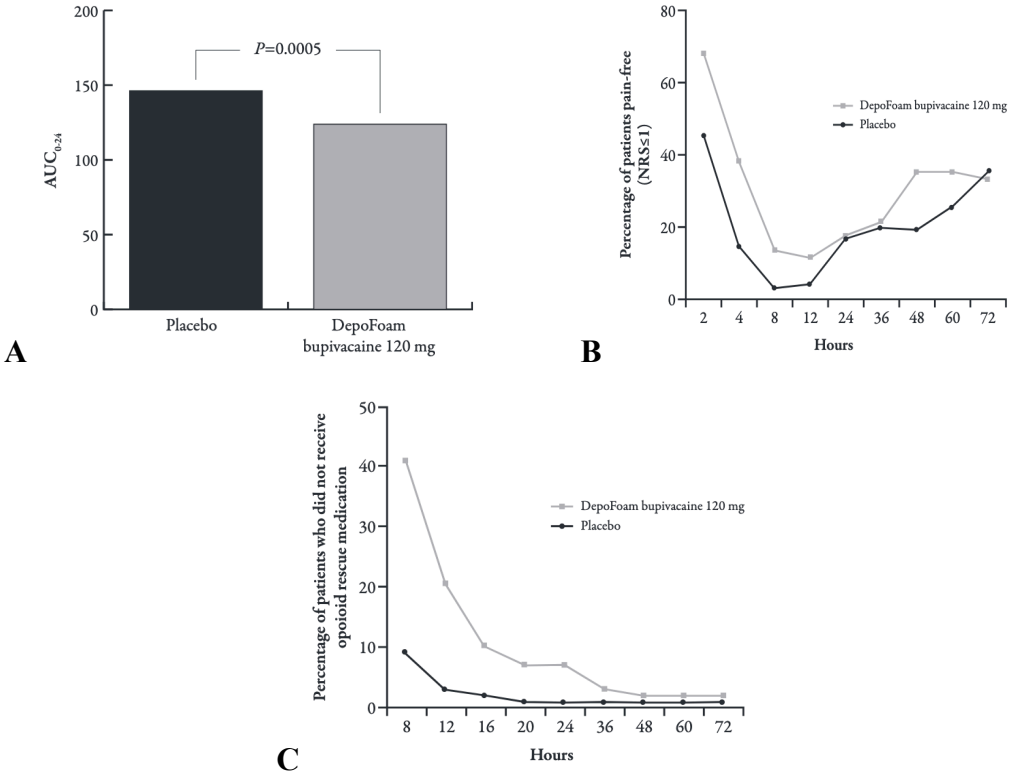

Figure 16. A) Primary measure of clinical efficacy as the adjusted mean of the area under the curve (AUC) of the numeric rating scale (NRS) pain intensity scores in the DepoFoam bupivacaine 120 mg group; B) Percentage of patients who went pain-free (NRS $\leq$ 1) for 120 mg DepoFoam bupivacaine compared to placebo; C) Percentage of patients who received no opioid rescue pain medication with 120 mg DepoFoam bupivacaine compared to placebo. Figures and captions adapted from [70].

In Fig. 16C, the percentage of patients of who received no opioid rescue medication with the study drug treatment when compared with the placebo treatment was statistically significant up to 24 hours, upon which both treatment groups had comparable levels of patients who now needed opioid rescue medication following postoperative surgery [70]. Based on this data, it was suggested that liposomal bupivacaine provides clinical benefit up to 24 hours for therapeutic efficacy over placebo treatment.

Several, additional clinical studies have been registered and completed by Pacira Pharmaceuticals for the evaluation of Exparel® bupivacaine liposomes. Given the recent approval of the new generic developed by Jiangsu Hengrui Pharmaceutical Company in 2024, characterizwo additional, investigational clinical studies have been registered with the National Library of Medicine on ClinicalTrials.gov for their generic bupivacaine liposome formulation. The first study is to evaluate the safety and efficacy of the generic, bupivacaine liposome

injection for local infiltration analgesia in pediatric orthopedic surgery for acute postoperative pain and is currently recruiting subjects between the ages of 6 and 17 years old [71]. The second study is not yet recruiting and is to evaluate the efficacy, safety and tolerability of the generic, liposomal bupivacaine formulation for paravertebral nerve block to treat thoracoscopic postoperative pain and evaluate human pharmacokinetics [72].

1.2.2 FDA-approved products with no approved generics

1.2.2.1 Onivyde

Onivyde® is an *irinotecan* liposome injection for intravenous use developed by Ipsen Pharmaceuticals approved in 2015 (U.S. Food & Drug Administration, 2024). Onivyde® is indicated for first-line treatment of adult patients with metastatic pancreatic adenocarcinoma as a combination therapy with oxaliplatin and/or fluorouracil and leucovorin following gemcitabine-based therapy (U.S. Food & Drug Administration, 2024). Onivyde® is available in one dosage strength, 43 mg/10 mL (4.3 mg/mL), as a single-dose vial [73].

The liposome is a unilamellar vesicle (ULV) approximately 110 nm in size, encapsulating irinotecan in its aqueous core in a precipitated or gelated state [73, 74]. An active drug loading process using sucrose octasulfate as the tapping agent via a transmembrane concentration gradient loads therapeutic levels of irinotecan into the aqueous core of the ULVs in the form of crystalline bundles [74]. The composition of the liposome consists of 1,2-distearoyl-SN-phosphatidylcholine (DSPC) at 6.81 mg/mL, cholesterol at 2.22 mg/mL and methoxy-terminated polyethylene glycol (MW 2000)-distearoylphosphatidyl ethanolamine (MPEG-2000-DSPE) at 0.12 mg/mL. Formulation buffer was HEPES buffer at 4.05 mg/mL and sodium chloride was used in the formulation as an isotonicity agent at 8.42 mg/mL [73].

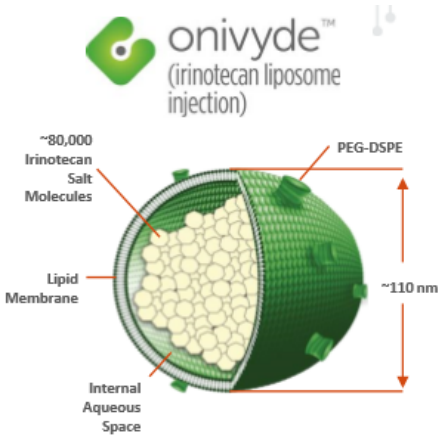

Figure 17. Schematic depiction of Onivyde (irinotecan liposome injection) [75].

Liposome characteristics of the irinotecan liposome product include liposome composition, drug and lipid concentration, state of the encapsulated drug, internal environment of the liposome, liposome size distribution, number of lamellae, grafted PEG at the liposome surface, electrical surface charge and *in vitro* release rates comparable to the reference standard as detailed in the draft guidance for irinotecan hydrochloride released by the FDA [76].

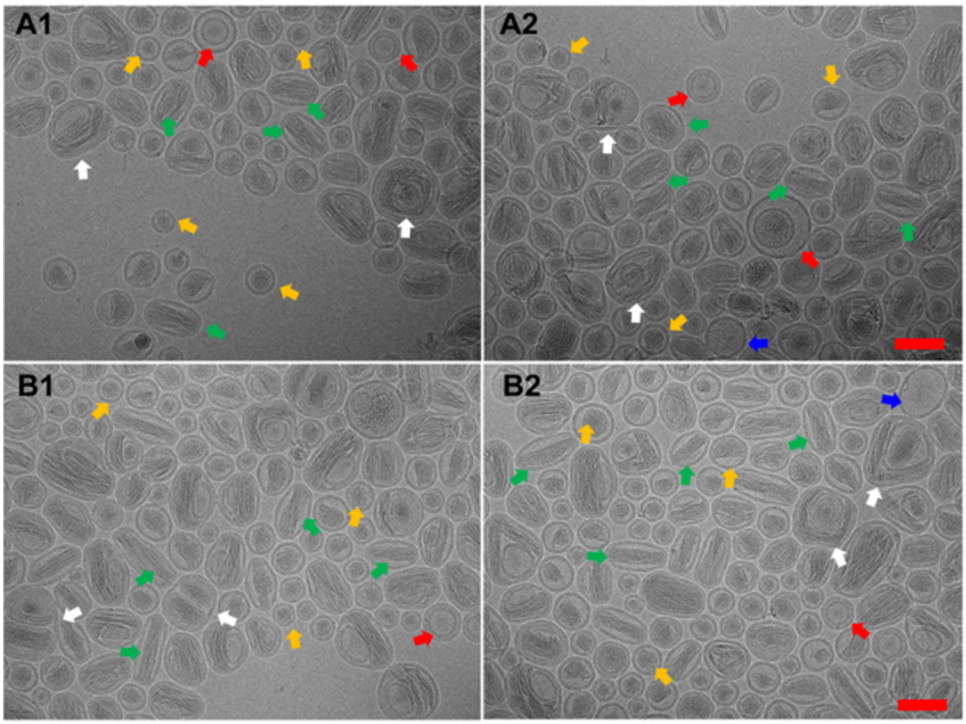

Figure 18. Cryo-TEM images of Onivyde®. Green arrows indicate the prolate spheroid with crystal bundle inside. Yellow arrows point out round shape particles. White arrows refer to complex structures with both liposome and drug crystal inside. Red arrows indicate symmetric multilamellar vehicles. Blue arrows point out empty liposomes. A1-A2 and B1-B2 are representative cryo-TEM images of batch #120518S and batch #200048A of Onivyde® respectively. Scale bar, 100 nm. Image adapted from [74].

The design and development of the irinotecan liposome is like that of the doxorubicin and amphotericin B liposomes and therefore, the strategic advantages of the design considerations are similar. Strategic liposome composition and concentrations consisting of DSPC, cholesterol and DSPE-PEG 2000 helped to reduce membrane fluidity due to incorporation of phospholipids such as DSPC with high phase transition temperatures (55°C) to prevent leakage of encapsulated irinotecan in the aqueous core of the unilamellar liposomes and cholesterol to increase liposome stability by altering the packing order of the phospholipid bilayer structure [47, 77]. The covalent attachment of polyethylene glycol (MW 2000) chains to liposome surface has been shown to increase steric stabilization, reduce clearance by the reticuloendothelial system, and increase circulation time in plasma of liposomes for passive targeting to tumor tissues, similar to that of Doxil® [74, 78].

The state of the encapsulated drug as an insoluble sucrose octasulfate salt precipitate is a critical design parameter to prevent premature drug release. Size distribution and zeta potential are critical parameters influencing release kinetics, biodistribution, liposome stability and interactions *in vivo*. The FDA label states that the Onivyde® is approximately 110 nm in size [73]. In characterization studies, irinotecan liposomes are reported to possess a negative surface charge or zeta potential which can help prevent liposome-liposome interactions due to electrostatic repulsions [79, 80].

The analytical methods used to characterize the quality characteristics of the Onivyde® include cryogenic transmission electron microscopy (cryo-TEM) for morphology as shown in Fig. 18, dynamic light scattering for particle size and size distribution, differential scanning calorimetry (DSC) for lipid phase transition temperature, ultra-performance liquid chromatography-evaporative light scattering detection (UPLC-ELSD), ultra-performance liquid chromatography-fluorescence detection (UPLC-FLR) and gas chromatography (GC) for quantification of irinotecan, lipid (DSPC, cholesterol, DSPE-PEG2k) and excipient concentrations [74]. Nanostructure was evaluated using small angle X-ray scattering (SAXS), and novel release methods developed by Gan and Juang *et al* used single-vial dialysis-based methods in phosphate buffered saline (PBS), HEPES buffer and human plasma to characterize the dissolution profiles of irinotecan from liposomes [74, 81].

Presently, there are no generic products available for the Onivyde® liposomal formulation. Four patents for the drug substance and product have expired and another patent for

a treatment indication has expired in May 2025 making it an attractive candidate for generic development. However, exclusivities have not yet expired preventing generic manufacturers from submitting their applications until 2031 [27]. Additionally, due to its complex liposomal formulation and manufacturing process, generic development of Onivyde® is challenging. Upon expiration patents and exclusivities, generic manufacturers must demonstrate bioequivalence to the reference listed product through qualitative (Q1) and quantitative (Q2) sameness and possess physicochemical similarity (Q3) through equivalent liposome characteristics as those described in the draft guidance for irinotecan hydrochloride [76].

1.2.2.2 Arikayce Kit

Arikayce® is an amikacin liposome inhalation suspension combination drug product developed by Insmed Incorporated. It received FDA approval in 2018 and is indicated for treatment of *Mycobacterium avium* complex (MAC) lung disease as part of a combination antibacterial drug regimen for patients who do not achieve negative sputum cultures after a minimum of 6 consecutive months of a multidrug background regimen therapy [82]. The recommended dosage in adults is once daily as an oral inhalation of the contents of a unit-dose glass vial containing 590 mg/8.4 mL (70 mg/mL) of amikacin sulfate using the Lamira Nebulizer System.



Figure 19. Lamira Nebulizer System and controller [83].

The FDA has yet to release a draft guidance for industry for Arikayce® given that patents and exclusivities have not expired. However, quality characteristics of the combination drug product detailed in the package insert include its liposome composition, drug and lipid concentration, mean delivered dose from the mouthpiece of the Lamira Nebulizer System, the

mass median aerodynamic diameter (MMAD) of the nebulized aerosol droplets and percentage of amikacin in liposomes released by nebulization [82].

The lipid composition of Arikayce® consists of cholesterol and dipalmitoylphosphatidyl choline (DPPC), and the lipid to drug weight ratio falls within the range of 0.60 – 0.79 for targeted delivery via the inhalation route [82]. The mean delivered dose of amikacin sulfate from the mouthpiece of the Lamira Nebulizer System was reported as approximately 312 mg (53% of label claim) and the MMAD of the nebulized aerosol droplets is approximately 4.7 microns [82]. Given the mode of delivery, nebulized Arikayce® administered through the oral inhalation route is delivered as a combination of free and liposomal amikacin.

In research conducted by Maxwell *et al*, optimized amikacin liposome formulations were developed by modified thin film hydration using different phospholipids were for its physico-chemical properties [84]. A high throughput, 96-well based spectrofluorimetric method was used to quantify the concentration of amikacin sulfate in *in vitro* samples and a LC-MS/MS bioanalytical assay was used to quantify amikacin concentration in plasma. Differential scanning calorimetry (DSC) was used to determine the thermal characteristics of amikacin and the excipients. Fourier Transform Infrared Spectroscopy (FTIR) was applied to assess the compatibility between the drug and excipients.

Particle size, size distribution and zeta potential were determined using dynamic light scattering (DLS). Surface morphology of amikacin-loaded liposomes was characterized using transmission electron microscopy (TEM). Drug encapsulation efficiency was quantified by measuring the diffusion of unencapsulated amikacin present in an entrapped volume of the liposomal amikacin formulation in a pretreated cellulose dialysis membrane into the external aqueous compartment at predetermined time intervals up to 10 hours [84]. Drug release of amikacin from liposomes was evaluated using double side open diffusion glass tubes with activated cellophane membranes, soaked overnight in Milli-Q water and tied to one end of the donor compartment, after removal of unencapsulated amikacin from the liposomal formulation and fluorescence intensity was measured to determine *in vitro* release profiles at predetermined time intervals using the spectrofluorimetric method for quantifying amikacin sulfate [84].

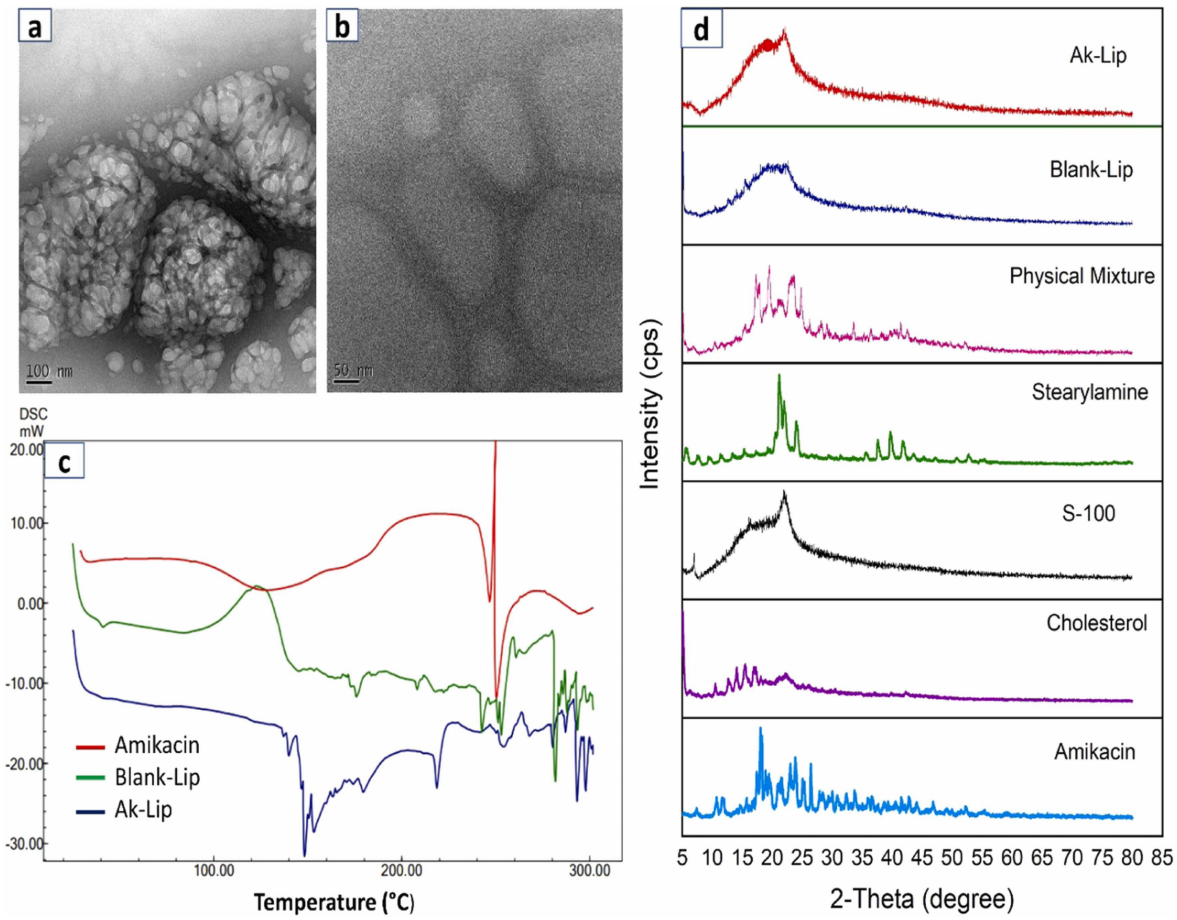

Figure 20. Transmission Electron Microscopy (TEM) image of amikacin loaded liposomes (Ak-lip) at 100 nm scale (a) and 50 nm scale (b). DSC thermogram of Amikacin, Amikacin loaded liposomes (Ak-lip) and Blank liposomes (Blank-Lip) (c); X-ray diffraction pattern of pure Amikacin, cholesterol, Soy phospholipid S-100, stearylamine, physical mixture, Blank-Lip and Ak-lip (d). Caption adapted from [84].

TEM images of amikacin-loaded liposomes in Fig. 20A revealed unique inner structures resembling non-spherical, honeycomb-like structures similar to the MVL structure of the Exparel® formulation. It is not yet understood whether the microstructure of the amikacin loaded liposome is comparable to the commercial product as these liposomes were prepared using a modified thin film hydration method and was formulated with soy phosphatidycholine (S100) instead of DPPC, cholesterol, stearylamine and amikacin sulfate in 5 mL of Milli-Q water under probe sonication [84]. Regardless, the physicochemical data provides useful insights into potential microstructure and thermal behavior of free and liposomal amikacin.

Fig. 21 shows the *in vitro* release profiles of the amikacin-loaded liposomes over 72 hours for pure amikacin and amikacin liposomes. Fig. 22 shows the *in vitro* release profiles of amikacin liposomes during a long-term stability study on days 15 and 90 at each storage temperature using a spectrofluorimetric assay for *in vitro* release evaluation.

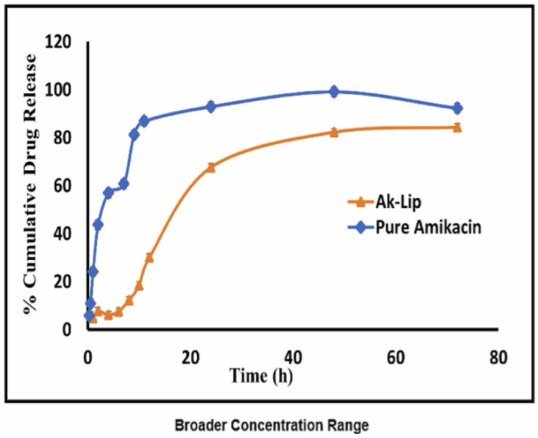

Figure 21. *In vitro* cumulative % drug release of pure amikacin and Ak-lip formulation. Image adapted from Maxwell *et al* [84].

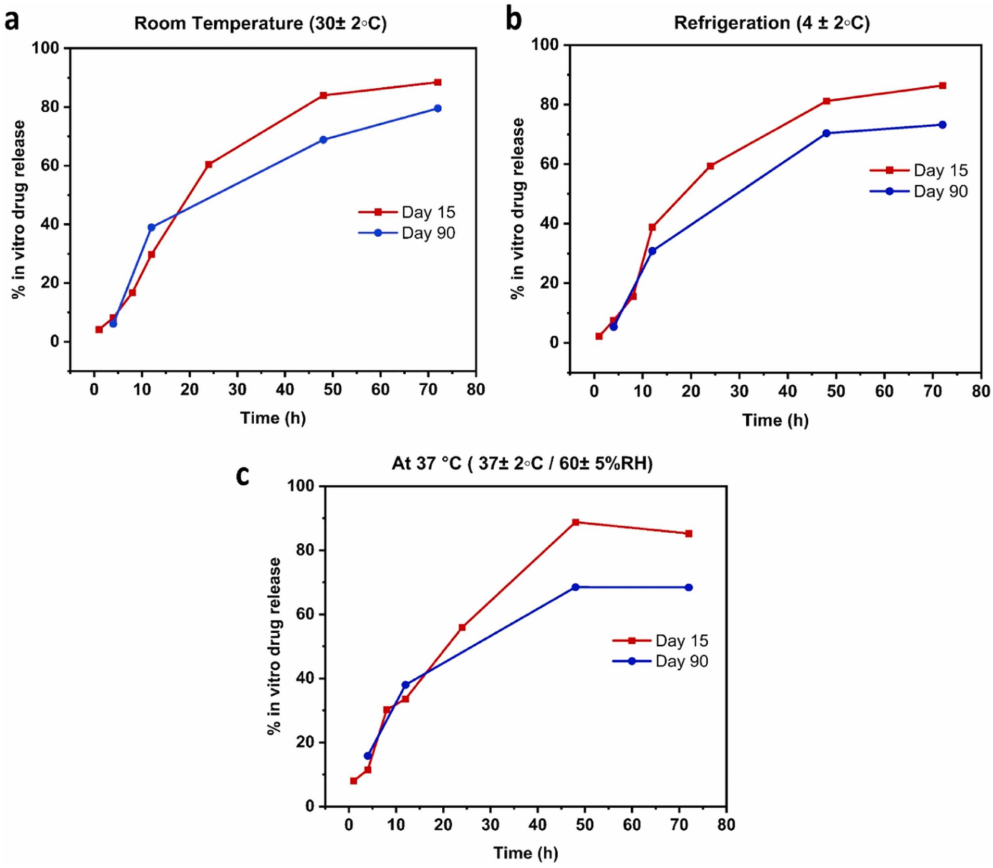

Figure 22.*In vitro* drug release profile of Ak-lip over 72 h, at Day 15 and 90, following storage at room temperature (a), refrigeration (b) and at 37°C (c) [84].

Additional quality characteristics were measured in the long-term stability study including drug content, particle size, polydispersity, and zeta potential in Table 5 [84]. Amikacin liposomes developed by Maxwell and colleagues showed a minor decrease in drug content and a minor increase in particle size, however, cumulative release within 72 hours on day 0 (87 ± 3.7%) at different temperatures showed insignificant differences over 90 days suggesting minimal effects on liposome stability over 3 months. *In vivo* pharmacokinetic studies were also performed in Sprague-Dawley rats and the concentration-time release profiles of free and liposomal amikacin are described in Table 6 and Fig. 23.

Table 6. Pharmacokinetic parameters for Ak-lip and Pure amikacin following i.v. injection [84].

Formulation	**C_{max}** ng/mL/ mg dose	**AUC** ng/ mL*h	**Cl** L/h
Amikacin sulfate dissolved in water for injection (10 mg/500 µL)	2.81	53.0	160.0
Ak-lip (10 mg/500 µL)	4.56	77.0	97.41

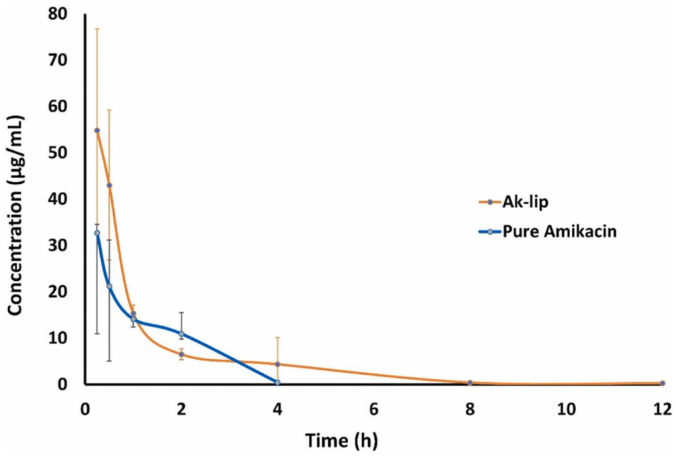

Figure 23. *In vivo* drug release of Ak-lip and Pure amikacin in Sprague-Dawley Rats.

Table 7. Stability study for optimized Ak-lip.

Parameter		**Day 0**	**Day 15**	**Day 30**	**Day 60**	**Day 90**
Drug Content (out of 10 mg)		9.91 ± 0.1	9.87 ± 0.02	9.95 ± 0.1	9.64 ± 0.4	9.45 ± 0.6
PS (nm)		93 ± 12	95 ± 14	93 ± 14	97 ± 15	102 ± 12
PDI		0.256 ± 0.03	0.211 ± 0.08	0.264 ± 0.04	0.241 ± 0.04	0.211 ± 0.18
ZP (+mV)		37 ± 2.2	35 ± 2.4	37 ± 2.0	40 ± 3.4	35 ± 2.3
***in vitro* drug release at 4 h** (%)	**Room temperature** (30 ± 2°C)	9.28 ± 1.7	8.1 ± 2.3	7.1 ± 1.7	7.8 ± 2.3	6.1 ± 1.1
	Refrigeration (4 ± 2°C)		7.4 ± 2.1	8.2 ± 2.9	8.2 ± 2.3	5.3 ± 3.2
	At 37°C (37 ± 2°C/ 60% ± 5%RH)		11.4 ± 3.4	11.3 ± 4.5	13 ± 1.6	15 ± 3.1
***in vitro* drug release at 72 h** (%)	**Room temperature** (30 ± 2°C)	87 ± 3.7	88 ± 1.8	81 ± 2.1	90 ± 2.5	79.5 ± 2.4
	Refrigeration (4 ± 2°C)		86 ± 0.7	81.2 ± 3	81 ± 3.2	86 ± 1.6
	At 37°C (37 ± 2°C/ 60% ± 5%RH)		85.2 ± 4.8	88.1 ± 3	82 ± 5.5	81 ± 4.7

PS, particle size; PDI, poly dispersibility index; ZP, Zeta potential.

Pharmacokinetic data shows sustained release and prolonged plasma exposure of amikacin in liposome form when compared to free amikacin sulfate. Free amikacin is fully cleared within 4 hours compared to 8 hours after intravenous administration of liposomal amikacin. Pharmacokinetic parameters detailed in Table 6 reveal greater C_{max} and AUC values and lower rates of clearance for the liposomal amikacin formulation when compared to the free amikacin sulfate formulation.

In a related study, the *in vivo* pharmacokinetics of amikacin liposomes was assessed in primates and determined the renal clearance to be 100-fold less than free amikacin. Liposomal amikacin had a longer plasma half-life ranging between 22.9–81.7 hours compared to free amikacin sulfate [86]. In rats, the reported half-life was 0.2 hours, whereas in humans it was 2.5 hours, requiring frequent dosing to maintain therapeutic concentrations in plasma [86, 87]. The pharmacokinetics demonstrated in the study by Maxwell *et al* and from prior studies reveal longer half-life, reduced clearance and a greater maximum plasma concentration for

amikacin liposomes showing that administration of amikacin sulfate using liposomes is suitable for sustained release and therapeutic activity at lower doses than the free amikacin formulation [84].

Currently, no generic versions of Arikayce® are available. The product was recently approved in 2018, and patents and exclusivities were filed to provide market protection for Arikayce® beyond its patent term to delay submission of generic drug applications. Orphan drug exclusivity (ODE) was filed for 7 years from approval year and is set to expire September 28, 2025. However, due to the rarity of the disease, GAIN exclusivity was also filed and added to the ODE for an additional 5 years of protection to prevent generic approvals until 2030. The first patent expired June 6, 2025 for its indication and the final patent is set to expire in January 2034.

1.2.3 Research Scope and Chapter Overviews

1.2.3.1 Summary

Five complex, liposomal drug products approved by the U.S. FDA for various indications were discussed, three of which has at least one generic approved within the last year. Despite differences in structure, lamellarity, morphology and route of administration among these products, similarities in the quality characteristics deemed relevant for formulation evaluation and quality control in manufacturing remained relatively consistent per recommendations provided in product-specific draft guidance documents released by the FDA. The most common characteristics included liposome composition, drug and lipid concentration, particle size, electrical surface charge, *in vitro* release rates, state of the encapsulated drug and/or the amount of free and encapsulated drug. Standard analytical characterization techniques (HPLC, DLS, DSC, TEM, IVRT etc) were used to evaluate each quality parameter using validated methods developed by researchers to characterize multiple batches of approved formulations from reference and generic manufactures to understand the subtle variations in processing, and some with meaningful differences introduced to study the impact of processing effects on *in vitro* drug performance.

The scope of this dissertation will focus on using Doxil® as our model drug to develop a physicochemical framework to support the *in vitro* and *in vivo* evaluation for generic development of similar, follow-on liposomal versions. Given the availability of preclinical and clinical data for Doxil® as the first liposomal drug approved by the FDA, its increasing generic

count, and lessons learned since development of Doxil® thirty years ago by Gabizon and colleagues [88], we seek to derive deeper insights and understandings about the critical quality attributes in processing that influence *in vitro and in vivo* liposomal drug performance to address the disparity between therapeutic performance of bioequivalent, complex liposomal generic products and their reference drug products to support complex liposomal generic drug development.

1.2.3.2 Chapter Overview

Chapter 2 will discuss the analytical methods developed to reverse engineer several batches of the reference Doxil® formulation and apply the same methods for characterization and comparative analysis of the physicochemical profiles of Doxil® and its FDA-approved, generic drug products. Analytical methodologies were established and validated for doxorubicin liposome characterization of particle size, zeta potential, drug and lipid concentration, drug and lipid impurities, and amount of free non-encapsulated doxorubicin. *In vitro* drug release was quantified using a previously validated in-house method, and morphology and nanostructure characterization was conducted in collaboration with the University of Michigan Life Sciences Institute CryoEM Core Facility and Lawrence Berkeley National Laboratory. The methods developed in this work served as a baseline for subsequent quantification methods for assay development and evaluation in Chapters 3 and 4.

Chapter 3 will discuss the development of single-vial drug release assay utilizing Bio-Bead SM-2 resin as a novel sink agent to evaluate the dissolution profile of doxorubicin liposomes. *In vitro* release testing is a critical measure of drug performance is crucial in generic development for formulation evaluation and quality control. The FDA and the United States Pharmacopeia (USP) outline a set of guidelines and regulations for the development of robust, reproducible assays evaluating drug release that were applied for this non-compendial system. The developed assay is based on rotational agitation using a rotator mixer, and assay conditions were optimized for Biobead weight for sink condition, release media, incubation temperature, and agitation speed. The method was assessed for discriminability and method robustness using commercial and stressed Doxil® formulations. Further optimization of the method is being explored to improve the discriminatory capability of the method to distinguish between formulations of the same composition with meaningful differences in processing methods. Overall, over 90% of doxorubicin is released from Doxil® liposomes within 24 hours under

varied assay conditions. When fully optimized and validated, this method has the potential to be a highly robust, cost-effective and simple tool for rapid evaluation of generic doxorubicin liposome products, helping to expedite formulation evaluation and optimization to support ANDA approvals for complex liposomal generic products.

Chapter 4 will discuss implications of the reliability of *in vitro* dissolution results related to the extent and rate of kinetics of drug adsorption to microtubes used in dissolution testing. Recently, it was discovered that certain drugs have a propensity for certain materials in different conditions that prevent complete drug recovery for sterols in neighboring labs. Upon further investigation, discrepancies in mass balance suggested drug adsorption to different plastic materials as the cause of incomplete drug recovery in their unpublished studies. Relatedly, Chapter 4 discusses the investigation into the critical parameters influencing the extent and rate of doxorubicin adsorption to microtubes using in *in vitro* release testing to evaluate the propensity of drug adsorption that could adversely affect the reliability of the dissolution results through invalidated mass balance. Solubility of doxorubicin hydrochloride was investigated in several solvents, and a suitable testing concentration was selected for the study. Test parameters included concentration, temperature, agitation speed, surface area, tube material, media composition for 6 different microtube brands/types and the time-dependent rate of adsorption kinetics was evaluated under standard dissolution assay conditions used in Chapter 3.

Chapter 5 discusses the broader context of this work and the implications for future studies. Chapter 2 is published in *The AAPS Journal*. Chapter 3 and 4 are under preparation for publication.

Chapter 2 A Comparative Study on Physicochemical and Analytical Characterizations of Doxil® and its Generic Drug Products

2.1 Abstract

Doxil®, a PEGylated liposomal doxorubicin (DOX) hydrochloride suspension, was the first liposome drug product approved by the U.S. Food and Drug Administration (FDA). Although off-patent, limited generic products have been approved due to challenges in achieving bioequivalence compounded by manufacturing complexity. Regulatory agencies require generic drug products to be bioequivalent to the reference listed drug. In this regard, we developed various analytical methods to analyze Doxil® and its generic drug products for multiple attributes, including liposome size distribution, zeta potential, DOX content, lipid content, purity, non-encapsulated doxorubicin, morphology, nanostructure similarity, and quantified *in vitro* release.

Batch-to-batch variation exists across attributes for different formulations. Minor differences in particle size and zeta potential were observed. Cryo-TEM imaging reveals the distinct coffee bean shape and morphology of the Doxil® liposome. SAXS similarity analysis shows a distinct difference in nanostructure for Dr. Reddy's formulation compared to the innovator formulation. Still, it is revealed to be a consequence of liposome uniformity and homogeneity as depicted in cryoTEM images. Several methods developed in this work can be complementary to provide a more thorough physicochemical analysis for generic evaluation. Size, morphology, and nanostructure evaluated by DLS, cryo-TEM, and SAXS should be readily employed to assess physicochemical similarity. Content, impurity identification, and amount of free non-encapsulated DOX are used to evaluate formulation sameness. The methods developed in this work provide a physicochemical framework for analytical comparison of complex liposomal generics and may support subsequent development efforts to improve generic drug availability for patient populations in need.

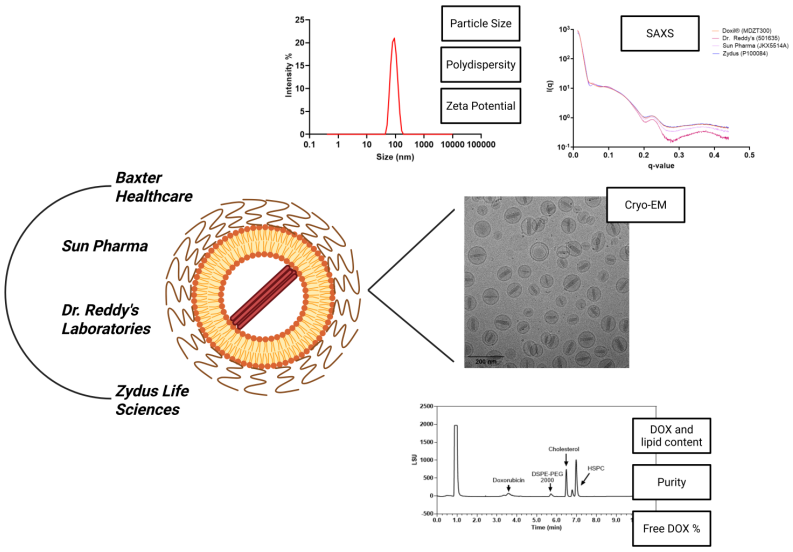

Figure 24. Chapter 2 Graphical Abstract

2.2 Introduction

Doxil® is a liposomal doxorubicin (DOX) hydrochloride suspension intended for intravenous infusion approved in 1995 by the United States (U.S.) FDA [89]. As the premier liposomal drug product, Doxil® became a highly sought-after product for generic development upon patent expiration in 2010. The global market for liposomal DOX has grown exponentially over the last decade. In 2020, the market was estimated at US $992.8 million and projected to reach US $1.3 billion in 2026, but the projection was actualized earlier as of 2024 [89]. The global market for liposomal DOX is currently estimated at US $1.28 billion and is expected to increase at a compound annual growth rate of 6.3% over the next decade [7]. In 2034, the projected market value is expected to nearly double to an estimated $2.37 billion [7]. An increase in the generic availability of liposomal DOX has been noted as a significant agent influencing the sales of liposomal DOX formulations, in addition to several advancements in developing and optimizing nanodrugs as chemotherapeutic medications.

However, developing generic drug products for Doxil® is challenging due to its manufacturing complexity and its direct correlation to *in vitro in vivo* bioequivalence. Minor variations in processing are known to significantly affect the physiochemical properties of liposomal drug products, and subsequently, drug performance [90]. Parameters such as liposome size, zeta potential, drug and lipid composition, the quantity of degradation products, and *in vitro* leakage are among some of the essential attributes for liposomal generic development as detailed in the FDA draft guidance for liposomal doxorubicin hydrochloride formulations [10].

Additional considerations for manufacturing should include *in vitro* measures to prove bioequivalence of the generic formulation to the reference listed drug (RLD) and be included in the submission of abbreviated new drug applications (ANDA). According to the FDA, a generic formulation is considered bioequivalent if it is qualitatively (Q1) and quantitatively (Q2) the same in comparison with the RLD and possesses physicochemical similarity (Q3). Q3 should demonstrate that the physical arrangement of matter in the formulation, characterized by nanostructure, is similar to the RLD. Q1/Q2(Q3)-compliant generics require extensive *in vitro* and *in vivo* evaluation, however, the FDA describes in the Code of Federal Regulations (21 CFR 320.22, 21 CFR 320.24) that different types of evidence may be used to establish bioequivalence between a generic and reference product [11, 12]. A waiver of evidence for *in vivo* bioequivalence for generic drug products that meet specific criteria can be obtained using sufficient *in vitro* data [11].

In this work, we developed a series of methods using techniques commonly employed for standard characterization of liposomal formulations to evaluate the similarities and differences of several approved generic, liposomal DOX products with the RLD. Comparative analysis of the measured *in vitro* physicochemical properties for different approved liposomal DOX formulations can inform formulators of the specification ranges deemed acceptable for the assessment of critical quality attributes (CQA) in subsequent development efforts [49, 65].

Few liposomal DOX generics have been successfully developed and approved by the U.S. FDA. Approved generic formulations include those from Sun Pharmaceuticals (Goregaon, Mumbai, India), Dr. Reddy's Laboratories (Hyderabad, Telangana, India), Zydus LifeSciences Global FZE (Ahmedabad, Gujarat, India), and Ayana Pharmaceuticals (Jerusalem, Israel) [91]. The work described in this manuscript details the physicochemical characterization and analytical comparison of the innovator (Baxter Healthcare) and generic liposomal DOX formulations developed by Sun Pharmaceuticals, Dr. Reddy's Laboratories, and Zydus LifeSciences.

Table I lists the drug vendor/manufacturer, batch number, and expiration date for each formulation tested. Few reports in literature detail a comparative physicochemical analysis for each generic, liposomal DOX formulation in reference to the RLD. Approval of generic, liposomal doxorubicin hydrochloride injection developed by Ayana Pharmaceuticals was approved in 2021 and was not available for purchase from our university pharmacy for testing

during our study period. Therefore, our work describes quantitative information about the physicochemical nature of each generic formulation, excluding Ayana Pharmaceuticals, and highlights the stability of formulations during their shelf-life that may impact *in vitro* drug performance.

Table 8. Sample inventory.

Vendor	Batch No.	Expiry Date
Doxil® (Baxter Healthcare)	KGZTG01	Feb 2022
	KIZTI00	Apr 2022
	KJZU901	May 2022
	LJZTS00	May 2023
	MDZT300	Nov 2023
Dr. Reddy's Laboratories	501451	Feb 2022
	501630	May 2022
	501635	Aug 2023
	501693	Aug 2023
Sun Pharmaceuticals	JKX5514A	May 2022
	HAC1612A	Sep 2022
Zydus Pharmaceuticals	P100084	Feb 2022

We developed several physicochemical assays using dynamic light scattering (DLS) and ultra performance liquid chromatography (UPLC) methods for accelerated evaluation and characterization of the following attributes of Doxil®: drug and lipid content, size distribution, zeta potential, free non-encapsulated doxorubicin present in each liposomal formulation, degradation products, and drug and lipid impurity profiles. We expanded our characterization to include properties and analyses relevant to determining the microstructure of liposomal formulations, such as morphology via cryogenic transmission electron microscopy (cryo-TEM) and structural similarity using small angle X-ray scattering (SAXS). Finally, we assess *in vitro* drug performance using an *in vitro* dissolution method to characterize release rates across manufacturers compared to the reference product. Using this framework, we can assess the *in*

vitro physicochemical similarity of generic, liposomal formulations with the same composition developed by different manufacturers in reference to the RLD.

Thus, the objective of the present research was to compare the physicochemical similarity of Doxil® with each FDA-approved generic, liposomal DOX formulation available on the market during the time of study. Existing literature only compares one generic formulation with the RLD, and we seek to evaluate the similarities and differences of several approved generic, liposomal DOX products with the RLD. This research provides measured specification ranges to evaluate the *in vitro* physicochemical sameness of the CQAs measured in formulations of the same composition, which were developed by different manufacturers. From this work, the current knowledge of the CQAs associated with developing Q1/Q2(Q3) compliant generic formulations can be expanded to encourage subsequent development and approvals of generic products.

2.3 Materials

Doxil® was manufactured by Baxter Healthcare (Deerfield, IL, USA) and Doxorubicin Hydrochloride Liposome Injection formulations (2 mg/mL) manufactured by Sun Pharmaceuticals (Goregaon, Mumbai, India), Dr. Reddy's Laboratories (Hyderabad, Telangana, India) and Zydus LifeSciences Global FZE (Ahmedabad, Gujarat, India) were purchased from the University of Michigan Hospital Pharmacy. Daunorubicin hydrochloride was purchased from Sigma Aldrich (St. Louis, MO, USA). Doxorubicinone and daunorubicinone were purchased from Cayman Chemical (Ann Arbor, MI, USA). Hydrogenated soy phosphatidylcholide (HSPC) and 1,2-distearoyl-sn-glycero-3-phosphoethanolamine-N-[amino (polyethylene glycol)-2000] (ammonium salt) (DSPE-PEG 2000) were purchased from Lipoid GmbH (Ludwigshafen, Germany). Lyso-PC (16:0) and Lyso-PC (18:0) were purchased from Avanti Polar Lipids (Birmingham, AL, USA). Cholesterol and ammonium acetate were purchased from Sigma Aldrich (St. Louis, MO, USA). Poly-Prep chromatography columns (Cat No. 731-1550 and 731-1553) were purchased from Bio-Rad Laboratories (Hercules, CA, USA). TOYOPEARL HW-55F resin in ethanol was purchased from Tosoh Bioscience (Grove City, OH, USA). Holey carbon grids (R 1.2/1.3, 300 Mesh, Copper) were obtained from Quantifoil (Großlöbichau, Germany). Round cryo grid boxes with lids were obtained from MiTeGen (Ithaca, NY, USA). C-clips and c-clip rings were purchased from Thermo Fisher (Waltham, MA, USA). Liquid nitrogen and dewars were provided by the University of Michigan Life Sciences Institute Cryo-

EM Core Facility (Ann Arbor, MI, USA). Axygen 96-well full-skirt clear PCR microplate and nonsterile, 96 Round Well Sealing Mat for PCR microplates were purchased from Corning (Corning, NY, USA). All other solvents and reagents were of analytical grade and were purchased from Fisher (Waltham, MA, USA).

2.4 Methods

2.4.1 Particle Size

Particle size was measured using the Malvern ZetaSizer Nano ZSP (Worcestershire, England, UK). Liposomal doxorubicin samples were diluted 10-fold in deionized water and transferred to Plastibrand® semi-micro disposable cuvettes (BRAND GMBH, Wertheim, Germany) for analysis. Water and liposome were selected as the dispersant and material, respectively, and the measurement temperature was 25°C. The refractive index for water and liposome were set to 1.33 and 1.45. The viscosity was 0.8872 cp for water at 25°C and sample equilibrium time was set to 120 seconds. All samples were measured in triplicates, and the particle size data obtained was zeta average, an intensity-based harmonic mean, plotted as a function of intensity (%) versus particle size (nm). Particle size data was directly obtained from the built-in software.

2.4.2 Zeta Potential

Zeta potential measurements were performed using the samples prepared for particle size analysis. A 1 mL syringe was used to handle and transfer the sample solution from semi-micro disposable cuvettes to DTS1070 folded capillary cells (Malvern Panalytical Ltd, England). Sufficient volume of solution covered the electrodes on both sides of the capillary cell. Zeta potential was measured using the Malvern ZetaSizer Nano ZSP under the same system parameters for the particle size method and the dielectric constant was set to 78.5. Data was reported in millivolts.

2.4.3 Doxorubicin Content

DOX content was quantified using ultra performance liquid chromatography (UPLC). An Acquity UPLC-TUV detector system with Empower 3 software was used with a BEH C18 column (100 × 2.1 mm, 1.7 μm) (Waters Corporation, Milford, MA, USA) under isocratic conditions consisting of deionized water with 0.1% formic acid as aqueous solvent (A), and

methanol with 0.1% formic acid as organic solvent (B). Liposomal DOX samples were diluted 100-fold in methanol. A 45% to 55% ratio of mobile phase for solvent A to B was employed. Flow rate was set to 0.3 mL/min, injection volume was 10 µL, detection wavelength was 254 nm, and the run time lasted 15 minutes. A method description for standard curve generation is provided in Appendix A.

2.4.4 Lipid Content

Lipid concentration was quantified using an Acquity UPLC with an evaporative light scattering detector (ELSD) system with Empower 3 software (Waters Corporation, Milford, MA, USA). A gradient mobile phase was used to separate HSPC, DSPE-PEG (Mw 2000) and cholesterol, and consisted of two solvent systems: A) a mixture of 40% v/v deionized water and 60% v/v methanol with 10 mM ammonium acetate buffer pH 6.4, and B) a mixture of 90% v/v isopropanol and 10% v/v methanol with 10 mM ammonium acetate buffer pH 6.4. The 10 mM ammonium acetate buffer was prepared by adding 77 mg of ammonium acetate to 100 mL of deionized water, and the pH of the solution was adjusted to 6.4.

Liposomal DOX samples were diluted 40-fold in methanol and vortexed to mix. An Xbridge C18 column (4.6 x 150 mm, 3.5 µm) (Waters Corporation, Milford, MA, USA) was used to separate the lipids. The flow rate and column temperature were set to 1 mL/min and 45 °C. Injection volume was 10 µL and the run time was 15 min. ELSD gas pressure was set to 40 psi, data rate was set to 10 points per second and the temperature of the drift tube was set to 55 °C. Gain was set to 150 and the nebulizer was set to heating at 45%. Compressed gas was used for ELSD operation. A method description for the gradient and standard curve generation is provided in Appendix A.

2.4.5 Doxorubicin Purity

Another UPLC-TUV method was developed to identify DOX impurities. The mobile phase consisted of two solvents: A) deionized water with 0.1% formic acid, and B) a mixture of 80% v/v acetonitrile and 20% v/v methanol with 0.1% formic acid. Daunorubicin hydrochloride, doxorubicinone, and daunorubicinone are designated as doxorubicin process and product-related impurities by the United States Pharmacopeia (USP). Liposomal DOX samples were prepared by diluting the samples 10-fold in methanol. A UPLC BEH C18 column (100 × 2.1 mm, 1.7 µm) was used to separate impurities from doxorubicin. Column temperature and flow rate were set to

35 °C and 0.5 mL/min. An injection volume of 10 µL, run time of 10 minutes, and dual detection wavelengths (220 and 254 nm) were used to identify doxorubicin and impurity peaks. The relative retention time (RRT) for each impurity standard in reference to the doxorubicin standard was calculated and impurities were identified by assigning corresponding peaks in each sample based on standard RRT ± 5%. Doxorubicin and impurity concentration were calculated using the linear regression equation from the standard curve (Appendix A).

2.4.6 Lipid Purity

Lipid purity was determined using a UPLC assay with an evaporative light scattering detector (ELSD) under the same conditions detailed in section 2.2.4. Lysophosphatidylcholine (Lyso-PC) 16:0 and 18:0 are two common lipid degradants from hydrolysis that often occurs in dissolution. Impurity stock solutions (1 mg/mL) were prepared in methanol and diluted to 0.05 mg/mL. Liposomal DOX samples were diluted 40-fold in methanol. The UPLC-ELSD method for lipid purity was performed and a doxorubicin standard was spiked with Lyso-PC (16:0) and Lyso-PC (18:0) to identify the retention time of each impurity peaks in our sample. The concentration of each lipid impurity was quantified by calculating the percentage ratio of peak area for the lipid impurity to the cumulative lipid peak area.

2.4.7 Free, Non-Encapsulated Doxorubicin in Liposomal Formulations

Separation of free, non-encapsulated DOX from liposomal DOX was achieved using size exclusion chromatography. Poly-Prep columns were washed with methanol and water. 600 µL of TOYOPEARL HW-55F resin (in ethanol) was added to the column and installed on a vacuum manifold processing station. Excess water was drained from the columns before loading the sample and the resin surface was kept flat. Liposomal DOX (10 µL) was carefully added to the resin surface. A free DOX solution (20 µL) prepared at a concentration of 1 mg/ml in methanol was loaded onto an equivalent resin bed volume (600 ul) for equivalent measurement of free doxorubicin recovery. Deionized water (400 µL) was slowly added to the column and the wash solution was collected under vacuum into a microtube. The water wash was repeated three times and 1.2 mL of water wash solution was collected. Next, 400 µL of a 50:50 acetonitrile/methanol solution was slowly added to the column. The same wash procedure was performed using the organic solution and 1.2 mL of organic wash solution was collected. The wash solution tubes were transferred to a nitrogen evaporator set to 50 °C to dry the samples. Dry sample residues

were reconstituted with 250 µL of methanol. A reference sample was prepared by adding 240 µL of methanol to 10 µL of liposomal DOX. Samples were transferred to UPLC vials and free, non-encapsulated doxorubicin content was quantified using the previously developed UPLC-TUV method described in section 2.2.5. Free doxorubicin content was calculated using the following equation:

$$\%\ Free\ Doxorubicin = \frac{Peak\ Area\ of\ DOX\ in\ test\ sample}{Peak\ Area\ of\ DOX\ in\ reference\ sample} \times 100 \qquad \text{(Eqn. 1)}$$

2.4.8 Cryogenic Transmission Electron Microscopy (Cryo-TEM)

Doxorubicin liposome morphology was determined utilizing the cryo-TEM technique in collaboration with the University of Michigan (U-M) Life Sciences Institute (LSI) CryoEM Core Facility. Liposomal DOX formulations at a doxorubicin concentration of 2 mg/mL were plunged frozen in liquid ethane cooled to freezing point in liquid nitrogen using a Vitrobot plunge freezer (ThermoFisher Scientific, Waltham, MA, USA). 3 µL of liposomal DOX samples were deposited onto glow-discharged (PelcoEasiGlow discharger) Cu 300 R 1.2/1.3 holey carbon grids (Quantifoil, Großlöbichau, Germany) and samples were frozen on the grids using the following Vitrobot parameters (10 second wait time, 5 second blot time, 100% humidity, 4°C). Samples were visualized under cryogenic conditions on a Talos Arctica (ThermoFisher Scientific, Waltham, MA, USA) operated at 200 kV. Images were recorded using a Gatan K2 Summit direct electron detector (Gatan, Pleasanton, CA, 94588) in counting mode at 17.5 kx magnification, corresponding to a pixel size of 2.48 Å/pixel. SerialEM v4.1 was used to control microscope and camera functionality [10,11]. The exposure time was set to deliver 20 electrons/Å2 cumulative dose to the area of interest. Representative images of each sample were recorded from the center of the holes. FIJI/ImageJ was used to manually measure particle dimensions of length, width, and membrane thickness using a minimum sample size of 500 liposomes [92].

2.4.9 Small Angle X-Ray Scattering (SAXS)

The SAXS technique was used to characterize the microstructure similarity of DOX liposomes present in liposomal DOX formulations developed by different manufacturers. Microstructure was analyzed using the high-throughput SAXS technique (HT-SAXS) and similarity between batches was compared using the SAXS Similarity tool developed and conducted by the SIBYLS Beamline (12.3.1) of the Advanced Light Source at the Lawrence

Berkeley National Laboratory (Berkeley, CA, USA), supported by the US Department of Energy and National Institutes of Health [93]. Liposomal DOX samples were added to an AXYGEN 96-well full-skirt clear PCR microplate with a consistent volume of 30 µL of buffer and sample at three concentrations between 1-10 mg/mL. Labeled concentration for liposomal doxorubicin hydrochloride formulations is 2 mg/mL. Therefore, the following concentrations were prepared for SAXS analysis: 1 mg/mL (low concentration), 1.5 mg/mL (medium concentration) and 2 mg/mL (high concentration).

Buffer preparation is critical for SAXS analysis as it can impact the scattering profile of the sample. The prepared formulation buffer should be as closely resemblant of the buffer present in the original sample. Therefore, the prepared formulation buffer was comprised of a 9.4% sucrose solution with 1.55 mg/mL histidine at pH 6.5 similar to the buffer used in the manufacturing of the commercial formulation. 100 mL of buffer was prepared by adding 9.4 g of sucrose and 155 mg of L-histidine to deionized water. The pH of the solution was adjusted to 6.5 with 1 N of sodium hydroxide and/or hydrochloric acid. Prepared buffer and sample solutions were transferred to two 96-well PCR microplates, sealed, and kept under cold conditions prior to analysis by the SIBYLS Beamline at the Lawrence Berkeley Laboratory.

2.4.10 In Vitro Dissolution

In vitro dissolution testing provides critical information to characterize the rate and extent of drug release from a finished dosage form, which can be correlative of *in vivo* drug performance. From a regulatory perspective, dissolution testing is used in formulation evaluation during product development for batch-to-batch quality control and assurance [94]. A dissolution method with discriminative capability, capable of characterizing release profiles of formulations of the same composition but from different manufacturers when compared to the reference product, is crucial to assess a product's performance and efficacy. Yuan et al developed a conventional release method using dialysis membranes and the referenced method was employed in the present work to evaluate dissolution profiles for one batch per manufacturer [53].

Briefly, 0.8 mL of each liposomal DOX formulation (C DOX = 2 mg/mL) was added to 300 kDa Float-a-lyzer dialysis tubes which were inserted into 50-mL centrifuge tubes containing 39.2 mL release media containing 100 mM ammonium bicarbonate, 75 mM MES buffer, 5% w/v hydroxypropyl-β-cyclodextrin, 5% w/v sucrose, 0.02% sodium azide at pH 6. The centrifuge tubes were placed on an orbital shaker (ThermoFisher MaxQ 6000) operating at 320 rpm speed

and incubated at 45°C. A free DOX solution was prepared with doxorubicin hydrochloride in the same release media at an equivalent concentration (C DOX = 2 mg/mL) as the liposomal formulation. 0.8 mL of the free DOX solution was added directly to a 50-mL centrifuge tube containing 39.2 mL of release media and was used as a positive control. At 0, 1, 2, 4, 8, 12, and 24 hours, 150 µL of release media was sampled for UV detection at 480 nm on a plate reader (Synergy NEO HTS Multi-Mode Microplate Reader (Bio-Tek) and replaced with an equal amount of fresh release media. Samples were prepared and analyzed in triplicate. The cumulative percent DOX release was calculated using the following equation:

$$Cumulative\ DOX\ release\ (\%) = \frac{C_{DOX}\ of\ liposome\ formulations}{C_{DOX}\ of\ free\ DOX\ control} \times 100\% \qquad \text{(Eqn. 2)}$$

2.5 Results

2.5.1 Size Characterization

We used dynamic light scattering (DLS) to determine the liposome size, size distribution and polydispersity index (PDI) for each batch formulation. All liposomal formulations were similar in liposome size on average around 90 nm using water as the diluent (Fig. 25a, Appendix Table 7). Particle size across all batches of the innovator formulation ranged between 86 – 95 nm, whereas the particle size across generic formulations was slightly smaller ranging from 84 – 90 nm (Appendix Table 7). Minor variations in PDI between innovator and generic formulations existed with PDI ranging from 0.045 ± 0.007 to 0.082 ± 0.035 (Fig. 25b, Appendix Table 7). The median PDI value was approximately 0.050 while batch no. MDZT300 from Baxter Healthcare (0.082 ± 0.035) and batch no. HAC1612A from Sun Pharmaceuticals (0.082 ± 0.015) showed the highest index value.

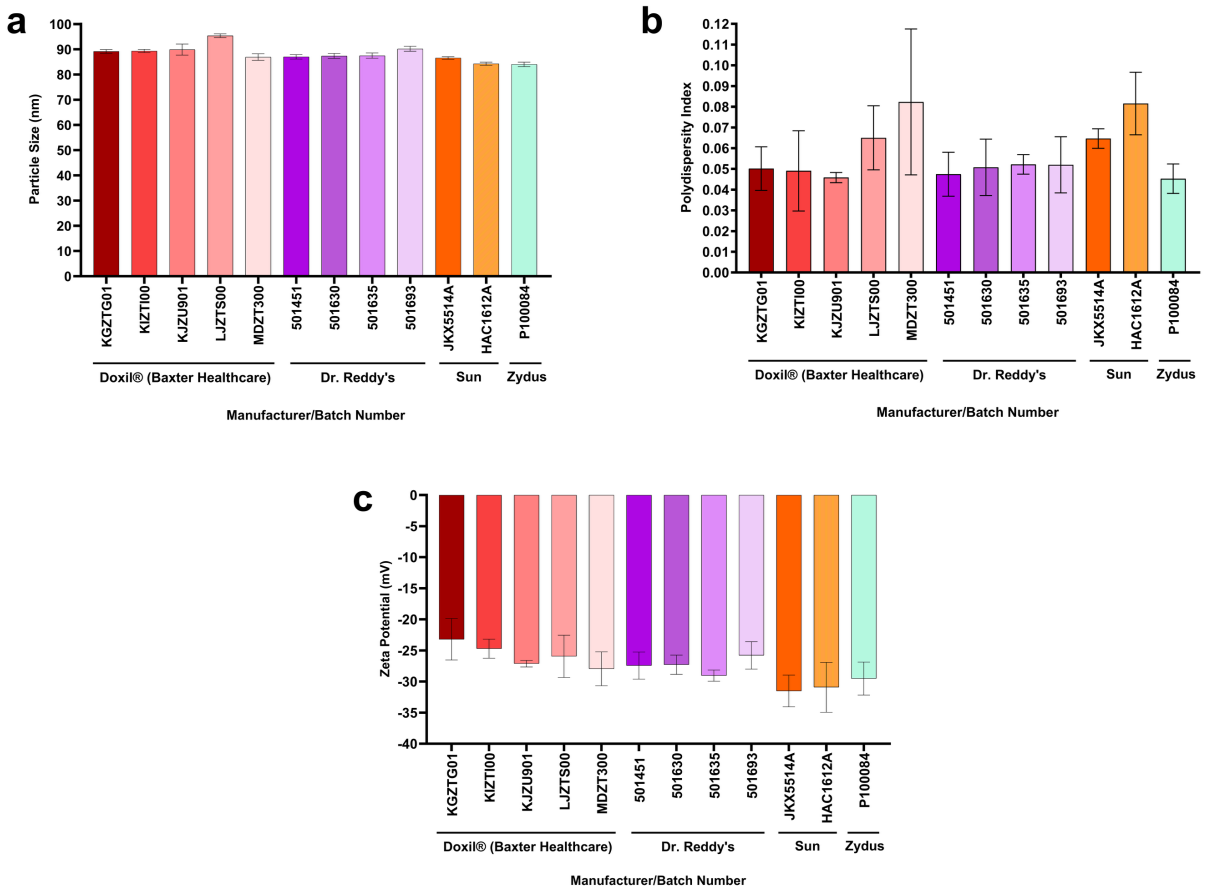

Figure 25. Size characterization of doxorubicin liposomes in formulation developed by innovator and different generic manufacturers: Baxter Healthcare, Dr. Reddy's Laboratories, Sun Pharmaceuticals and Zydus. a) Particle size, b) polydispersity index, and c) zeta potential was measured using the Malvern Zetasizer (mean ± SD, $n \geq 3$).

2.5.2 Zeta Potential

DLS was also used to determine the zeta potential of each formulation. The doxorubicin liposome possesses a negative surface charge that falls within –20 to –32 mV when diluted in water (Fig. 25c, Appendix Table 7). The most negatively charged formulation was developed by Sun Pharma (batch no. JKX5514A) with a zeta potential of –31.5 ± 2.5 mV. Batch-to-batch variation for innovator formulations ranged from –23.2 ± 3.34 mV to –27.9 ± 2.72 mV, and the least negatively charged liposomal formulation was batch no. KGZTG01. Minimal batch-to-batch variation in zeta potential existed between generic formulations, however, batch formulations developed by Sun and Zydus Pharmaceuticals measured were much more negatively charged than the innovator formulations. Dr. Reddy's batches fell between –25.8 ± 2.20 mV and –29.0 ± 0.90 mV, and Sun Pharma and Zydus batches were comparable, between –29.5 ± 2.65 mV and –31.5 ± 2.55 mV.

2.5.3 Doxorubicin & Lipid Content

Several ultra performance liquid chromatography (UPLC) methods for quantifying DOX and lipid ingredients were established. Label claim states that each vial of Doxil® contains 2 mg/mL of DOX hydrochloride, 9.58 mg/mL HSPC, 3.19 mg/mL of MPEG-DSPE, and 3.19 mg/mL of cholesterol [6]. Quantification was carried out on several batches of each product, and batch-to-batch variation falls within ± 5% of the label claim value. Measured DOX concentrations for innovator Doxil® formulations ranged between 1.94 ± 0.02 and 2.03 ± 0.06 mg/mL. Dr. Reddy formulations ranged between 1.97 ± 0.03 and 2.09 ± 0.06 mg/mL. Sun Pharma batch formulations #JKX5514A and #HAC1612A had measured DOX concentrations of 1.90 ± 0.04 and 1.91 ± 0.03 mg/mL, respectively, and Zydus batch formulation #P100084 had a measured DOX concentration of 2.09 ± 0.06 mg/mL (Fig. 26a, Appendix Table 8).

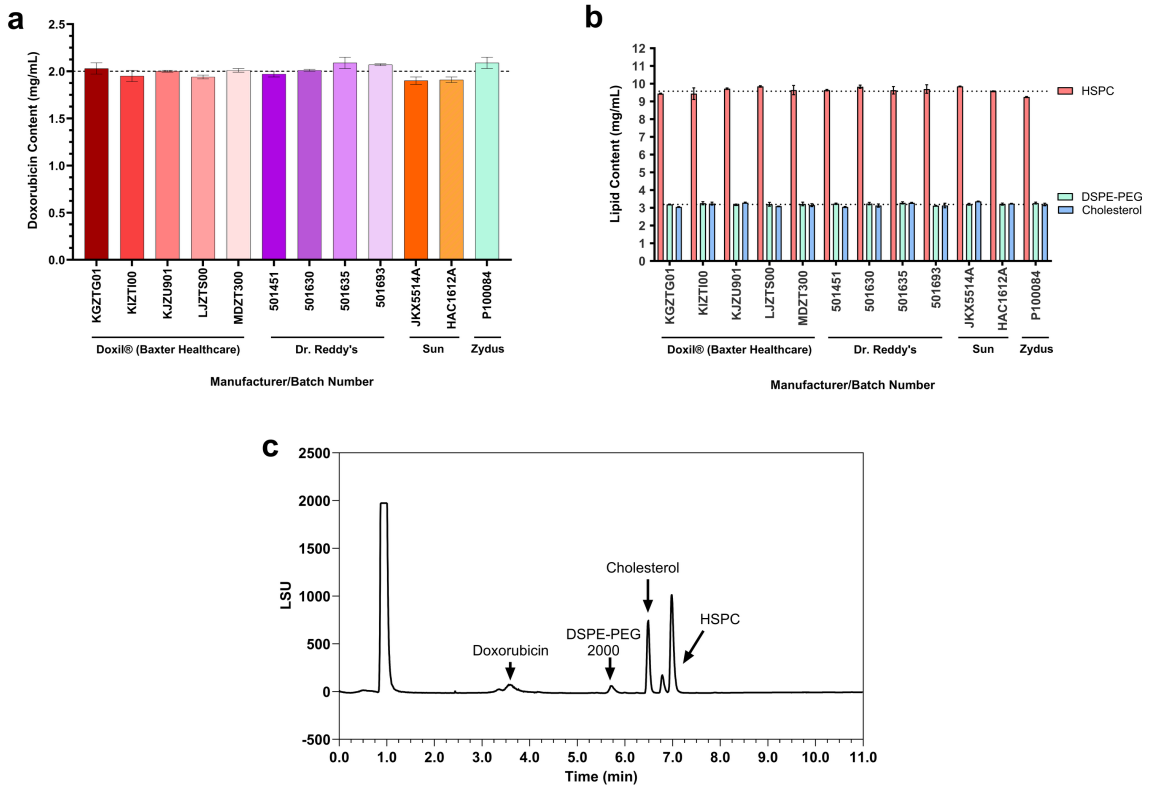

Figure 26. Measured doxorubicin and lipid content present in different liposomal preparations of doxorubicin hydrochloride produced by different manufacturers (mean ± SD, n = 3). a) Doxorubicin content, b) Lipid content for HSPC, DSPE-PEG (MW 2000) and cholesterol. **c**) Chromatographic separation of doxorubicin from lipid components using an UPLC-ELSD assay under a gradient mobile phase.

HSPC concentrations for innovator Doxil® formulations ranged from 9.44 ± 0.03 to 9.85 ± 0.04 mg/mL which fell within ± 5% of the label claim value (Fig. 26b, Appendix Table 8). Dr.

Reddy's batch formulations ranged from 9.63 ± 0.21 to 9.83 ± 0.09 mg/mL. HSPC content for Sun Pharma batch #JKX5514A and HAC1612A was 9.85 ± 0.02 and 9.58 ± 0.02 mg/mL, and HSPC content for Zydus batch #P100084 was measured at 9.25 ± 0.03 mg/mL (Fig. 26b, Appendix Table 8).

Cholesterol levels for innovator Doxil® formulations ranged between 3.05 ± 0.02 and 3.29 ± 0.03 mg/mL, which also fell within ± 5% of label claim concentration (Fig. 26b, Appendix Table 8). Cholesterol concentration for Dr. Reddy batch formulations fell within the same range from 3.05 ± 0.03 and 3.28 ± 0.03 mg/mL. Sun Pharma batch formulation #JKX5514A and #HAC1612A had measured cholesterol levels of 3.36 ± 0.02 and 3.24 ± 0.01 mg/mL, respectively, and Zydus batch formulation #P100084 had a measured cholesterol concentration of 3.19 ± 0.07 mg/mL (Fig. 26b, Appendix Table 8).

Measured DSPE-PEG (Mw 2000) concentration was comparable with label claim concentration (3.19 mg/mL), fell within acceptable limits of variation across all batch manufacturers and within a narrow range of measurement from 3.12 ± 0.02 and 3.26 ± 0.09 mg/mL (Fig. 26b, Appendix Table 8). Fig. 26c shows chromatographic separation and identification of lipids in reference to the elution profile of doxorubicin using the UPLC-ELSD method described in section 2.2 4. The initial peak in Fig. 26c corresponds to the sucrose/histidine buffer component present in the liposomal formulation.

2.5.4 Doxorubicin Purity

Greater than 99% DOX purity using the UPLC-TUV method was observed across innovator and generic batch formulations (Fig. 27a, Appendix Table 9). For innovator Doxil® formulations, impurity levels for doxorubicinone, daunorubicin and daunorubicinone ranged from 0.11 ± 0.20% to 0.33 ± 0.06%, 0.00 ± 0.00% to 0.18 ± 0.24%, and 0.00 ± 0.00% to 0.50 ± 0.07%, respectively (Fig. 27b-d, Appendix Table 9). The greatest impurity level measured for doxorubicinone is found in Sun Pharma batch #JKX5514A, HAC1612A and Zydus batch #P100084 at 0.67 ± 0.43%, 0.40 ± 0.35%, and 0.42 ± 0.24%, respectively (Fig. 27d, Appendix Table 9). In consideration of these results, method variability may be a probable cause for some variation; thus, the data should be interpreted with caution. Fig 27e shows a representative chromatogram of the elution profile for doxorubicin, daunorubicin, doxorubicinone and daunoribicinone at retention times of 5.50, 6.62, 6.83, and 8.37 minutes respectively.

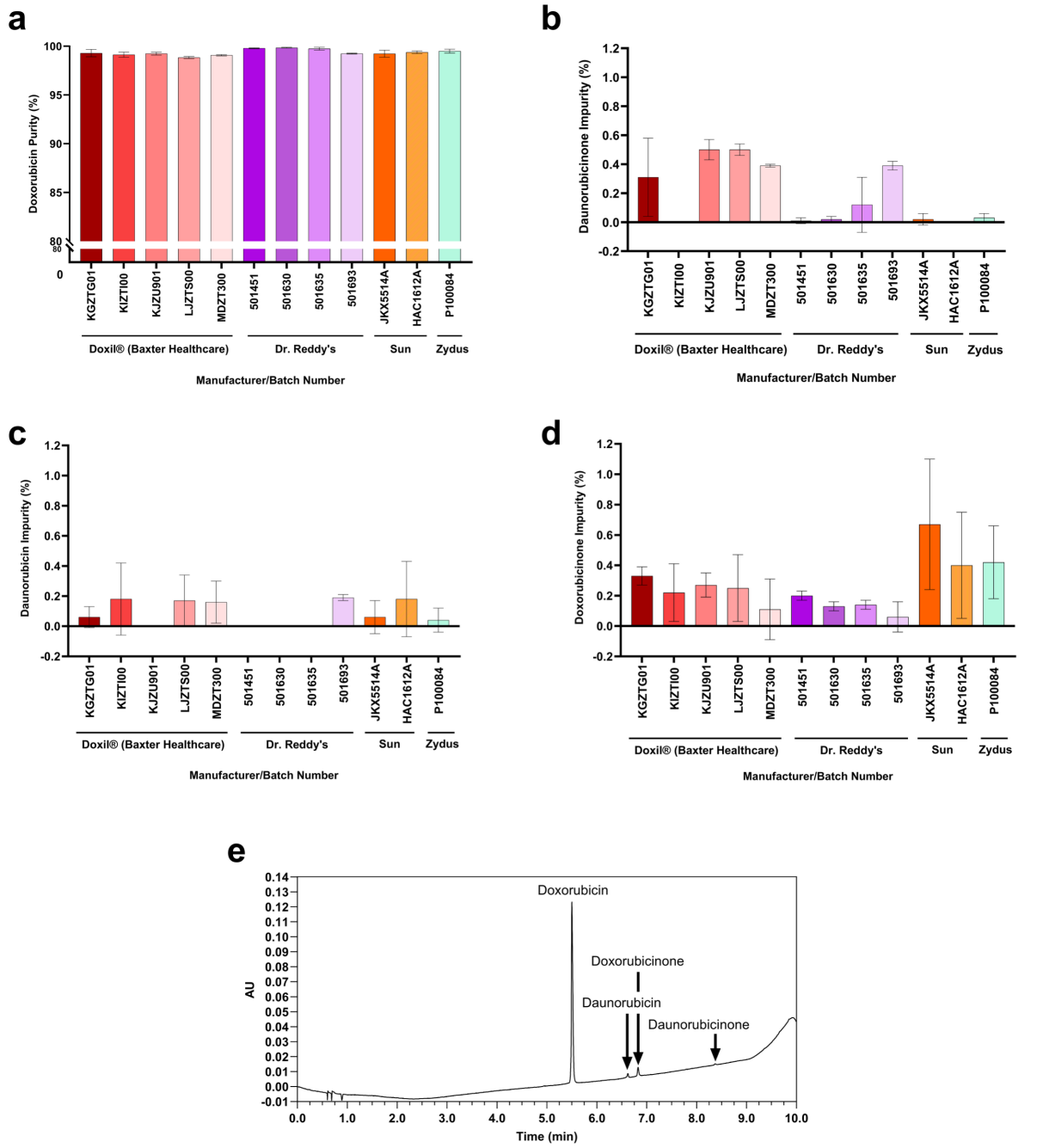

Figure 27. Purity of liposomal doxorubicin formulations quantified as a percentage of peak AUC over cumulative peak AUC in each sample using UPLC-TUV analysis. a) Doxorubicin purity (%), b) daunorubicinone impurity levels (%), c) daunorubicin impurity levels (%), d) doxorubicinone impurity levels (%), e) chromatographic separation of doxorubicin and the respective impurities (mean ± SD, $n = 3$).

2.5.5 Lipid Purity

Quantification of cumulative lipid impurities, lyso-PC 16:0 and 18:0, present in different liposomal DOX formulations ranged from 0.44 ± 0.21 to 2.21 ± 0.03 percent (Fig. 28a). The

elution of lyso-PC 16:0 and 18:0 standards compared with the chromatographic profile of Dr. Reddy's formulation in Fig. 28b shows lyso-PC 16:0 and 18:0 peaks that are slightly offset from the standards at low quantities in terms of peak area. We quantified the percentage of cumulative lipid impurity by calculating the ratio of cumulative impurity peak area to the cumulative lipid peak area.

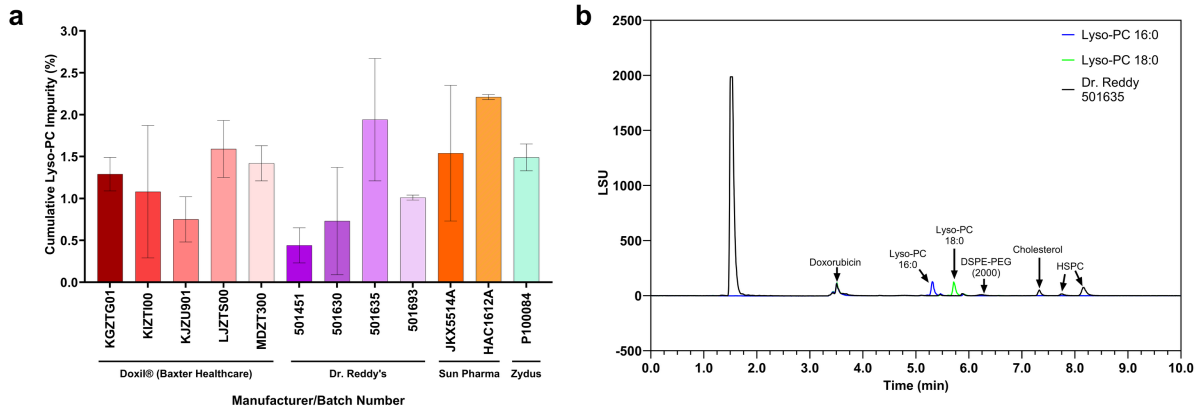

Figure 28. Quantification of lipid impurities in liposomal doxorubicin hydrochloride formulations. a) cumulative lyso-PC (16:0) and (18:0) impurities (mean ± SD, n ≥ 2). b) Chromatographic separation of lyso-PC (16:0) and (18:0) impurities in a representative, liposomal DOX sample manufactured by Dr. Reddy's Laboratories.

2.5.6 Free, Non-Encapsulated Doxorubicin in Liposomal Formulations

Varying levels of free, non-encapsulated doxorubicin were quantified in different liposomal formulations using the UPLC-TUV method described herein. All batches across manufacturers had non-encapsulated DOX levels less than 2%, ranging from 0.37 ± 0.04% for Sun Pharmaceuticals batch JKX5514A to 1.99 ± 0.03% for Dr. Reddy's batch 501451. The greatest level of non-encapsulated DOX present in Baxter formulations was 1.93 ± 1.01% for batch KIZTI00 whereas the amount of non-encapsulated DOX present in Zydus P100084 was 1.32 ± 0.92 % (Fig. 29, Appendix Table 10). The recovery of free doxorubicin hydrochloride loaded at an equivalent weight relevant for the test was 90.98 ± 0.18%.

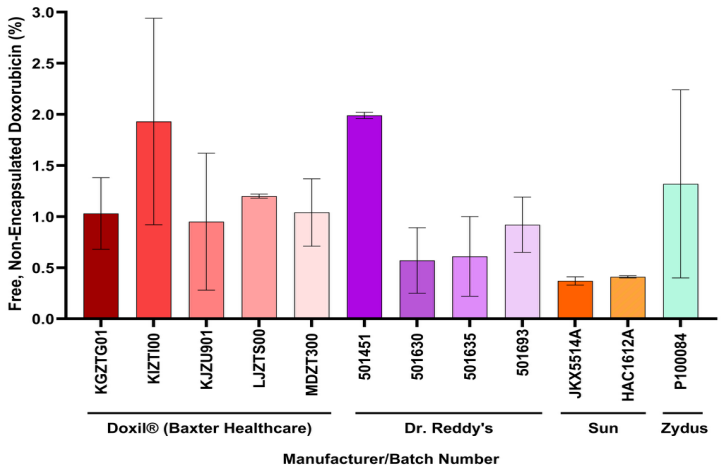

Figure 29. Quantification of free, non-encapsulated doxorubicin present in liposomal doxorubicin hydrochloride formulations produced by different manufacturers (mean ± SD, n ≥ 2).

2.5.7 Cryo-TEM

One representative batch of liposomal DOX was analyzed for morphology of the DOX liposome using the cryo-TEM technique, MDZT300 (Baxter Healthcare), 501635 (Dr. Reddy's), JKX5514A (Sun Pharmaceuticals), and P100084 (Zydus). The shape and morphology of the DOX liposome is consistent across formulations developed by each manufacturer. DOX liposomes possess a "coffee bean" like shape and thread-like filaments visible in the aqueous core of the liposome represent the insoluble, doxorubicin-sulfate crystal [95]. Differences in uniformity and homogeneity of particles can be directly observed in Fig. 8. While each formulation appears heterogeneous and less uniform, Dr. Reddy's batch no. 501635 (Fig. 30b) shows good uniformity of liposomes.

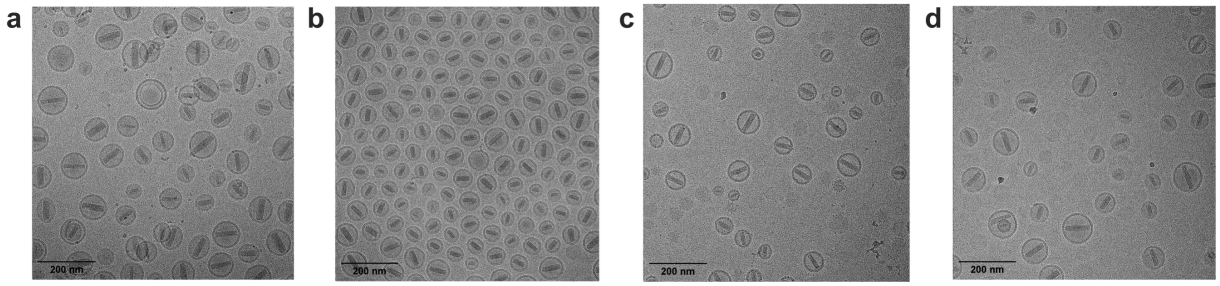

Figure 30. Morphology of the doxorubicin liposome from different formulations: a) Doxil® (batch no. MDZT300); b) Dr. Reddy's (batch no. 501635); c) Sun Pharmaceuticals (batch no. JX5514A); d) Zydus (batch no. P100084)

Appendix Table 11 describes the size dimensions and membrane thickness of doxorubicin liposomes measured manually via FIJI/Image J processing software (mean ± SD, n

≥ 500). The length of the DOX liposome from each formulation ranged from 60.9 ±15.1 nm to 73.3 ± 13.1 nm, whereas the width ranged between 57.6 ± 14.8 nm and 66.0 ± 13.0 nm (Appendix Table 11). Each generic batch imaged had dimensions that were smaller than those of the reference batch from Baxter. Sun Pharma was the smallest at a length and width of 60.9 ± 15.1 and 57.6 ± 14.8 nm, respectively. Membrane thickness was comparable between formulations between 4.5 ± 0.7 and 5.0 ± 0.4 nm among batches (Appendix Table 11). Appendix Figure 4 depicts the distribution histograms for the measured length and width of each formulation.

2.5.8 SAXS

For complementary analyses, SAXS scattering profiles were generated for the four liposomal DOX formulations imaged using the cryo-TEM technique (Fig. 31a). The scattering profiles were generated using the SAXS technique performed by the SIBYLS Beamline, Advanced Light Source (12.3.1) at the Lawrence Berkeley Laboratory. The data shown in Fig. 31b is matrix comparison of SAXS scattering profiles with formulations that are highly similar in structure clustered together in the upper left corner, while the most dissimilar formulations are clustered in the lower quadrants of a SAXS similarity map. The center diagonal compares each SAXS curve against itself, which results in perfect similarity agreement and zero radius of gyration, ΔR_G [96]. Our results demonstrate that the nanostructure of DOX liposomes developed by Dr. Reddy's is different from the innovator formulation and the generic formulations tested. Formulations developed by Zydus and Sun Pharma are more similar in nanostructure than the innovator formulation developed by Baxter Healthcare.

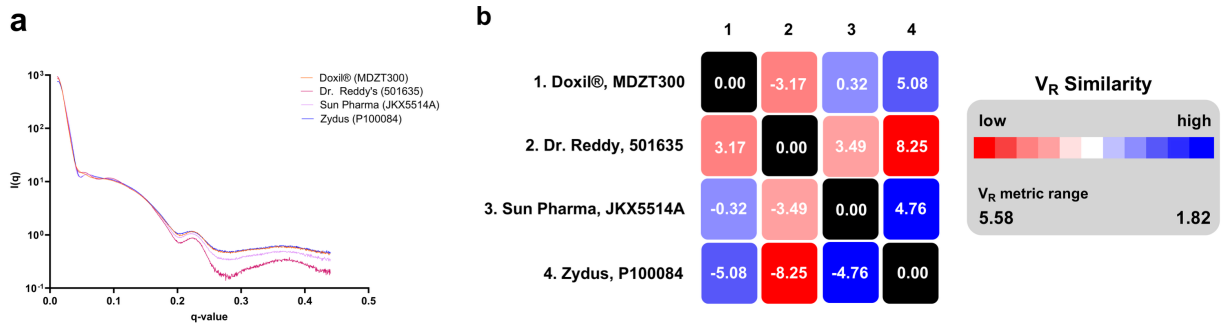

Figure 31. SAXS scattering profiles for a) one liposomal DOX formulation representative of each manufacturer (n = 4). b) Structural similarity between generic and reference, liposomal DOX formulations was compared and depicted using the SAXS similarity map (SSM) developed by SIBYLS at the Advanced Light Source (12.3.1), Lawrence Berkeley Laboratory. The Volatility of Ratio, V_R, correlation method was used to define similarity and dissimilarity between samples (mean ± SD, $n \geq 2$).

2.5.9 In Vitro Dissolution

To support the physicochemical evaluation of generic liposomal DOX formulations with the reference Doxil® formulation, we conducted dissolution testing using the conventional dialysis method published by Yuan and colleagues on an individual batch from each manufacturer in our sample inventory (Doxil® #KIZTI00; Dr. Reddy's #501630; Sun Pharma #HAC1612A; Zydus #P100084) (Fig. 32) [53].

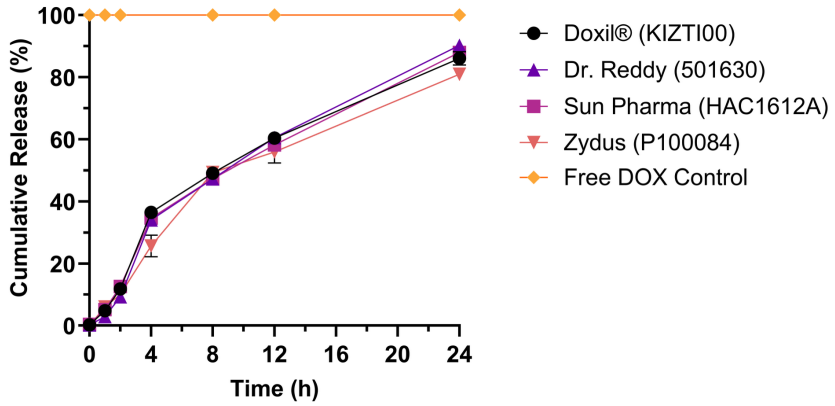

Figure 32. Characterization and comparison of *in vitro* dissolution profiles for individual batches of approved generic liposomal doxorubicin hydrochloride formulations with the reference Doxil® formulation (mean ± SD; n = 3)

Cumulative DOX release was 86.0 ± 2.12%, 90.2 ± 0.96%, 87.9 ± 1.00%, and 81.0 ± 1.31% for the batch formulations of Doxil®, Dr. Reddy's, Sun Pharma, and Zydus, respectively. We employed the f2 similarity test to evaluate the similarity of the dissolution profile of each generic formulation with the reference Doxil® formulation. f2 values for Dr. Reddy's (#501630), Sun Pharma (#HAC1612A) and Zydus (#P100084) compared to Doxil® (#KIZTI00) were 91.3, 92.2 and 89.8, respectively.

2.6 Discussion

Approval of ANDA submissions for generic, liposomal formulations are dependent upon the success of bioequivalence evaluation of the generic drug candidate. The FDA recommends *in vitro* and *in vivo* testing to establish bioequivalence as described in the draft guidance for liposomal doxorubicin hydrochloride [10]. Physicochemical characterization is critical for the evaluation of liposomal dosage forms as these properties dictate *in vivo* drug product behavior. Previous studies have identified critical quality attributes (CQA) relevant for drug performance in alignment with liposome characteristics detailed in the FDA draft guidance that should be equivalent to the reference listed drug in order for the generic drug candidate to become eligible

for bioequivalence studies [10, 23, 65, 90, 97]. These characteristics include liposome composition, size distribution, electrical surface potential, state of encapsulated drug, internal environment of the liposome, and *in vitro* leakage rates comparable to the reference standard [10].

Key attributes of Doxil® evaluated in this work included particle size, polydispersity, zeta potential, DOX and lipid content, DOX and lipid purity, the amount of non-encapsulated DOX present in the formulation, morphology, nanostructure and *in vitro* release. We identified these attributes as critical for *in vitro* drug performance for liposomal DOX formulations due to their *in vivo* implications related to drug safety and efficacy. Changes in size and zeta potential between generic and reference formulations may influence the stability, circulation and adsorption of the liposomal nanoparticle [98]. Our results confirmed the similarity of particle size and polydispersity between different products despite dilution in water which would subsequently decrease the 9.4% sucrose content of the liposomal formulations. Given that the formulation was diluted 10-fold by water, the final sucrose concentration was 0.94%. At such low concentration, sucrose has a minimal impact on the viscosity and refractive index of the solution. Thus, we sought to characterize particle size in water using the viscosity (0.8872 cP) and refractive index (1.330) of water at 25°C for size analysis via DLS.

For zeta potential, the pH of the dissolving media plays a crucial role as it influences ionization of the functional groups on the particle surface and ion distribution within the electrical double layer. At acidic conditions, these surface groups may become protonated which could reduce the net negative charge making the zeta potential less negative or even give a positive charge. At basic conditions, surface groups may become deprotonated which would increase the negative charge on the liposome surface [99, 100]. Diluting these liposomal samples in water at neutral pH reflected pH values that were very similar to the original, undiluted suspensions minimizing the impact on zeta potential. Differences in drug and lipid content can affect the drug-to-lipid ratio and consequently, membrane rigidity and liposome stability in plasma. Quantification of non-encapsulated DOX present in liposomal formulations can provide insight into the state of the drug in each formulation. The package insert states that greater than 90% of DOX is encapsulated in liposomes, however, an increase in non-encapsulated drug may present safety and toxicity concerns related to the free drug analog [101].

Morphology and nanostructure assessment utilizing electron microscopy and x-ray light scattering techniques is particularly useful for visualization and comparison of different liposomal formulations of the same composition. Qualitative visualization using cryo-TEM imaging complements quantitative characterization for assessing formulation similarity and *in vitro* bioequivalence evaluation. We observed the heterogeneous inner structure of the liposome, whose impact on drug performance may warrant further investigation as differences in nanostructure may impact the rate and extent of drug release. The liposomes imaged in Fig. 30B from the Dr. Reddy's batch display a greater degree of liposome uniformity in terms of size, shape, density and morphology when compared to the representative innovator Doxil® batch, as well as Sun Pharma and Zydus batches. Possible explanations for these differences may lie in minor processing differences in during liposome formation lending itself to increased uniformity of the liposome population. In this regard, the application of cryo-TEM can serve as a useful tool to evaluate liposome uniformity during the formulation development stage.

Selective characterization of these properties *in vitro* can highlight the similarities and differences between approved, generic and innovator formulations for liposomal dosage forms containing DOX and provide the rationale for future work to develop an *in vitro in vivo* correlation using drug release assays. Subsequent evaluation of *in vitro* release for individual batches from each manufacturer revealed similar cumulative release rates for Doxil®, Dr. Reddy's, Sun Pharma and Zydus formulations, suggesting a high degree in formulation sameness and physicochemical similarity necessary for bioequivalence evaluation. For liposomal formulations, dissolution testing can provide critical insights into the release kinetics of the active ingredient, and determination of a faster or slower release rate may adversely influence the product's performance and efficacy when considered among other physicochemical properties as a predictive correlation of *in vivo* performance.

This manuscript provides a framework for multiple tests which strengthens the comparative assessment between generics and innovator products. Although, the methods when repeated in our labs showed high reliability, additional research at other laboratories to confirm the integrity of the framework is useful. Cost of testing with the SIBYLS Beamline, Advanced Light Source at the Lawrence Berkeley Laboratory is not onerous as it is largely funded by the NIH and the DOE through the ALS-ENABLE and High-End Instrumentation grants. Other costs associated with sample preparation and shipping cold transport are with the originating

laboratory which otherwise makes this method to structurally characterize liposomal samples using HT-SAXS highly accessible. However, CryoTEM can be costly, requires extensive training and access to a core facility that offers or specializes in electron microscopy. CryoTEM and SAXS can be used as complimentary methods for structural characterization and comparative analysis of complex liposomal products, however, with subsequent model fitting and simulation, SAXS analysis can also be used to estimate size parameters in lieu of direct measurement from cryoTEM images.

2.7 Conclusion

In this work, we devised a series of analytical methods for the physicochemical characterization and comparison of DOX liposomes in formulations with the same composition developed by different manufacturers. Size distribution, zeta potential, drug and lipid content, impurity identification, free non-encapsulated DOX in formulation, morphology via cryo-TEM, microstructure via SAXS, and *in vitro* release were parameters assessed for the Q1/Q2(Q3) evaluation of the selected sample population. Several batches from three FDA-approved, generic products and the reference Doxil® formulation developed by the innovator company, Baxter Healthcare, were compared in each of our characterization studies with representative batches used for TEM/SAXS analysis.

Our results showed formulation similarities and minor variation across different attributes assessed in the Q3 evaluation of generic, liposomal DOX products. DOX purity, lipid purity, and the amount of free non-encapsulated DOX within liposomal formulations are critical to ensure the safety, efficacy, stability, and quality of each liposomal product. Our experimental results show a low prevalence of drug and lipid impurities and acceptable levels of non-encapsulated DOX in each formulation. Complementary methods using DLS, cryo-TEM, and SAXS provide useful information to elucidate the morphology and nanostructure similarity of different liposomal DOX formulations, which are essential to minimize differences that could adversely impact drug performance. Ultimately, structural characterization techniques can support physicochemical evaluation and uphold the commitment to product safety and quality for patients. It is our intent that the comparative analysis and methods outlined in this study may provide a useful framework for subsequent evaluation of complex, liposomal generics and similar follow-on products to increase the generic availability of complex, liposomal products on the market.

2.8 Author Contributions & Acknowledgements

2.8.1 Author Contributions

Adaeze Eneli was responsible for conceptualization, design of methodology, validation, formal analysis, investigation, data curation, visualization, writing/editing/revising of the original manuscript draft, project administration and supported funding acquisition. Kaikai Wang was responsible for design of methodology, validation, formal analysis, investigation, and writing/editing /revising of the original manuscript draft. Adaeze Eneli and Kaikai Wang are co-first authors on this publication.

Jingyao Gan was responsible for formal analysis, investigation and writing and editing/revising the original manuscript. Rimpy Diwan was responsible for visualization, writing and revising/editing the manuscript. Ziyi Lu was responsible for validation, formal analysis, investigation and editing/revising the manuscript. Minzhi Yu was responsible for editing and revising the manuscript. Rose Ackermann was responsible for design of methodology, validation, procurement of materials and resources, and editing/revising the manuscript. Brian Shay was responsible for validation, procurement of materials and resources, data curation and editing/revising the manuscript. Anna Schwendeman was responsible for conceptualization, design of methodology, validation, procurement of materials and resources, editing/revising of the manuscript, project administration, project supervision and funding acquisition.

2.8.2 Funding & Acknowledgements

This research was funded by the NIH T32 Pharmacological Sciences Training Program (PSTP) GM007767, the National Institute of Health project ALS-ENABLE (P30 GM124169) and a High-End Instrumentation Grant (S10OD018483), the University of Michigan Bioscience Initiative Bioinnovations in Brain Cancer (BIBC) grant, and the Rackham Merit Fellowship awarded to Adaeze Eneli by the University of Michigan Rackham Graduate School.

Research reported in this publication on cryo-EM was supported by the University of Michigan Cryo-EM Facility (U-M Cryo-EM). U-M Cryo-EM is grateful for support from the U-M Life Sciences Institute and the U-M Biosciences Initiative. We thank Vinson Lam for his assistance in collecting TEM images of Doxil® liposomes. Research conducted for the data acquisition and processing of SAXS scattering profiles for Doxil® liposomes was conducted at the Advanced Light Source (ALS), a national user facility operated by Lawrence Berkeley

National Laboratory on behalf of the Department of Energy, Office of Basic Energy Sciences, through the Integrated Diffraction Analysis Technologies (IDAT) program, supported by DOE Office of Biological and Environmental Research. Additional support comes from the National Institute of Health project ALS-ENABLE (P30 GM124169) and a High-End Instrumentation Grant S10OD018483.

Chapter 3 Development of an *In Vitro* Drug Release Assay Utilizing Bio-Beads SM-2 Resin to Evaluate Doxorubicin Liposomes

3.1 Abstract

Developing *in vitro* drug release (IVR) methods is essential for evaluating formulation performance, ensuring quality, and supporting bioequivalence for generic liposomal drug products. Traditional dialysis-based assays are commonly used for liposomal drug products but present serious limitations in dissolution testing. *In vitro* release methods using dialysis membranes inaccurately and inadequately reflect drug release kinetics from nanocarriers due to barrier effects of the dialysis membrane. Barrier effects artificially slow the rate of drug diffusion into the sampling compartment for quantification of *in vitro* drug release, which indicates that the traditional dialysis technique is actually a measure of the rate of drug diffusion across the dialysis membrane instead of drug release from the nanocarrier. Batch-to-batch variation in manufacturing, challenges in maintaining sink condition and drug/membrane interactions in solution also present additional limitations for the utility of dialysis membranes for IVR assays as a regulatory requirement in practice.

This study aimed to develop a simple, robust, single-vial IVR assay using Bio-Beads SM-2 resin as a hydrophobic sink material to assess the release kinetics of doxorubicin from Doxil®. A spectrofluorometric method was established to quantify cumulative release and adsorption by normalizing the fluorescent intensity of doxorubicin for the following assay test parameters: resin weight, drug concentration, temperature, agitation speed, and media composition. Sink conditions were validated for a select resin weight, and key study objectives included: achieving >80% drug release within 24 hours, ensuring rapid adsorption of released drug by the resin, maintaining liposome structural integrity, and demonstrating the discriminative capacity of the assay under formulation stress.

Under optimized conditions using 200 mg Bio-Beads, 10 µg/mL Doxil® in PBS (pH 7.4) with 5% w/v α-cyclodextrin, greater than 90% doxorubicin release was achieved within 24 hours. The addition of α-cyclodextrin preserved liposome integrity while promoting controlled

release. While the assay showed limited ability to distinguish formulations based on free drug content, it effectively detected release differences from formulations exposed to freeze-thaw stress. This simplified IVR method offers a cost-effective, reproducible approach for evaluating liposomal drug release, while highlighting cyclodextrins as excipients that support liposome stability. Further optimization is warranted to enhance the assay's discriminatory power for detecting differences in free drug content across liposomal formulations.

3.2 Introduction

Doxil® is a PEGylated doxorubicin liposome formulation, the first of its kind, which became the model nanomedicine featuring advantageous pharmacological properties including controlled drug release, prolonged circulation times in plasma, and enhanced permeability and retention (EPR) effect for passive targeting [88]. In the 30 years since its initial FDA approval, only five generic versions of Doxil® have been approved, reflecting the scientific and manufacturing complexities involved in replicating the liposomal structure and ensuring equivalent quality attributes. *In vitro* release evaluation is a critical parameter in formulation evaluation and batch-to-batch quality control to support the development of complex, liposomal generic versions [94]. *In vitro* release assessment can also be used to develop predictive correlations for *in vivo* drug performance, and therefore, it is paramount to develop an *in vitro* release assay with discriminative power and *in vivo* relevance.

Of all the methods used to evaluate encapsulated drug release from nanocarriers like liposomes, dialysis methods are the most common. In traditional dialysis-based methods, the released drug is separated from its nanocarrier using a semi-permeable membrane contained in a system with a donor and receiver compartment [102]. Sampling of released drug in the receiver compartment can be directly measured without need for further separation. This is advantageous, but the validity of the dialysis method and reliability of the release data generated have been questioned due to the relationship between the apparent and actual release kinetics from nanocarriers measured using dialysis membranes [102, 103].

Yu *et al* demonstrated that drug release kinetics are influenced by the barrier effects of dialysis membranes [103]. Previously, it was generally assumed these barrier effects were negligible because drug diffusion through the dialysis membrane was rapid with little to no interactions between the drug and the membrane [104]. As a result, apparent drug release in the sampling compartment outside of the dialysis bag was assumed to be the actual drug release

from the nanocarrier within the dialysis bag. Further investigation, however, in other studies investigating the release kinetics of poorly soluble drugs from nanoparticles, emulsions, and microgels suggested otherwise [104–109]. Slower and/or incomplete rates of drug release over the specified assay duration were observed in these analogous studies with each investigation attributing the inadequate/slow rate of release to drug diffusion limitations through dialysis membranes of varying types and materials [104–108].

Due to the growing evidence of barrier effects on drug diffusion through dialysis membranes, Yu and colleagues applied a mathematical model to determine the actual drug release kinetics from liposomal nanocarriers from the apparent release data generated using the dialysis method [104]. A calibration experiment was conducted initially to define the diffusion barrier properties of several dialysis membranes using a doxorubicin solution [104]. Doxil® was used as a model drug and a mathematical model representing dialysis with volume changes and appreciable receiver drug concentration was fitted to the experimental data [104]. Excellent agreement was found between the predicted and measured drug concentration inside the dialysis bag correcting for the apparent release kinetics [104]. This mathematical approach serves as one way to overcome the diffusion limitation of using dialysis bags in dissolution testing. However, batch-to-batch variation in dialysis membranes, challenges in maintaining sink condition and interactions between the drug and dialysis membrane presents additional limitations in the utility of dialysis bags for the reliability of dissolution testing.

Relatedly, several approved dialysis methods for industry are no longer suitable for dissolution testing due to manufacturing changes that have significantly altered the properties of the dialysis membrane resulting in no drug diffusion for sampling [52, 53, 81]. This is a significant issue for developers and regulatory agencies as a need emerges for a simple and natural *in vitro* drug release assay capable of characterizing the true drug release kinetics from nanocarriers and other, complex drug products.

Bio-bead SM-2 resin offers several advantages over traditional dialysis and sample-and-separate methods for liposome drug release evaluation. Bio-bead SM-2 resin beads are macro-porous, non-polar adsorbent beads comprised of polystyrene-divinyl-benzene ranging from 300 – 1180 microns in size capable of absorbing organic molecules less than 2000 kDa in molecular weight, like doxorubicin hydrochloride, from aqueous solutions. Table 1 details the properties of the bio-bead resin including its pore diameter, wet density and adsorption capacity to remove

detergents. Bio-bead adsorption of organics in aqueous solutions functions from the principles of hydrophobic interaction chromatography [110].

Table 9. Physicochemical properties of Bio-beads SM-2 resin.

	Bio-Beads SM-2 Adsorbent
Chemical nature	Polystyrene-divinyl-benzene
Polarity	Nonpolar
Dipole moment	0.3 Debye
Average pore diameter (dry beads)	90 Å
Wet density (g/cc)	1.02
Capacity (Triton® X-100 detergent) g/g	0.07

Bio-Bead SM-2 resin operate from the principles of hydrophobic interaction chromatography, adsorbing to hydrophobic regions of amphiphilic small molecules in high-salt buffers [111]. In buffers containing high salt concentrations, solute-solvent interactions between the amphiphilic drug and buffer solvent decrease, exposing the hydrophobic regions of the amphiphilic drug molecule for adsorptive binding to the Bio-bead resin [111]. As the encapsulated drug is released from liposomes into release media, drug adsorption by Bio-beads effectively removes the drug from the media "separating" the released drug from the free solution and trapping it within or on the surface of the Bio-beads in solution. The novelty in using Bio-bead SM-2 resin as a sink agent for dissolution testing is in its use for non-compendial, small-volume systems to achieve sink conditions while enabling the robust and discriminative evaluation of drug dissolution profiles for formulations of identical composition manufactured by different processes or introduced to meaningful structural differences.

In this study, we have developed a simple, robust, non-compendial *in vitro* release assay to evaluate doxorubicin release from Doxil® liposomes using Bio-beads SM-2 resin as a novel sink agent. This assay employs a small volume microtube system using the Bio-bead resin to remove released doxorubicin molecules from aqueous solutions. The United States Pharmacopeia (USP) outlines the recommendations and considerations for dissolution assay development in USP <1092> [112]. Four study objectives were developed including: 1) to design an IVR assay with discriminatory capacity between formulations of the same

composition; 2) achieve ≥ 80% cumulative release within 24 hours; 3) validate that encapsulated drug released from liposomes is immediately absorbed by the Bio-bead resin; and 4) ensure the quality of the liposome structure remains intact while facilitating controlled doxorubicin release from the liposomes.

We optimized key release parameters, including Bio-bead weight, drug concentration, temperature, agitation speed, and media composition. We determined the solubility of doxorubicin hydrochloride in various buffers and solvents relevant to our study investigation and developed a rapid, spectrofluorometric analysis method using 96-well microplates to quantify the amount of drug released from liposomes and absorbed by Bio-beads by normalizing the reduction in fluorescence intensity over the time-course of the study. Our IVRT method can differentiate between formulations of different qualities and achieve greater than 90% cumulative release in 24 hours using this accelerated release method. Discriminative capability of *in vitro* release methods is critical for formulation evaluation and quality assessment of reference and generic drug products. Additional work is necessary to continue optimization of the assay to increase assay sensitivity to detect and distinguish between formulations with intrinsic differences in free and liposomal doxorubicin content. However, the assay is sensitive enough to detect meaningful differences induced by freeze-thaw stress which has implications on processing, storage and drug product stability.

In sum, our release method serves as a promising, robust and reproducible, cost-effective tool for formulation evaluation, quality control and assurance. Establishment of this assay will enable the rapid evaluation of *in vitro* release kinetics for bioequivalence assessment of generic Doxil® formulations, advancing regulatory science and supporting the approval of complex, generic liposomal drug products.

3.3 Materials

Doxil® (liposomal doxorubicin hydrochloride injection) was purchased from the University of Michigan Hospital Pharmacy (Ann Arbor, MI, USA). Doxorubicin hydrochloride (Pharmaceutical Secondary Standard; Certified Reference Material) was purchased from MilliporeSigma (Burlington, MA, USA). Gibco Phosphate Buffered Saline (1X, pH 7.4), methanol (LC/MS grade, 99% purity, ethanol (LC/MS grade, 99% purity) and sucrose were purchased from Thermo Fisher Scientific (Waltham, MA, USA). α-cyclodextrin, (2-

hydroxypropyl)-β-cyclodextrin, γ-cyclodextrin, and L-histidine were purchased from Sigma-Aldrich (St. Louis, MO, USA). Dextrose was obtained from VWR International (Radnor, PA, USA). Eppendorf Natural Microtubes (5 mL), Eppendorf microtube clips (5 mL) and Fisherbrand Microcentrifuge Tubes (0.5 mL) were purchased from Fisher Scientific (Waltham, MA, USA). Bio-bead SM-2 resin was purchased from Bio-Rad Laboratories (Hercules, CA, USA). Microplate reader with SoftMaxPro software was obtained from Molecular Devices (San Jose, CA, USA). Benchmark rotating mixer was purchased from Benchmark® (Sayreville, NJ, USA). 96-well microplates were purchased from Corning® (Corning, NY, USA). Sealing film was purchased from Axygen/Corning (Corning, NY, USA). Malvern Zetasizer Nano ZSP was obtained from Malvern Pananalytical (Worcestershire, England, UK). Plastibrand® semi-micro disposable cuvettes were purchased from BRAND GMBH (Wertheim, Germany). All other solvents and reagents were of analytical grade and were purchased from Fisher Scientific (Waltham, MA, USA).

3.4 Methods

3.4.1 Pretreatment for Bio-Bead SM-2 resin material

Bio-bead SM-2 resin (Bio-Rad Laboratories, Hercules, CA, USA) was pretreated to remove entrapped air from the macroporous adsorbent to facilitate maximum adsorption capacity of organic molecules in aqueous solutions. Pretreatment followed the column method described in the "Instructions for Use" manual (Bio-Rad, n.d.) using methanol as the solvent. Bio-Bead SM-2 resin was washed with 100% methanol and degassed in a sonicator until the Bio-beads no longer floated on the solution surface, indicating successful removal of air from Bio-bead pores. The methanol/resin solution was then decanted and saturated overnight in deionized water. The hydrated resin solution was transferred to Poly-Prep chromatography columns to drain the excess liquid and was stored at 4°C until use.

3.4.2 Solubility determination of doxorubicin hydrochloride in various solvents

Saturation solutions of doxorubicin hydrochloride were prepared by adding the compound in excess to 1.5 mL microtubes containing 1 mL of organic and aqueous solvents at 37°C. Solvents used for solubility analysis included phosphate buffered saline (1X PBS, pH 7.4), PBS with dextrose, PBS with α-cyclodextrin, PBS with hydroxypropyl-β-cyclodextrin, PBS with γ-cyclodextrin, 100% methanol, 100% acetonitrile and the Doxil® formulation buffer (9.4%

sucrose and 1.55 mg/mL L-histidine, pH 6.5). Solutions were prepared in triplicate and vortexed continuously for 5 minutes. The initial pH of each solution was measured before the microtubes were affixed to tube clips on a Benchmark® rotating mixer (Sayreville, NJ, USA) set to 40 RPM maximum speed under incubation at 37°C for 24 hours. Calibration standards (25-125 μg/mL) were prepared from a 1 mg/mL stock solution of doxorubicin hydrochloride dissolved in the respective solvents.

After 24 hours, the final pH of each solution was measured, and doxorubicin content was quantified by UPLC-TUV using an Acquity UPLC-TUV detector system with Empower 3 software (Waters Corporation, Milford, MA, USA). Quantification of doxorubicin concentration was based on peak area (AUC) relative to prepared calibration standards. The previously validated UPLC-TUVmethod described in Chapter 2 Section 2.3 was used. Briefly, an isocratic mobile phase consisting of 45% deionized water with 0.1% formic acid (A) and 55% methanol with 0.1% formic acid (B) was pumped through an Acquity BEH C18 column (100 x 2.1 mm, 1.7 μm) (Waters Corporation, Milford, MA, USA) at a flow rate of 0.3 mL/min for a run time of 15 minutes. The injection volume was 10 μL and the UV detection wavelength was 254 nm. Doxorubicin solubility in each solvent was determined by applying a linear regression model to convert sample AUC values to concentrations, based on calibration curves with a correlation coefficient (R^2) greater than 0.99.

3.4.3 Spectrofluorometric analysis method for quantifying DOX release/adsorption under assay development conditions

Fluorescent intensity of sample aliquots at each time point was measured using a microplate reader equipped with SoftMax Pro software (Molecular Devices, San Jose, CA, USA). Measurements were taken at the fluorescence maximum excitation, auto cutoff, and emission wavelengths of 470, 550 and 560 nm. Samples were prepared by diluting aliquots 5-fold in 100% methanol to a final volume of 100 μL in a 96-well microplate. The microplate was sealed with Axygen® sealing film, wrapped in aluminum foil, and incubated at 55°C in a water bath for 20 minutes prior to fluorescence measurement. Raw fluorescence data was recorded in relative fluorescence units (RFU), and subsequently transformed into percentages representing cumulative release of doxorubicin under each test condition using the following equation:

$$Cumulative\ release\ (\%) = \left(1 - \left(\frac{RFU_t}{RFU_0}\right)\right) \times 100 \quad \text{(Eqn. 1)}$$

where RFU_t represents the fluorescent intensity of doxorubicin sample aliquots at time t, and RFU_0 represents the initial fluorescent intensity of the doxorubicin sample aliquot withdrawn at 0 hours.

3.4.4 Determining the optimal Bio-bead amount for complete DOX release and adsorption in aqueous release media

To begin assay development, we optimized the quantity of pretreated Bio-beads SM-2 resin to achieve 100% adsorption of free doxorubicin and doxorubicin released from liposomes. Using select assay conditions from the flow-through dissolution assay utilizing the USP-4 apparatus to evaluate doxorubicin liposomes [53], we tested three resin quantities–50 mg, 100 mg, and 200 mg– for their ability to enable complete doxorubicin release and adsorption. A 4 mL doxorubicin solution was prepared in PBS (1X, pH 7.4) at a test concentration of 10 μg/mL and run in triplicate. PBS was used as the baseline release medium for dissolution assay development. Samples were subject to rotational agitation (40 RPM) using a Benchmark® rotating mixer for 24 hours. Aliquots were withdrawn and replaced with fresh PBS at 0, 1, 2, 4, 8, 12, and 24 hours. DOX release and adsorption were quantified using the spectrofluorometric analytical method described in Section 3.4.3.

3.4.5 Determining the optimum testing concentration for encapsulated doxorubicin release and free doxorubicin adsorption by Bio-beads SM-2 resin in aqueous release media

The optimal concentration used to evaluate the dissolution profile of liposomal doxorubicin formulations with Bio-beads SM-2 resin was determined in PBS. Three test concentrations- 10 ug/mL, 20 ug/mL, and 40 μg/mL– of Doxil® diluted in PBS were assessed to evaluate the rate and extent of encapsulated doxorubicin release and adsorption by Bio-beads SM-2 resin.

Initial aliquots were withdrawn and replaced with fresh PBS for each replicate for 0-hour measurement. Two hundred milligrams of Bio-bead SM-2 resin were added to 5 mL Eppendorf® Natural microtubes containing the sample solution after sampling at 0 hours. Each 5 mL microtube was capped using Eppendorf® tube clips to prevent solution leakage during agitation and each vial was affixed horizontally to the Benchmark rotating mixer contained within an incubator set to 37°C. The rotator speed was set to 40 RPM to provide maximal

agitation during dissolution testing. Subsequent aliquots were taken and replaced with fresh PBS (1X, pH 7.4) at 1, 2, 4, 8, 12, 24 hours.

Particle size was measured after sampling at each time point using the Malvern Zetasizer Nano ZSP (Worcestershire, England, UK). For each analysis, sample aliquots were diluted 10-fold in deionized water in Plastibrand® semi-micro disposable cuvettes (BRAND GMBH, Wertheim, Germany). System parameters for particle size measurement are detailed in Section 2.4.1 of Chapter 2. Doxorubicin release and adsorption was quantified using the spectrofluorometric analytical method described in Section 3.4.3.

3.4.6 Requirement and validation of sink condition using Bio-bead SM-2 resin in aqueous release media

Following determination of the optimal concentration and Bio-bead resin quantity for complete release and adsorption of doxorubicin (Section 3.4.3), a validation experiment was performed to determine if sink conditions were achieved under these parameters. Bio-bead resin was evaluated as a novel sink agent for dissolution due to its unique physicochemical properties enabling the adsorption of small organic molecules (<2,000 kDa) from aqueous solutions (Bio-Rad, n.d.). To test sink conditions, sample solutions were prepared at concentrations 3- to 10-fold higher than the optimal doxorubicin concentration of 10 µg/mL in PBS (1X, pH 7.4). These solutions were incubated with 200 mg of Bio-Beads SM-2 resin to determine whether the resin quantity is capable of fully absorbing free doxorubicin present at concentrations 10-fold the selected concentration to investigate drug-bead saturation in PBS media.

Initial aliquots were withdrawn and replaced with fresh PBS for each replicate for 0-hour measurement. Two hundred milligrams of Bio-bead SM-2 resin were weighed and added to 5 mL Eppendorf® Natural microtubes containing the sample solution after sampling at 0 hours. Each 5 mL microtube was capped using Eppendorf® tube clips to prevent solution leakage during agitation and each vial was affixed horizontally to the Benchmark rotating mixer contained within an incubator set to 37°C. The rotator speed was set to 40 RPM to provide maximal agitation during dissolution testing. Subsequent aliquots were taken and replaced with fresh PBS (1X, pH 7.4) at 1, 2, 4, 8, 12, 24 hours. The spectrofluorometric analytical method described in Section 3.4.3 was applied to quantify the percentage of doxorubicin adsorption.

3.4.7 Validating rapid absorbance of free DOX to Bio-bead SM-2 resin in aqueous release media

A key assumption requiring validation is that free DOX is rapidly absorbed by Bio-Bead SM-2 resin in aqueous media, ensuring that DOX released from liposomes is immediately removed from the release media by the resin. This experiment also aimed to confirm that DOX removal is not attributed to alternative mechanisms. To evaluate this, sample conditions of the target concentration (10%, 20%, 50%, 75%, and 100% of 10 μg/mL) were prepared in PBS and tested under the standard assay conditions. Each condition was performed in triplicate using 200 mg of Bio-Beads SM-2 resin per sample, and samples were subject to rotational agitation set to 40 RPM using a Benchmark® rotating mixer and incubated at 45°C.

Aliquots (200 μL) were withdrawn with fresh PBS (1X, pH 7.4) at 0, 1, 2, 4, 8, 12, and 24 hours. Particle size was measured after sampling at each time point using the Malvern Zetasizer Nano ZSP (Worcestershire, England, UK). For analysis, aliquots were diluted 10-fold in deionized water and transferred to Plastibrand® semi-micro disposable cuvettes (BRAND GMBH, Wertheim, Germany). System parameters for particle size measurement are detailed in Section 2.4.1 of Chapter 2. The spectrofluorometric method described in Section 3.4.3 was applied to quantify the percentage of DOX adsorption.

3.4.8 Assay optimization to retain empty liposome structural quality and facilitate DOX release

3.4.8.1 Agitation

Bio-bead SM-2 resin (200 mg) was added to 4 mL of Doxil® diluted in PBS to a concentration of 10 μg/mL. Samples were affixed to a Benchmark® rotating mixer and incubated at 45°C under rotational agitation for 24 hours. To evaluate the impact of agitation rate, slower agitation speeds (10 and 20 RPM) were tested on successive days and compared to the initial 40 RPM condition. Aliquots (200 μL) were withdrawn and replaced with fresh PBS at 0, 1, 2, 4, 8, 12, and 24 hours.

Particle size was measured at each time point using the Malvern Zetasizer Nano ZSP (Worcestershire, England, UK). Sample aliquots were diluted 10-fold in deionized water in Plastibrand® semi-micro disposable cuvettes (BRAND GMBH, Wertheim, Germany) for analysis. System parameters for particle size measurement are detailed in Section 2.4.1 of

Chapter 2. DOX release was quantified using the spectrofluorometric method described in Section 3.4.3.

3.4.8.2 Temperature

Bio-bead SM-2 resin (200 mg) was added to 4 mL solution of Doxil® diluted in PBS to a concentration of 10 μg/mL. Sample solutions were affixed to a Benchmark® rotating mixer and incubated under rotation at 40 RPM for 24 hours. To evaluate the effect of temperature on DOX release, reduced temperatures (25° and 37°C) were tested on successive days and compared to the initial assay temperature of 45°C.

Aliquots (200 μL) were withdrawn and replaced with fresh PBS at 0, 1, 2, 4, 8, 12, and 24 hours. Particle size was measured after sampling at each time point using the Malvern Zetasizer Nano ZSP (Worcestershire, England, UK). Aliquots were diluted 10-fold in deionized water and transferred to Plastibrand® semi-micro disposable cuvettes (BRAND GMBH, Wertheim, Germany) for analysis. System parameters for particle size measurement are detailed in Section 2.4.1 of Chapter 2. DOX release was quantified using the spectrofluorometric method described in Section 3.4.3.

3.4.8.3 Reduced agitation and temperature

The effects of reduced agitation and temperature were assessed by conducting dissolution and particle size analysis at 20 RPM and 37°C. Doxil® solutions (4 mL) were prepared in PBS (1X, pH 7.4) at 10 μg/mL, 20 μg/mL, and 40 μg/mL and incubated under these conditions. Aliquots (200 μL) were withdrawn and replaced with fresh PBS at 0, 1, 2, 4, 8, 12, and 24 hours. Particle size was measured at each time point using the Malvern Zetasizer Nano ZSP (Worcestershire, England, UK). Aliquots were diluted 10-fold in deionized water and transferred to Plastibrand® semi-micro disposable cuvettes (BRAND GMBH, Wertheim, Germany). System parameters for particle size measurement are detailed in Section 2.4.1 of Chapter 2. Doxorubicin release was quantified using the spectrofluorometric method described in Section 3.4.3.

3.4.8.4 Cyclodextrin addition to release media

α-cyclodextrin, 2-hydroxypropyl-β-cyclodextrin, and γ-cyclodextrin (5% *w/v*) were added to standard dissolution media consisting of PBS (1X, pH 7.4) in separate conical vials. Doxil® solutions (4 mL) were prepared in each PBS/cyclodextrin solution at 10 μg/mL in triplicate. Initial aliquots were withdrawn and replaced with fresh PBS/cyclodextrin solution

corresponding to the sample replicate for measurement. Two hundred milligrams of Bio-bead SM-2 resin were added to 5 mL Eppendorf® Natural microtubes containing each sample solution after sampling at 0 hours. Each microtube was capped using tube clips to prevent leakage during agitation, affixed horizontally to the rotating mixer set to 20 RPM, and incubated at 37°C. Subsequent aliquots were taken and replaced with the corresponding, fresh PBS/cyclodextrin solution at 1, 2, 4, 8, 12, 24 hours.

Particle size was measured at each time point using the Malvern Zetasizer Nano ZSP (Worcestershire, England, UK). Aliquots were diluted 10-fold in deionized water and transferred to Plastibrand® semi-micro disposable cuvettes (BRAND GMBH, Wertheim, Germany). System parameters for particle size measurement are detailed in Section 2.4.1 of Chapter 2. Doxorubicin release was quantified using the spectrofluorometric method described in Section 3.4.3.

3.4.9 Discriminative capability of developed assay

Following establishment of assay conditions for the *in vitro* dissolution test, the method must be evaluated for its discriminative ability to detect meaningful differences between formulations of identical composition produced by different manufacturing processes. To assess this, stress conditions were applied to the Doxil® formulation used in assay development to introduce controlled variations. This evaluation tested whether the proposed, developed assay could distinguish between formulations of the same composition. Demonstrating the discriminative ability of the assay supports its application for the robust evaluation of complex, liposomal generic drug candidates in comparison with the reference formulation.

3.4.9.1 Free DOX spike test in liposomal DOX formulations

The first stress test evaluating the discriminative ability of the developed assay includes distinguishing between formulations with increasing levels of free, non-encapsulated DOX present in liposomal DOX formulations. Doxil® (2 mg/mL) samples spiked with 0, 2.5, 5, 10, 15 and 20% *v/v* of a 2 mg/mL free DOX solution prepared in Doxil® formulation buffer consisting of 9.4% sucrose and 1.55 mg/mL L-histidine at pH 6.5 were diluted to 10 µg/mL in PBS (1X, pH 7.4) and prepared in triplicate. Aliquots were withdrawn at the 2 mL mark of the 5 mL microtubes at pre-determined time intervals at 0, 1, 2, 4, 8, 12 and 24 hours and replaced with fresh PBS (1X, pH 7.4) after the bio-beads settled following agitation.

At time zero, prior to addition of the bio-bead resin, the 5 mL microtubes were inverted to mix 3 times to ensure liposome distribution throughout the media before withdrawing the initial aliquot. Two hundred milligrams of bio-bead resin were weighed and added to each sample replicate for each free DOX spike level in individual Doxil® samples. Sample solutions contained in the 5 mL microtubes capped with tube clips were affixed in a horizontal orientation to the rotator in the direction of rotation. Particle size was measured after sampling at each time point using the Malvern Zetasizer Nano ZSP (Worcestershire, England, UK). Sample aliquots were diluted 10-fold in deionized water in Plastibrand® semi-micro disposable cuvettes (BRAND GMBH, Wetheim, Germany) for analysis. System parameters for particle size measurement are detailed in Section 2.4.1 of Chapter 2. Initial and final pH of the 0 hour and 24-hour samples were measured using a pH reader. DOX release was quantified using the spectrofluorometric method described in Section 3.4.3.

3.4.9.2 Freeze-thaw stress test

The second test to evaluate the discriminative ability of the developed assay involved subjecting the liposomal doxorubicin formulation to freeze-thaw cycles in order to simulate thermal stress related to storage and drug product stability. Doxil® samples (2 mg/mL) were rapidly frozen in 0.5 mL microtubes using liquid nitrogen at -80°C for 3 minutes, then immediately thawed in a water bath at 55°C. The freeze-thaw process was repeated 4, 7, and 10 times to represent increasing stress cycles. Following treatment, sample solutions were prepared in triplicate by preparing 4 mL drug-in-media solutions (10 µg/mL Doxil® in PBS) for each freeze-thaw condition.

Aliquots were withdrawn at the 2 mL mark of each microtube at pre-determined time intervals (0, 1, 2, 4, 8, 12, and 24 hours) after settling of bio-beads following agitation and were immediately replaced with fresh PBS (1X, pH 7.4). Prior to addition of the Bio-bead SM-2 resin at time zero, microtubes were inverted three times to ensure uniform distribution of liposomes throughout the media. 200 mg of Bio-bead SM-2 resin were added to each sample replicate for each freeze-thaw stressed Doxil® sample. Sample solutions were contained in 5 mL microtubes, capped securely with tube clips, and horizontally affixed to the rotator in the direction of rotation.

Particle size was measured after sampling at each time point using the Malvern Zetasizer Nano ZSP (Worcestershire, England, UK). Aliquots were diluted 10-fold in deionized water in

Plastibrand® semi-micro disposable cuvettes (BRAND GMBH, Wetheim, Germany) for analysis. System parameters for particle size measurement are detailed in Section 2.4.1 of Chapter 2. Initial and final pH of the 0-hour and 24-hour samples were measured using a pH reader. DOX release was quantified using the spectrofluorometric method described in Section 3.4.3.

3.5 Results & Discussion

3.5.1 Solubility determination of doxorubicin (DOX) hydrochloride in various solvents

To select an appropriate medium for dissolution method development, it is critical to assess the influence of different buffers, solvents, surfactants and pH on the solubility and stability of the drug substance [112]. Selecting a dissolution medium that doxorubicin hydrochloride may be poorly soluble and instable in at room and elevated temperatures can compromise the reliability of formulation testing and evaluation for *in vitro* release. Using the shake-flask solubility method described in USP <1236>, we tested the solubility of doxorubicin hydrochloride in the buffer used to develop to the Doxil® formulation at pH 6.5, phosphate buffered saline (1X, pH 7.4) with different surfactants, and two organic solvents. The Doxil® formulation buffer consists of 9.4% sucrose and 1.55 mg/mL L-histidine at pH 6.5. The concentration of each cyclodextrin evaluated was 5% *w/v* of α-cyclodextrin, hydroxypropyl-β-cyclodextrin, and γ-cyclodextrin.

In Table 10, saturation solubility for doxorubicin hydrochloride powder dissolved in the Doxil® formulation buffer was 5.79 mg/mL and was used as a baseline for solubility comparison. DOX is most insoluble in 100% ethanol at 85.22 μg/mL, but soluble in 100% methanol at 3.07 mg/mL. The effect of short-chain alcohols on lipid bilayers were investigated using microscopic molecular dynamic simulations on fully hydrogenated phosphatidylcholine (PC) membranes and discovered that ethanol and methanol increase bilayer fluidity and permeability [113]. Ethanol has a stronger effect than methanol on the structural properties of lipid bilayer membranes which is due rapid membrane penetration on the order of magnitude of nanoseconds related to hydrogen bonding to lipid molecules [113]. However, due to the poor solubility of DOX in ethanol, its use in our dissolution assay for analytical method development is limited. Therefore, due to greater DOX solubility in methanol, methanol was selected as the organic solvent in order to disrupt the liposomes that remain in each sample aliquot to release and dissolve DOX in methanol for fluorescence detection during analysis.

Table 10. Solubility of DOX in various solvents.

	DOX Solubility	
PBS (1X, pH 7.4) + 5% w/v γ-CD	9.13	mg/ml
PBS (1X, pH 7.4) + 5% w/v α-CD	9.01	mg/ml
PBS (1X, pH 7.4) + 5% w/v HP-β-CD	8.20	mg/ml
PBS (1X, pH 7.4) + 5% w/v dextrose	7.93	mg/ml
PBS (1X, pH 7.4)	6.05	mg/ml
9.4% sucrose + 1.55 mg/mL L-histidine, pH 6.5	5.79	mg/ml
100% methanol	3.07	mg/ml
100% ethanol	85.22	µg/ml

Cyclodextrins are oligosaccharides formed by cyclization of dextrose units linked together by α-(1→4) glycosidic bonds. Cyclodextrins are known for solubilizing hydrophobic compounds, such as DOX hydrochloride, by sequestering cholesterol and small hydrophobic molecules in its inner cavity and forming inclusion complexes [114, 115]. Cyclodextrin addition to phosphate buffered saline (PBS, 1X, pH 7.4) increases DOX solubility in PBS with increasing cyclodextrin size. An increase in DOX solubility was also observed upon addition of 5% *w/v* dextrose to PBS, however, lower solubility was observed with the addition of hydroxypropyl- β-cyclodextrin when compared to α-cyclodextrin.

Reduced solubility with addition of hydroxyalkylated β-cyclodextrin to PBS (1X, pH 7.4) can be attributed to a moderate increase in hydrophobicity due to presence of hydroxyalkyl groups. In a review article by Saokham *et al*, the solubility of cyclodextrins, drug/cyclodextrin complexes and their properties were discussed to evaluate the use of cyclodextrins to improve the solubility and oral bioavailability of BCS Class II and IV drugs and other dosage forms intended for other routes of administration [115]. It was determined that the $LogP_{o/w}$ value for hydroxypropyl- β-cyclodextrin (-11) is more positive than that of α-cyclodextrin (-13) which provides a plausible explanation for the moderate increase in hydrophobicity that is responsible for the slight decrease in DOX solubility when added to PBS.

Based on the solubility results, PBS (1X, pH 7.4) was selected as the baseline media for subsequent assay development.

3.5.2 Determining the optimal Bio-bead amount for complete DOX release and adsorption in aqueous release media

The optimal quantity of Bio-bead SM-2 resin to enable 100% DOX release from Doxil® liposomes and adsorption by the Bio-beads in the dissolution medium was investigated, as illustrated in Fig. 33. Within only 20 minutes under the assay conditions, 50% of free DOX is absorbed by 50 mg of Biobeads whereas 70% and 90% is absorbed with 100 mg and 200 mg of Biobeads, respectively. In comparison, the rate of cumulative DOX release from the Doxil® liposome increases with increasing bio-bead quantity. Within the same 20 minutes, only 20% DOX release is achieved with 50 mg of Biobeads whereas 38% and 49% DOX release is achieved with 100 mg and 200 mg of Biobeads, respectively.

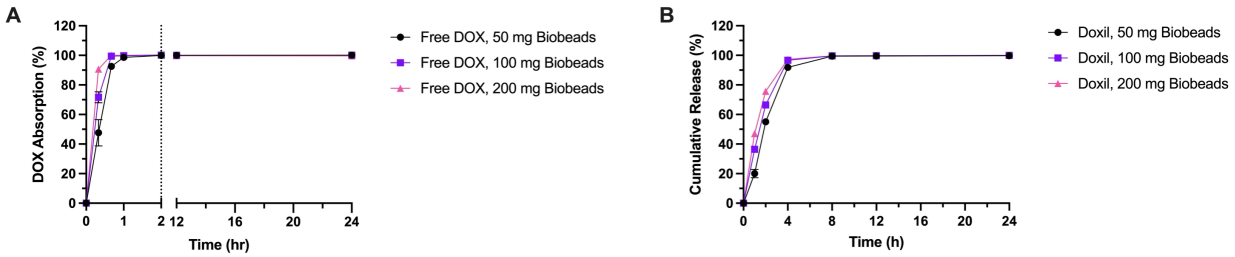

Figure 33. Rate of DOX adsorption and release in free and liposomal formulations to determine the quantity of Biobead resin necessary for rapid, complete DOX adsorption in release media consisting of phosphate buffered saline (1X, pH 7.4) under rotational agitation at 40 RPM and incubation at 45°C using an *in vitro* release assay under development (mean ± SD, n = 3).

In this study, our objective was to develop an accelerated drug release assay for Doxil® using Bio-Bead SM-2 resin achieving greater than 80% release within 24 hours, providing a practical and robust test to evaluate dissolution behavior and formulation performance [94]. According to the *FDA Guidance for Industry on Dissolution Testing of Immediate Release Solid Oral Dosage Forms*, a minimum of 80% cumulative release must be achieved within the testing period for assay validity (U.S. Food & Drug Administration, 2024). Moreover, a fundamental assumption for the validity of this assay necessitates that the rate limiting step is slow DOX release from liposomes and that the released drug is rapidly absorbed by the Biobeads, eliminating alternative mechanisms for DOX adsorption upon release from liposomes. Greater than 90% DOX release is observed within 4 hours and complete release is achieved in 8 hours for each test condition. Two hundred milligrams were selected as the bio-bead quantity for subsequent assay development due to the rapid and complete adsorption of DOX in PBS.

3.5.3 Determining the optimum testing concentration for encapsulated DOX release and free DOX adsorption by Bio-beads SM-2 resin in aqueous release media

Fig. 34 details the results of our concentration investigation to select the optimal test concentration for DOX samples prepared in the dissolution medium using 200 mg of Biobeads to facilitate complete DOX release and adsorption. The dissolution profiles for Doxil® are highly similar for test conditions at 10 µg/mL and 20 µg/mL, reaching over 80% release in 12 hours, whereas DOX release for 40 µg/mL is 10% slower.

As Doxil® concentration increases, the volume of liposomes present in each solution will increase under a fixed volume, surface area and temperature resulting in a greater frequency of collisions between the constituents in the dissolution system - the liposomes, bio-beads, molecular components of the dissolution medium and potentially, the polypropylene molecules comprising the chemical composition of the microtube material due to the microenvironment influencing dissolution. However, compared with lower concentrations, the slower release rate observed at 40 µg/mL may be attributed to the number of liposomes that had not been disrupted and released its drug cargo upon evaluation with 200 mg of bio-beads. Based on these findings, we selected 10 µg/mL as the optimal concentration for further testing.

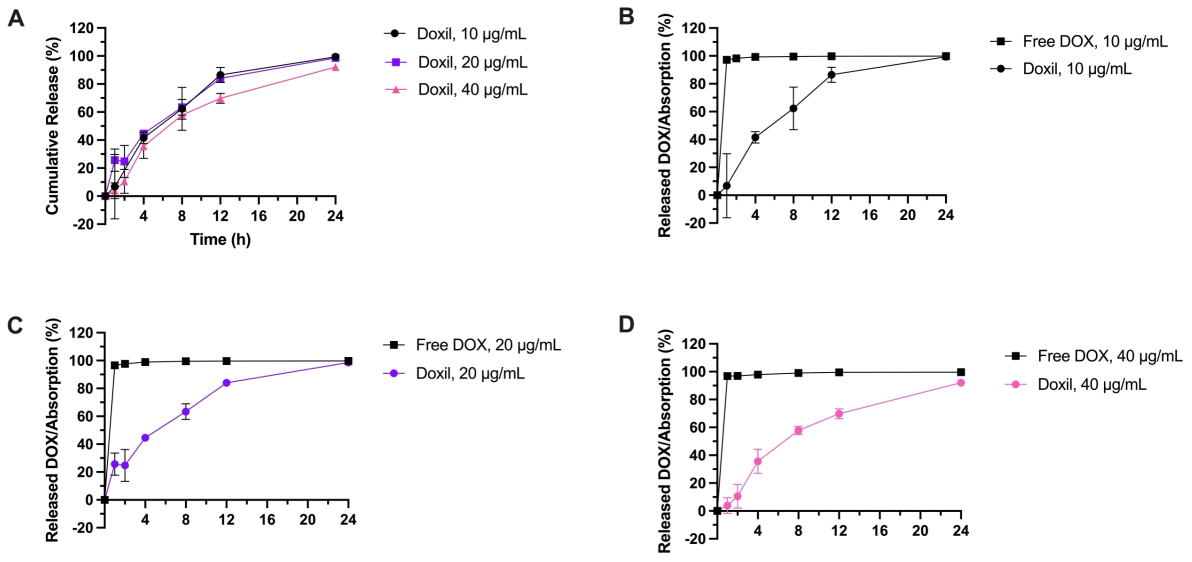

Figure 34. Evaluation of released and absorbed DOX in free and liposomal formulations by 200 mg of Biobeads at increasing concentrations in release media consisting of phosphate buffered saline (1X, pH 7.4) under rotational agitation at 40 RPM and incubation at 45°C using an *in vitro* release assay under development (mean ± SD, n = 3).

3.5.4 Requirement and validation of sink condition using Bio-bead SM-2 resin in aqueous release media

When developing a dissolution assay, one goal is to achieve sink condition to create a more realistic environment for *in vitro* dissolution to increase relevance to *in vivo* conditions. From an *in vivo* perspective, the biological processes of adsorption, distribution, and metabolism function collectively as a continuous sink for drug dissolution preventing drug saturation at the site of adsorption that would slow the rate of drug dissolution. To simulate *in vivo* conditions, sink condition is achieved by defining the volume of media necessary to dissolve at least 3 times the amount of drug required to form a saturated solution [112]. However, the volume selected to achieve sink condition should not be too large as the dissolution assay may lose its sensitivity to detect critical differences in the intrinsic properties of drug formulation or changes in the manufacturing process [116, 117].

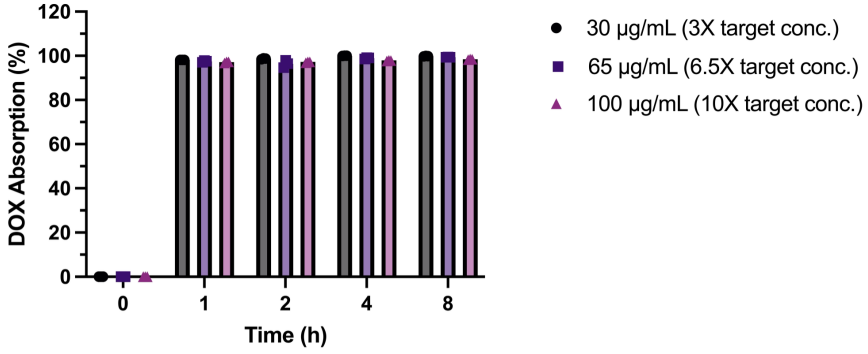

Figure 35. Experimental validation for sink condition using a free DOX solution (2 mg/mL) prepared in Doxil® formulation buffer diluted to concentrations 3-10 times the target concentration of 10 µg/mL in phosphate buffered saline (1X, pH 7.4) under rotational agitation and incubation at 40 RPM and 45°C (mean ± SD, n = 3).

For our release assay, we sought to develop a non-compendial single vial method in a 5-mL microtube to create a simple, robust and cost-effective means to evaluate the dissolution profile of complex, liposomal drug products. Fixing our solution volumes to 4 mL for this non-compendial assay, we evaluated 200 mg of Bio-bead SM-2 resin as the quantity necessary to completely absorb DOX from three solutions prepared at concentrations equivalent to 3-10 times the optimal concentration (10 µg/mL) selected in Section 3.5.3. Fig. 35 shows the results of DOX adsorption at concentrations three to ten times the target concentration to assess sink condition using a free DOX solution (2 mg/mL) prepared in Doxil® formulation buffer and dissolved in PBS to a final test concentration of 10 µg/mL. Within one-hour, rapid adsorption of virtually all free DOX in each solution was absorbed by 200 mg of the Bio-bead resin: 98.2 ±

0.02%, 97.5 ± 0.3% and 97.1% ± 0.3% for 30, 65 and 100 μg/mL free DOX solutions in PBS media. Rationale for the minor decrease in free DOX adsorption at increasing concentration likely stems from the same rationale for slower release of encapsulated DOX from liposomes. However, in the absence of liposomes, the rate of drug adsorption is more rapid in the presence of bio-beads due to the principles of hydrophobic interaction chromatography.

3.5.5 Validating rapid absorbance of free DOX to Bio-bead SM-2 resin in aqueous release media

Fig. 36 shows a comparison of the rate of free DOX absorbance and encapsulated DOX release in the presence of Bio-bead SM-2 resin at incremental levels of the target concentration to validate the assumption that upon DOX release from the Doxil® liposome, free DOX will be immediately absorbed by the resin in the aqueous release media using rotational agitation for physical mixing and incubation at 40 RPM and 45°C. Free DOX adsorption remained constant with complete adsorption within one hour across all conditions. At 10% of the target concentration at 1 μg/mL, 80% of encapsulated DOX is released within 1 hour compared to nearly 60% release at 2 μg/mL (20% target) and 45% release at 5 μg/mL (50% target). Interestingly, less than 5% release is observed at 75% of the target concentration when compared to 20% release at 100% of the target concentration. Discrepancies in the 75% test condition may be due to random error and variability in fluorescence detection for sample analysis.

Experimental results in Fig. 36 confirm the assumption that as DOX is slowly released from the liposome, it will be rapidly absorbed by Bio-bead SM-2 resin within less than an hour, supporting the data from Fig. 33 which showed the discriminative adsorption of 90% free DOX with 200 mg of bio-beads within 20 minutes.

After determining the optimal bio-bead quantity, drug concentration, validating sink condition and the rapid absorbance of released DOX from liposomes, the next research objective was to investigate the quality of the liposome structure upon release of DOX from liposomes and employ strategies to improve or retain its structural quality upon drug release. Fig. 37 shows the results of the time-dependent particle size analysis run in conjunction with the *in vitro* release study to validate the rapid absorbance of released DOX from liposomes. At 0 hr in each condition, a singular peak is observed at approximately 90 nm which is representative of the intact liposome population in media prior to agitation in the dissolution apparatus. Within one

hour of the release study, a significant reduction in peak intensity (%) is observed in purple and subsequent reductions are observed with an increasing prevalence of a second peak with a size of approximately 1000 nm.

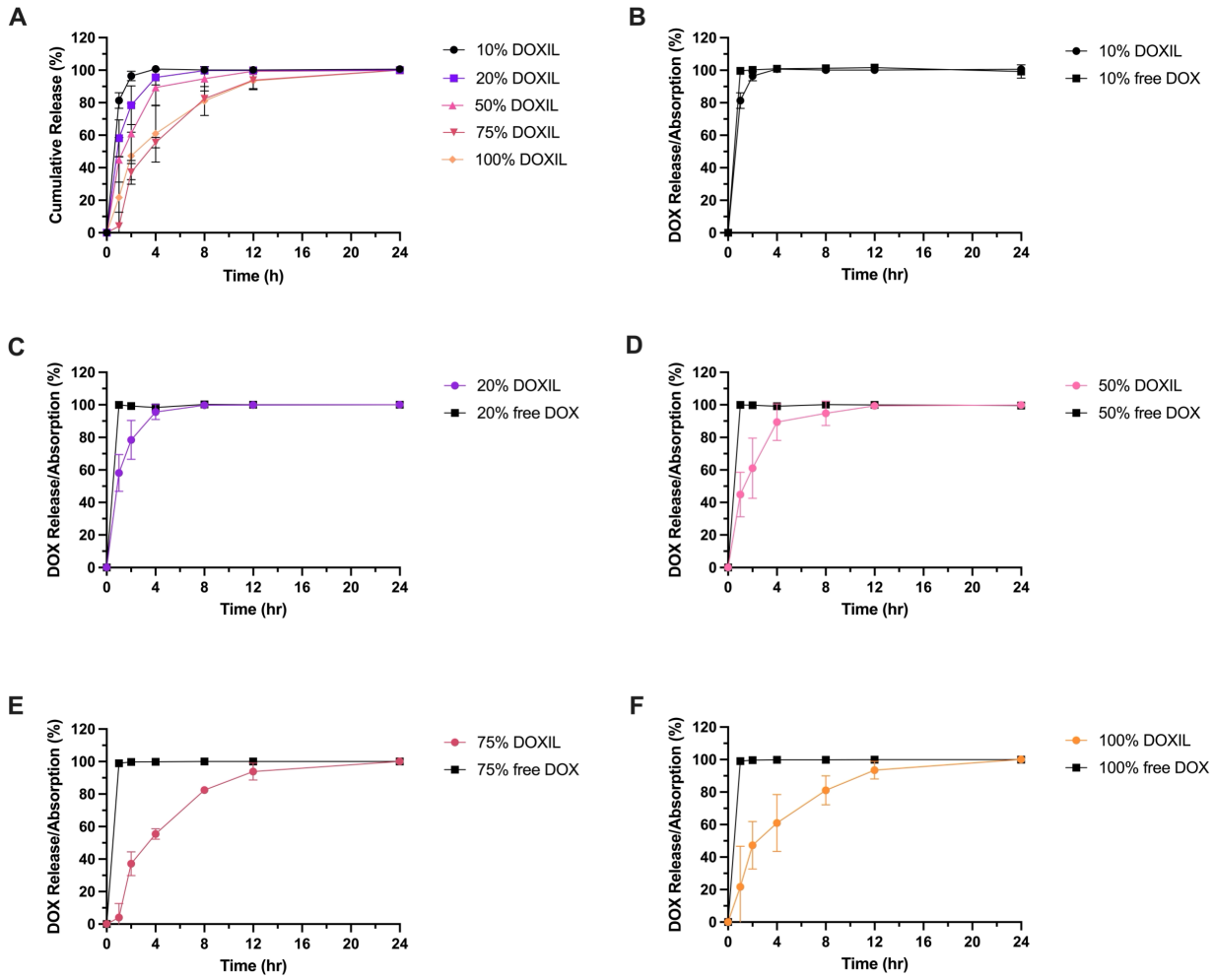

Figure 36. Validate that free DOX is rapidly absorbed by Biobeads in media and encapsulated DOX is released at a slower rate from liposomes in the same media consisting of phosphate buffered saline (1X, pH 7.4) under rotational agitation and incubation at 40 RPM and 45C using an *in vitro* release assay under development (mean ± SD, n = 3).

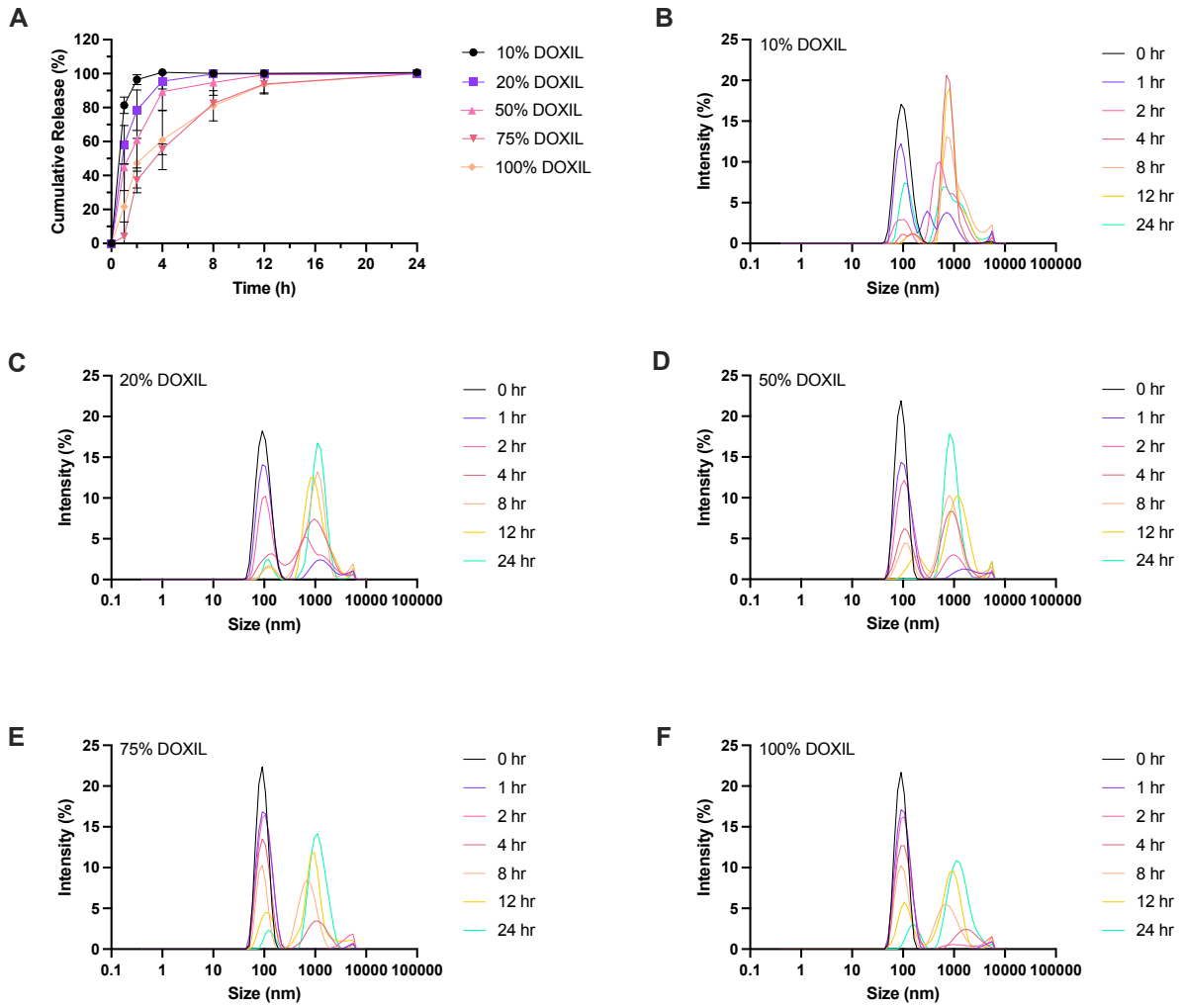

Figure 37. Particle size distribution analysis for an experimental study validating the slow-release rate of encapsulated DOX from liposomes and rapid adsorption of free, released DOX in release media consisting of phosphate buffered saline (1X, pH 7.4) under rotational agitation and incubation at 40 RPM and 45C using an *in vitro* release assay under development (mean ± SD, n = 3).

Sample aliquots for particle size measurements are diluted 10-fold in water, therefore, it is plausible that liposome membranes were destroyed by particle collisions induced by physical agitation via rotation during the release study and are reflected in the results by the detection of lipids aggregating in the water dispersant for analysis.

3.5.6 Assay optimization to retain liposome structural quality during dissolution

Considering that gradual destruction of the Doxil® liposome is the mechanism by which DOX is completely released evidenced in Fig. 37, strategies for assay optimization were explored to improve structural quality of the liposome during dissolution. Reducing the rotational agitation speed, reducing temperature and studying the effect of cyclodextrin addition

to the release media on liposome structure during dissolution were explored tangentially to the dissolution assay under the proposed conditions.

3.5.6.1 Agitation

Fig. 38 shows the effect of agitation speed on the release profiles and liposome structure of Doxil® at 45°C. Cumulative release of DOX for each speed condition reached 100% within 24 hours, however, the slower the agitation speed, the slower the release rate of doxorubicin. Moreover, the release profile at 10 RPM is distinct from the release profiles at 20 RPM and 40 RPM, where two burst release phases can be observed at 1 hr and 8 hrs. Gradual rate of release is observed in the dissolution profiles for Doxil® at 10 and 20 RPM, and while 100% release is achieved at 40 RPM within 12 hrs, greater than 80% is achieved within the same time frame for complete release within 24 hrs.

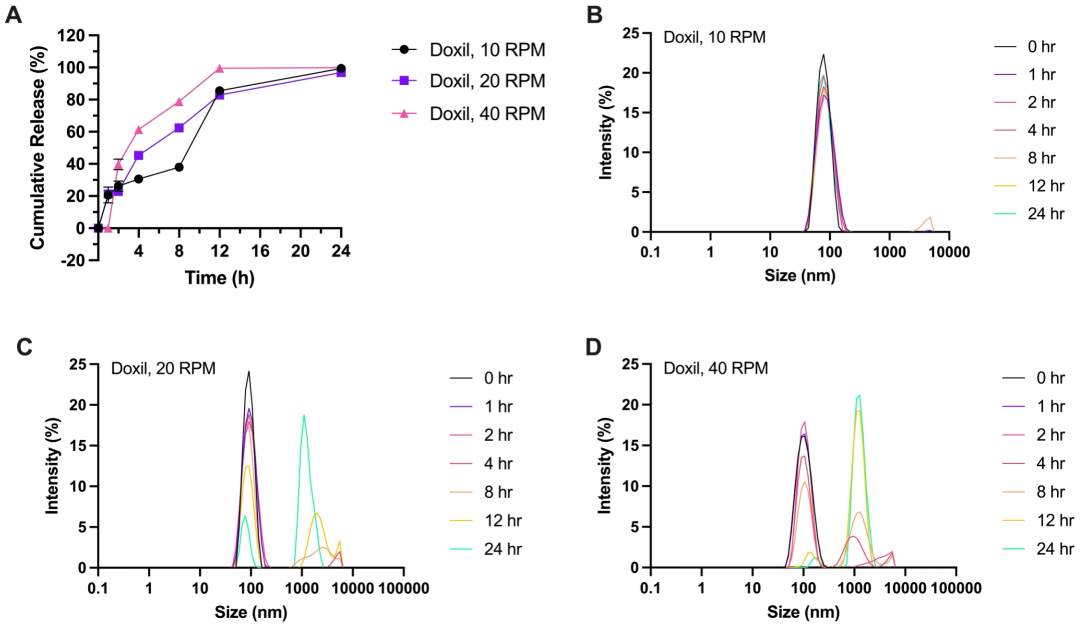

Figure 38. (A) Rate of DOX release from liposomes in release media consisting of phosphate buffered saline (1X, pH 7.4) under incubation at 45°C and rotational agitation at different test speeds using an *in vitro* release assay under development; (B-D) Particle size distribution analysis to evaluate the impact of agitation speed on empty liposome structural quality while facilitating DOX release (mean ± SD, n = 3).

Particle size analysis in Fig. 38 also shows greater intensity of liposomes at time 0 in the 20 RPM test condition when compared with 40 RPM in Fig. 38C and 38D, and in Fig. 38C, a remnant liposome population exists among the lipid aggregates at the 24 hr time point that is nonexistent in Fig. 38D suggesting that all liposomes were destroyed at the high speed test condition.

3.5.6.2 Temperature

The impact of temperature on the dissolution profile and retention of Doxil® liposome structure at 40 RPM were investigated. In Fig. 39A, greater than 90% release was achieved in 24 hrs at 37°C and 45°C whereas 71.8 ± 6.7% was achieved at 25°C. Particle size analysis at 37°C and 40 RPM showed minor disruption of the liposome structure with most of the liposome population still present at 24 hrs when compared with the size intensity peak at 0 hrs.

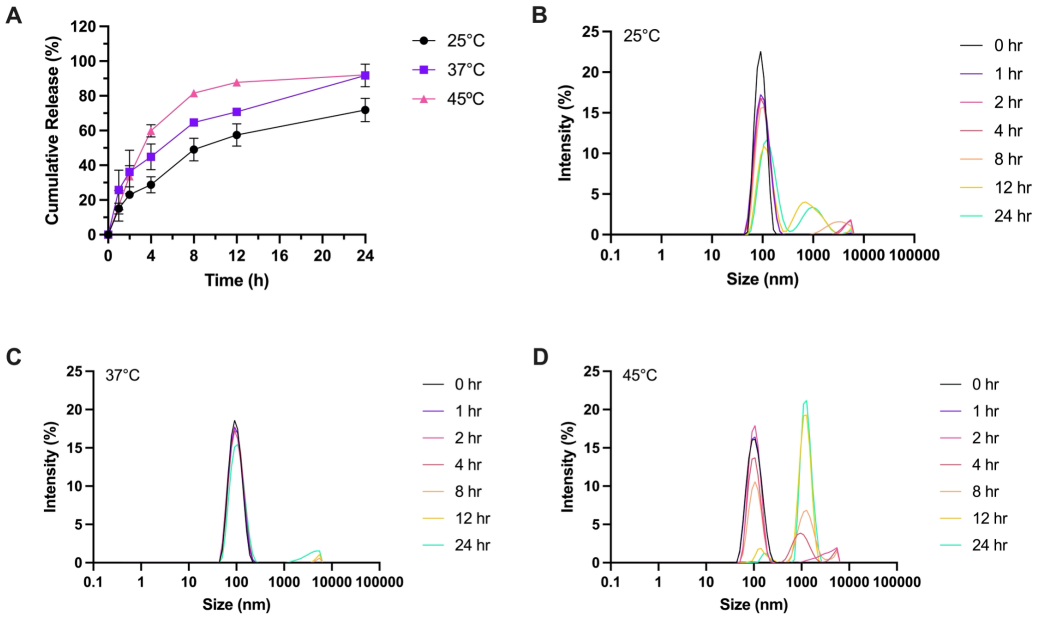

Figure 39. (A) Rate of DOX release from liposomes in release media consisting of phosphate buffered saline (1X, pH 7.4) under rotational agitation at different incubation temperatures using an *in vitro* release assay under development; (B-D) Particle size distribution analysis to evaluate the impact of temperature on empty liposome structural quality while facilitating DOX release (mean ± SD, n = 3).

3.5.6.3 Concentration study at reduced agitation & temperature

Based on the results of the agitation and temperature studies in Fig. 38 and 39, the dissolution profile of Doxil® was evaluated at the reduced agitation speed and temperature, 20 RPM and 37°C to study its influence on the quality of the liposome structure during dissolution. Fig. 40 shows the concentration-dependent dissolution profiles of Doxil® at reduced agitation and temperature, and Fig. 41 shows its impact on the liposome quality during dissolution.

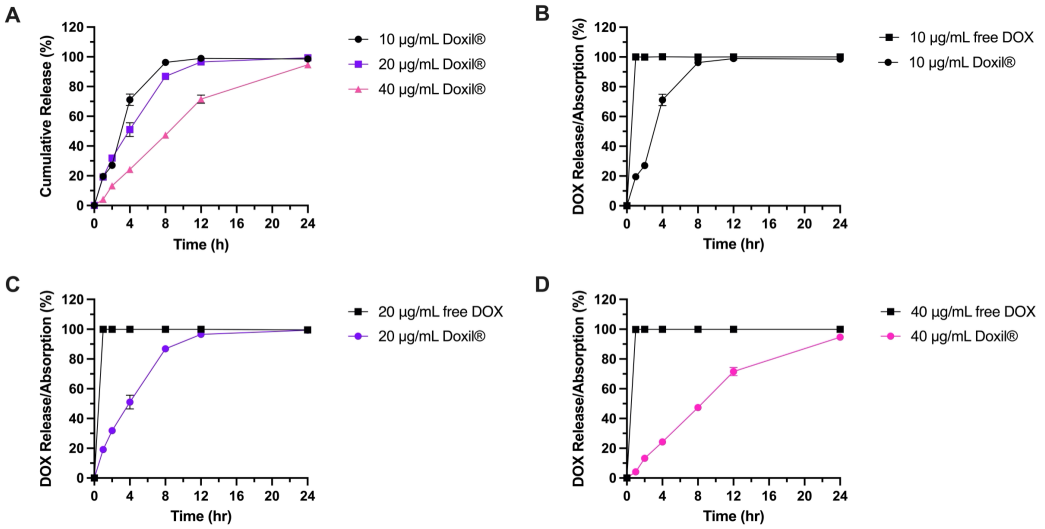

Figure 40. Rate of DOX release from liposomes at increasing concentrations using 200 mg Biobeads to absorb released DOX tested at lower agitation speed and temperature, 20 RPM and 37C, to evaluate the ability to retain the empty liposome structure upon DOX release (mean ± SD, n = 3).

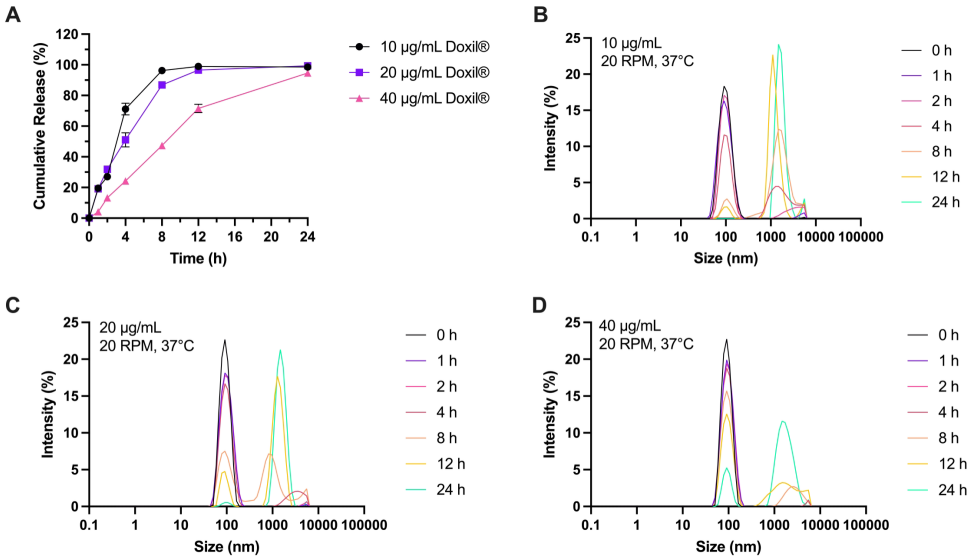

Figure 41. Time-dependent particle size analysis for DOX release assay under development at reduced agitation speed and temperature, 20 RPM and 37°C, to improve the structural quality of the empty liposome while facilitating complete drug release from the liposome (mean ± SD, n = 3).

Rate of DOX release in Fig. 40 at the reduced speed and temperature follows the same trend as in the data shown in Fig. 34 under initial speed and temperature of 40 RPM and 45°C, but with a greater degree of discrimination between test concentrations and a slower, more controlled release profile at the 10 and 20 µg/mL conditions. Greater than 90% cumulative release is achieved within 8 hours converging to complete release at 12 hours for both test

conditions when compared with an equivalent free DOX control. However, slower agitation at the reduced temperature of 37°C reintroduces liposome breakage at 20 RPM in Fig. 41C and a remnant liposome population observed in Fig. 41D for the 40 µg/mL test condition.

3.5.7 Cyclodextrin addition to release media

Fig. 42 shows the effect of adding 5% *w/v* of cyclodextrin or dextrose to the PBS dissolution medium to the dissolution profile of Doxil® and its liposome structural quality at 20 RPM and 37°C. Addition of γ-cyclodextrin to PBS when dissolved with the Doxil® formulation to its drug-in-media test concentration of 10 µg/mL results in near elimination of the liposome population from the dissolution media in Fig. 42D and formation of lipid aggregates

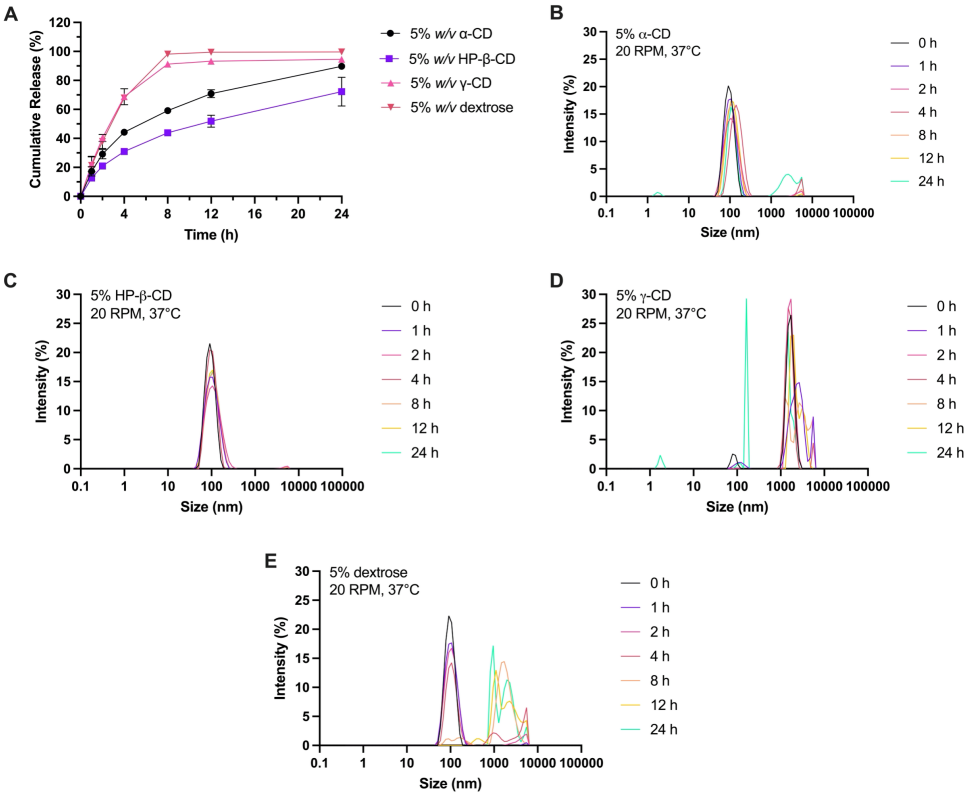

Figure 42. Effect of cyclodextrin type on DOX release from liposomes (10 µg/mL) and liposome structural quality upon DOX release in phosphate buffered saline (1X, pH 7.4) with 200 mg Biobeads at 20 RPM and 37°C (mean ± SD, n =3).

in the water dispersant within 1 hour of dissolution for detection in particle size analysis. However, only 22.2 ± 5.1% of encapsulated DOX is released and detected by fluorescence spectrometry in 1 hr.

Addition of α- and hydroxypropyl-β-cyclodextrin resulted in slower, more gradual release rates in the dissolution medium with little to no liposome breakage observed over the duration of the dissolution study in Fig. 42B and C, respectively. A compromise in cumulative release was observed with the addition of hydroxypropyl-β-cyclodextrin to retain the empty liposome structure in Fig. 42C, achieving 72.3 ± 9.9% DOX release within 24 hours. Greater than 80% cumulative release was observed with a slower rate and extent of liposome structure disruption within 24 hours upon addition of 5% *w/v* of α-cyclodextrin to the PBS dissolution medium.

Adding dextrose also results in the disruption of the liposome membrane, although slower than γ-cyclodextrin, resulting in complete destruction within 8 hrs. However, within 8 hours, 100% of DOX encapsulated in liposomes is released in dissolution media containing PBS (1X, pH 7.4) and 5% *w/v* dextrose. For γ-cyclodextrin, it appears that the previous assumption that free, released DOX is immediately absorbed by bio-beads in aqueous media is violated in this case due to the disparate difference in the expected and actual quantity of released DOX despite experimental evidence that the liposome structure has been severely compromised and thus, drug release may be rapid. However, due to the unique physicochemical properties of cyclodextrins and doxorubicin, an alternative explanation may account for the reduced release rate.

Cyclodextrins can form inclusion complexes with hydrophobic drugs in its inner cavity, and in aqueous solution, drug molecules under complexation exist in dynamic equilibrium with free drug molecules in solution [115]. Therefore, with either media dilution upon sampling and replacement during the dissolution study or by competitive complexation by other molecules like cholesterol from the liposome membrane, the rate of drug release will also be influenced by the rate of complexation by cyclodextrins. The same study reported inner cavity diameters for α-, HP-β-, and γ-cyclodextrins ranging from 4.7-5.3 for α, 6.0 for HP-β, and 7.5-8.3 angstroms for γ-cyclodextrin [115]. Another study by Peng *et al* applied molecular modeling to determine the complexation modes of DOX with HP-β-CD and determined the simulated distance between H_a and H_b on the antherene ring in the chemical structure of doxorubicin in Fig. 43 was 7.6 angstroms [114]. Given the property data for γ-cyclodextrin, it may be possible that released DOX from liposomes could fit in the inner cavity of γ-cyclodextrin molecules, and competitive

mechanisms for complexation and adsorption were at play which resulted in the difference between apparent and actual rate of DOX release from liposomes.

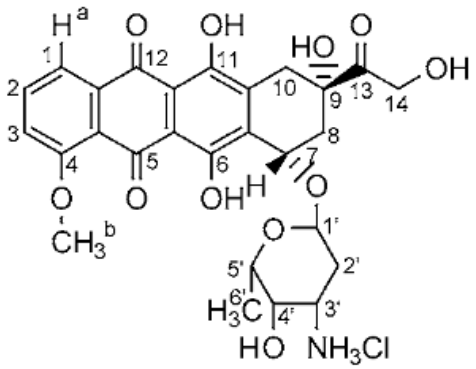

Figure 43. Chemical structure of doxorubicin [114].

3.5.8 Discriminative capability of developed assay

After establishment of the assay conditions for *in vitro* release method development, the discriminative capability of the assay must be assessed to determine the assay's sensitivity to distinguish minor variations in processing, formulation and/or structural differences that influence the dissolution profile of the liposomal drug product. A study by Yuksel *et al* evaluated the application, usefulness and considerations utilizing ANOVA-based, model-dependent methods and model-independent f_1 *and* f_2 methods for the comparison of *in vitro* dissolution profiles [118]. Results of ANOVA based methods and model-dependent methods were described as more discriminative, given validation of statistical assumptions necessary for use of the model and detailed information in level and shape of the dissolution profile that can be accomplished using ANOVA-based methods [118]. For the purposes of rapidly determining the discriminative capability in each assay for further optimization, ANOVA-based methods using Tukey's multiple comparisons were applied. This was done to determine if a statistical significance existed between liposomal DOX formulations compromised with increasing levels of free DOX or freeze thaw stress.

3.5.8.1 Differentiating between Doxil® formulations with increasing free drug ratios

We evaluated the ability of the optimized assay to distinguish between Doxil® formulations containing different amounts of free DOX. Prepared mixtures consisting of 0 to 20% free DOX were spiked into a corresponding amount of Doxil® totaling 100% to prepare a

10 µg/mL drug-in-media solution for each test condition. As illustrated in Fig. 44, dissolution profiles were largely similar and was confirmed through statistical analysis methods to determine discriminative capability. Non-significant differences exist between dissolution profiles of Doxil® compromised with 2.5 to 20% of free DOX when compared with the 100% Doxil (0% free DOX) sample ($F(25, 50) = 0.8022$; $p = 0.72$). This indicates that the single-vial assay developed using 200 mg of Bio-bead SM-2 resin at 20 RPM and 37°C is not capable of distinguishing between formulations with intrinsic differences, like the amount of free versus encapsulated drug present in each formulation.

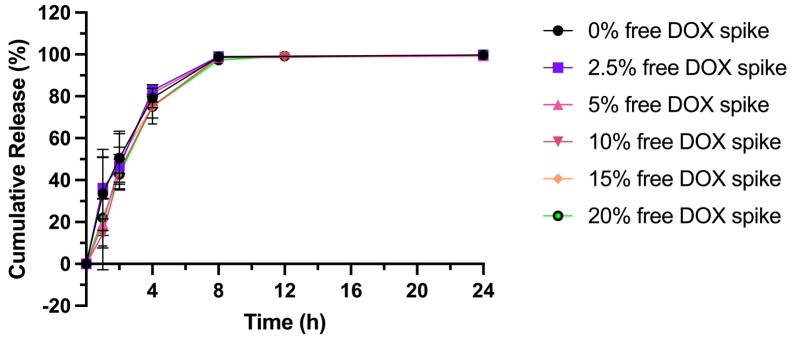

Figure 44. First evaluation for discriminatory ability of the *in vitro* release assay under development using Biobead SM-2 resin as sink agent by spiking increasing levels of free DOX (2 mg/mL) prepared in 9.4% sucrose, 1.55 mg/mL L-histidine, pH 6.5 to Doxil® (liposomal doxorubicin hydrochloride formulation) under optimized assay conditions (20 RPM, 37°C) with 200 mg Biobeads for sink condition (mean ± SD, n = 3).

3.5.8.2 Application of freeze-thaw stress for storage and handling considerations

Lastly, we applied different amounts of freeze thaw stress to Doxil® formulations to determine if the assay was capable of distinguishing between compromised formulations due to variations in processing, storage and handling. Doxil® samples were rapidly frozen for 3 minutes with liquid nitrogen and immediately thawed in a water bath at 55°C for an equivalent amount of

time for 4, 7 or 10 cycles. A negative control with zero freeze thaw stress applied was included for comparison.

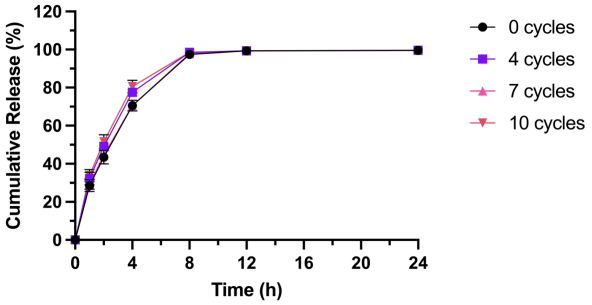

Figure 45. Second evaluation for discriminatory ability of the *in vitro* release assay under development by applying freeze thaw stress to a commercial Doxil® formulation to introduce meaningful differences to the liposome structure and assess the capability of the assay to distinguish between these formulations under optimized assay conditions (20 RPM, 37°C) using 200 mg Biobeads for sink condition (mean ± SD, n = 3).

In Fig. 45, the difference between dissolution profiles of Doxil compromised by freeze thaw stress is statistically significant, indicating that this single-vial assay is capable of distinguishing between formulations of the same composition with meaningful differences due to variations in processing, storage and/or handling ($F(18, 36) = 4.015$; $p < 0.001$). Evaluation of freeze thaw stress is relevant storage and drug product stability, and the ability of the assay to reliably assess the performance and distinguish between formulations kept under different storage conditions. We acknowledge that this is only one method to evaluate the impact of storage and drug product stability on the *in vitro* performance of compromised and uncompromised liposomal DOX products, however, the intent was to assess the discriminative capability of the assay in relevant conditions related to manufacturing, storage, and/or handling.

3.6 Conclusion

Using a non-compendial microtube system, we have developed and optimized an *in vitro* release method for Doxil® using Bio-bead SM-2 resin as a novel sink agent. We optimized parameters such as concentration, temperature, agitation and media composition to achieve sink conditions using the bio-beads and conducted preliminary tests to evaluate the discriminative ability of the developed assay. The optimized assay conditions include release media consisting of 1X phosphate buffered saline at pH 7.4 with 5% *w/v* α-cyclodextrin, 10 µg/mL drug-in-media concentration, rotational agitation at 20 RPM, and incubation temperature of 37°C. These

conditions were then used to evaluate the discriminative ability of the assay to distinguish between Doxil® formulations subjected to varying cycles of freeze thaw stress and increasing free drug content. The method proved reliable for distinguishing between formulations subjected to different cycles of freeze thaw stress but was insensitive to detect intrinsic differences in liposomal formulations with levels of free doxorubicin content up to 20%. Further optimization of the release assay is warranted to increase the sensitivity of the release assay for its use in formulation evaluation and quality control of generic and innovator drug product development.

Chapter 4 Drug Adsorption to Microtubes Impacting the Reliability of *In Vitro* Dissolution Testing: A Case Study on *Doxorubicin Hydrochloride*

4.1 Abstract

Accurate *in vitro* release testing is essential for evaluating the performance and quality of complex formulations, particularly for assessing the bioequivalence of generic liposomal drug products. However, incomplete drug recovery due to non-specific drug adsorption can compromise mass balance and dissolution data integrity. This study investigates the critical assay parameters influencing the rate and extent of doxorubicin hydrochloride (DOX) adsorption to microtubes during dissolution. Using a validated UPLC-TUV method, we quantified DOX adsorption under various conditions, including drug concentration, temperature, agitation speed, tube material, volume-to-surface area ratio, and media composition.

Standard, untreated polypropylene microtubes, specifically Eppendorf® Natural 1.5 mL microtubes, exhibited the greatest extent of DOX adsorption compared with other microtube brand types, with up to 35.5% loss in 24 hours at 37°C. DOX adsorption decreased with increasing drug concentration, saturating adsorptive binding sites in polypropylene microtubes at 180 µg/mL. Higher temperatures increased adsorption, while faster agitation reduced adsorption. Inner surface area to volume ratio significantly influenced DOX binding in 2.0 mL microtubes, with less pronounced effects in 1.5 and 5.0 mL microtubes.

Tube material and composition affected drug adsorption, with polyethylene and polypropylene copolymers demonstrating reduced binding compared to untreated polypropylene and polystyrene. Media composition also played a role; organic solvents and cyclodextrin-containing buffers reduced DOX adsorption due to different mechanisms for surface interaction. These findings highlight the critical need to consider material-based drug loss due to adsorption in dissolution assay design. Optimizing assay parameters and selecting appropriate microtubes can mitigate non-specific adsorption and improve the reliability of *in vitro* release testing, particularly for amphiphilic drugs with a propensity to adsorb to plastic materials. This work

offers practical insights for regulatory and quality control settings involving complex liposomal generics.

4.2 Introduction

In vitro dissolution testing is a critical quality attribute used to evaluate product performance and establish quality control for drug formulations [119, 120]. The purpose of dissolution testing is to identify and assess the variables affecting the rate and extent of drug release from the final dosage form under conditions that reflect and simulate *in vivo* performance [119]. When used as a comparative tool for generic drug development, matching dissolution profiles and cumulative release specifications suggests a degree of physicochemical similarity likely to translate to comparable therapeutic performance.

Reliable assessment of drug dissolution depends on accurately measuring drug recovery in the release media over time to generate a dissolution profile reflecting the rate and extent of release [119, 121]. Maintaining accurate mass balance in dissolution testing is essential. If mass balance is compromised, the credibility of the data is undermined, potentially misrepresenting the release characteristics of the test formulation which could lead to adverse implications for clinical performance.

Failures in maintaining mass balance during dissolution testing may arise from various sources, including the drug substance, assay conditions, or the dissolution apparatus. Drug instability in the release medium due to degradation, sampling loss, absorption into or adsorption to materials of the dissolution system are probable sources for drug loss from the solution affecting mass balance. Other sources include precipitation, molecular interactions with media components and self-association, particularly for amphiphilic molecules such as doxorubicin [122–124]. For other drug products, precipitation is often associated with insolubility in certain solvents but an alternate mechanism for doxorubicin precipitation was proposed in a research study by Yamada [122].

Yamada observed doxorubicin precipitation in neutral buffers such as phosphate buffered saline at pH 7.2 and 5-fluorouracil and heparin drug solutions [122]. Using mass spectrometry and a reaction model with hydroxylamine, the mechanism of doxorubicin precipitation was determined to be due to dimerization of doxorubicin molecules, occurring due to deprotonation of the α-hydroxy ketone carbon-14 group of one doxorubicin molecule and the molecular interaction of the resultant product with the amine group of a second doxorubicin molecule

followed by oxidation [122]. Yamada investigated the temperature dependence of doxorubicin precipitation in phosphate buffered saline at 25, 37 and 60°C which revealed rapidly increasing levels of precipitation at higher temperatures up to ~90% within 24 hours, and the pH dependence on doxorubicin precipitation [122]. For pH dependence, ~90% precipitation was observed in alkaline solutions while ~10% precipitation was observed in acidic solutions [122]. In reference to the conditions evaluated in the prior study, drug precipitation is a significant factor to consider for mass balance in dissolution testing because it may decrease the apparent concentration of doxorubicin in the dissolution medium, which may result in an underestimation of drug release and recovery and could compromise mass balance [123].

Drug loss may also result from chemical degradation or molecular interactions with media components reducing the effective drug concentration in the dissolution media and compromise mass balance. Kaushik and Bansal demonstrated the impact of chemical degradation on doxorubicin using forced degradation studies testing acidic, neutral and basic hydrolytic stress at various temperatures, and oxidative and photolytic stress under conditions in accordance with the International Conference for Harmonization (ICH) Q1(R2) guidelines [125]. Several doxorubicin degradation products were formed and identified using liquid chromatography-mass spectrometry techniques for the stress conditions tested due to chemical degradation. Stability of the drug substance is critical for accurate measurement of dissolution performance as indicated in the guidance from the United States Pharmacopeia (USP) for dissolution method development [112]. Therefore, drug loss due to chemical degradation pathways could affect the integrity of the mass balance by reducing the amount of doxorubicin present in the dissolution media for drug release and recovery. Relatedly, molecular interactions with certain media additives, such as cyclodextrins, with the ability to form inclusion complexes with amphiphilic molecules like doxorubicin could adversely affect the amount of drug available in the dissolution medium for drug recovery.

Several studies have also demonstrated the propensity of doxorubicin to self-associate in aqueous solutions to form dimers, trimers and higher-order aggregates at very low concentrations [124, 126–128]. While solubility refers to the equilibrium concentration of a drug in its monomeric form, these aggregates can accumulate, and form supersaturated solutions at concentrations near or above its solubility limit that may appear clear but are thermodynamically unstable. Under certain stress conditions during dissolution with agitation, incubation, or pH

shifts, these supersaturated solutions may destabilize, causing the aggregates to precipitate out and decrease the dissolved drug concentration although the total drug content remains unchanged. Supersaturation and precipitation due to the self-association behavior of doxorubicin molecules is another significant issue for maintaining accurate mass balance in dissolution testing that may adversely influence analytical test results and data interpretation.

Prior literature has also explored drug adsorption in related contexts—for example, the non-specific adsorption of probe drugs to plastic containers in bioassays, the loss of acidic or basic drug content due to adsorption to polystyrene during cell culture transport experiments, and the adsorption of chloroquine to glass and plastic surfaces [129–131]. However, the impact of drug adsorption on the reliability and quality of dissolution testing remains unexplored.

Using doxorubicin hydrochloride as a model drug, this study aims to investigate the key factors influencing the rate and extent of drug adsorption under standard dissolution conditions. Our objective was to determine how various assay parameters affect drug adsorption to microtubes used in dissolution testing, and how this, in turn, influences the accuracy and reliability of dissolution results. To guide our hypothesis development, we focused on the following research questions: 1) What are the critical assay parameters that significantly influence drug adsorption to microtubes for *in vitro* dissolution testing? 2) How do the kinetics of drug adsorption contribute to discrepancies in mass balance, thereby affecting the reliability of *in vitro* drug release assessment?

We investigated parameters including drug concentration, temperature, internal surface area-to-volume ratio, tube material composition, and media composition. We hypothesized that drug adsorption would increase with higher drug concentrations, elevated temperatures, and greater surface area-to-volume ratios. Additionally, we examined the use of certain aqueous and organic additives that have been previously reported to mitigate drug adsorption in other applications. Microtubes composed of different materials were also evaluated to identify brands with low-binding affinities for amphiphilic drug molecules commonly used in accelerated release testing.

Ensuring mass balance accuracy is paramount for reliable *in vitro* release profiling of liposomal drug products and their follow-on versions. This work is critical to overcoming limitations in dissolution methods and may help explain disparities in therapeutic performance between complex generic liposomal products and their reference counterparts. It also provides

insight for regulatory agencies, offering strategies to minimize drug adsorption to enhance the reliability of bioequivalence assessments for complex generics.

4.3 Materials

Doxorubicin hydrochloride (Pharmaceutical Secondary Standard; Certified Reference Material) was purchased from MilliporeSigma (Burlington, MA, USA). Ethanol was purchased from Decon Labs, Inc. (King of Prussia, PA, USA). Gibco Phosphate Buffered Saline (PBS) (1X, pH 7.4) was purchased from Thermo Fisher Scientific (Waltham, MA, USA). 2-(N-morpholino) ethanesulfonic acid (MES), α-cyclodextrin (α-CD), (2-hydroxypropyl)-β-cyclodextrin (HP-β-CD), γ-cyclodextrin (γ-CD), and L-histidine were purchased from Sigma-Aldrich (St. Louis, MO, USA). Dextrose was obtained from VWR International (Radnor, PA, USA). Eppendorf Natural Tubes (1.5 - 5.0 mL), Eppendorf Biopur Tubes (1.5 mL), Fisherbrand Premium MCT Natural Tubes (1.5 mL,2 mL), Eppendorf Protein LoBind Tubes (1.5 mL, 5 mL), and Fisherbrand Polyethylene Sample Vials (2.5 mL) were purchased from Fisher Scientific (Waltham, MA, USA). VWR Polystyrene Microcentrifuge Tubes (2.0 mL) and Polycarbin Microcentrifuge Tubes (1.5 mL) were purchased from Avantor (Radnor, PA, USA). Axygen MaxyClear Tubes (1.7 mL) and Falcon Round Bottom Polystyrene Test Tube (5 mL) were purchased from Corning (Corning, NY, USA). Low Background Borosilicate Glass Vials (8 mL) were obtained from RPI, Corp (Mount Prospect, IL, USA). All other solvents and reagents were of analytical grade and were purchased from Fisher Scientific (Waltham, MA, USA).

4.4 Methods

4.4.1 Solubility determination for DOX in various solvents and dissolution media

Saturation solutions of doxorubicin hydrochloride were prepared by adding an excess amount of drug to 1.5 mL microtubes containing 1 mL of various organic and aqueous solvents, followed by incubation at 37°C. Solvents used for solubility analysis included (1) phosphate buffered saline (1X PBS, pH 7.4); (2) PBS solutions containing 5% w/v dextrose, α-cyclodextrin, 2-hydroxypropyl-β-cyclodextrin, or γ-cyclodextrin; (3) methanol (100%); (4) acetonitrile (100%); and (5) Doxil® formulation buffer consisting of 9.4% sucrose and 1.55 mg/mL L-histidine at pH 6.5. Each solution was prepared in triplicate and vortexed continuously for 5 minutes. The initial pH of each solution was measured and recorded.

The microtubes were then affixed to the tube clips attached to a rotating mixer (Benchmark®, Sayreville, NJ, USA) set at a maximum speed of 40 RPM and incubated at 37°C for 24 hours. Calibration standards (25-125 µg/mL) were prepared from a 1 mg/mL stock solution of doxorubicin hydrochloride dissolved in the respective solvents. Following incubation, the final pH of each solution was recorded, and doxorubicin content was quantified by UPLC-TUV.

Doxorubicin content was quantified using an Acquity UPLC-TUV detector system with Waters Empower 3 software to measure the peak AUC of doxorubicin samples in each solvent, as described in the validated method (Chapter 2, Section 2.3). Briefly, an isocratic mobile phase consisting of 45% deionized water with 0.1% formic acid (A) and 55% methanol with 0.1% formic acid (B) was pumped through an Acquity BEH C18 column (100 x 2.1 mm, 1.7 µm) at a flow rate of 0.3 mL/min for a run time of 15 minutes. The injection volume was 10 µL, and UV detection was performed at 254 nm. Solubility concentrations were determined by applying a linear regression model to the peak AUC values, with $R^2 > 0.99$ for all standard curves.

4.4.2 Selecting a model microtube for investigations of DOX adsorption

To evaluate the extent of doxorubicin (DOX) adsorption to microtubes, a pilot study was conducted using various commercially available microtubes under standard *in vitro* assay conditions. Based on prior solubility data for doxorubicin hydrochloride, test solutions were prepared in phosphate buffered saline (PBS, 1X, pH 7.4) at a sample concentration of 60 µg/mL, approximately 100-fold lower than saturation solubility. One milliliter of each solution was deposited into replicate tubes of the following microtube types: Eppendorf® Natural, Eppendorf® Biopur, Eppendorf® Protein LoBind and Fisherbrand MCT Natural microtubes. All sample tubes were affixed to tube clips attached to the rotating mixer (20 RPM) and incubated at 37°C. Prior to incubation (0-hr),100 µL aliquots were withdrawn and transferred into UPLC vials for initial concentration measurement. Withdrawn volumes were replaced with an equivalent volume of excess sample solution at 60 µg/mL to maintain constant concentration and volume. After 24 hours, final aliquots were collected from each tube type and added to UPLC vials for time 24-hour UPLC analysis.

Calibration standards (20-100 µg/mL) were prepared in PBS (1X, pH 7.4) at both timepoints, and a linear regression model was applied to determine DOX concentration using the validated UPLC-TUV method described in Chapter 2 Section 2.3. Mass balance was used to

calculate percent recovery of DOX, which was then used to calculate the percentage of DOX lost to tube adsorption (Eqn. 1).

$$Adsorbed\ DOX\ (\%) = (1 - \frac{C_{DOX,final}}{C_{DOX,initial}}) \times 100 \qquad \text{(Eqn. 1)}$$

4.4.3 Concentration dependent DOX adsorption analysis

To determine the concentration at which doxorubicin (DOX) saturates adsorption binding sites within polypropylene microtube material, a concentration-dependent DOX adsorption study was conducted. A 1 mg/mL DOX stock solution was prepared in PBS (1X, pH 7.4) using borosilicate glass vials to minimize nonspecific binding. The stock was diluted to obtain test concentrations of 60, 120, 180, and 240 µg/mL. One milliliter of each solution was dispensed into triplicate 1.5 mL Eppendorf® Natural microtubes.

The samples were incubated at 37°C for 24 hours on a Benchmark® rotating mixer set to 20 RPM. Aliquots were collected at 0 and 24 hours, and DOX concentrations were quantified using the UPLC-TUV method described in Section 4.4.1, and validated in Chapter 2, Section 2.3. Mass balance was used to calculate percent recovery of DOX, which was then used to calculate the percentage of DOX lost to tube adsorption. Equation 1 was used to calculate DOX adsorption for all subsequent studies.

4.4.4 Temperature dependent DOX adsorption analysis

Temperature-dependent adsorption of doxorubicin (DOX) adsorption to polypropene microtubes was evaluated under three test conditions: 25°C, 37°C, and 45°C. Each test condition was subjected to rotation agitation. A 60 µg/mL DOX solution was prepared by diluting a 1 mg/mL stock solution in PBS (1X, pH 7.4). One milliliter of the working solution was transferred into triplicate 1.5 mL Eppendorf® Natural microtubes for each temperature condition.

Sample tubes were affixed to tube clips on a Benchmark® rotating mixer set to 20 RPM and incubated for 24 hours at the respective temperatures. At 0 hours, 100 µL aliquots were withdrawn from each solution and transferred to UPLC vials for baseline measurements. Withdrawn volumes were replaced with fresh 60 µg/mL DOX solution in PBS. At 24 hours, final aliquots were similarly collected for analysis. Calibration standards (20-100 µg/mL) were prepared in PBS (1X, pH 7.4) at each sampling time point. DOX concentrations at 0 and 24

hours were quantified using the UPLC-TUV method described in Section 4.4.1 and validated in Chapter 2, Section 2.3.

4.4.5 Speed dependent DOX adsorption analysis

The effect of agitation speed on doxorubicin (DOX) adsorption to microtubes was evaluated by varying rotational speeds during incubation. A 1 mg/mL DOX stock solution was prepared in PBS (1X, pH 7.4) using a glass vial to minimize nonspecific adsorption. The stock was diluted to a final concentration of 60 µg/mL. For each test condition, 1 mL of the 60 µg/mL DOX solution was transferred into triplicate 1.5 mL Eppendorf Natural microtubes. Sample tubes were incubated at 37°C for 24 hours on a Benchmark® rotating mixer set to one of three agitation speeds: 10, 20, or 40 RPM. Aliquots were withdrawn at 0 and 24 hours for quantification. DOX concentrations were measured using the UPLC-TUV method described in Section 4.4.1 and validated in Chapter 2, Section 2.3.

4.4.6 Effect of inner surface area per volume ratio on DOX adsorption

The influence of microtube surface area on DOX adsorption was evaluated by varying the ratio of sample solution volume to the maximum hold volume of different microtube sizes. The maximum hold volume in 1.5, 2.0, and 5.0 mL microtubes corresponds to the surface area for DOX adsorption, and different test ratios for solution volume to microtube surface area were tested. A 60 µg/mL DOX sample solution prepared from a 1 mg/mL stock solution of DOX dissolved in PBS (1X, pH 7.4). Aliquots of varying volumes were added to 1.5 mL, 2.0 mL and 5 mL Eppendorf® Natural microtubes in triplicate to achieve volume-to-surface area ratios ranging from 0.1-1.0 (Eqn. 2). The specific sample volumes used for each tube size and condition are summarized Table 2 below.

$$V/_{SA} = \frac{Volume\ of\ DOX\ sample\ solution}{Maximum\ hold\ volume\ of\ microtube} \qquad \text{(Eqn. 2)}$$

Table 11. Sample solution volumes added to Eppendorf Natural microtubes with varied surface areas ranging from 0.1 – 1.0.

	Sample Volumes (mL)		
Volume/Surface Area Ratio	*1.5 mL Eppendorf® Natural Microtubes*	*2 mL Eppendorf® Natural Microtubes*	*5 mL Eppendorf® Natural Microtubes*
0.10	0.15	0.20	0.50
0.20	0.30	0.40	1.00
0.50	0.75	1.00	2.50
0.75	1.125	1.50	3.75
1.00	1.50	2.00	5.00

Initial and final DOX concentrations were quantified using the UPLC-TUV method described in Section 4.4.1 and validated in Chapter 2, Section 2.3. Calibration curves were generated from standards ranging from 20-100 μg/mL, prepared in PBS (1X, pH 7.4) at both 0 and 24 hours.

4.4.7 Effect of microtube material on DOX adsorption

Eight commercially available tubes composed of different materials were tested to assess the effects of tube material on DOX adsorption. Materials included various types of polypropylene, polyethylene, and polystyrene. Details regarding microtube brand, product name, capacity, and material are provided in Table 12.

Table 12. Specifications of microtubes with different material compositions.

Brand	*Product Name*	*Capacity (mL)*	*Material*
Eppendorf	Safe-Lock Tubes (Natural)	1.5	Standard polypropylene
Eppendorf	Protein LoBind Tubes	5.0	Fluorinated polypropylene
Fisherbrand	Microcentrifuge Tubes with Locking Snap Cap	2.0	Medical-grade polypropylene
Avantor (VWR)	Microcentrifuge Tubes with Socket Screw-Cap	2.0	Gamma-resistant polypropylene
Axygen	MaxyClear Snaplock Microcentrifuge Tube	1.7	Polypropylene copolymer
Polycarbin	Microcentrifuge Tubes	1.5	Polypropylene (20% Circular Economy)
Fisherbrand	Polyethylene Sample Vials	2.5	Polyethylene

Falcon	Round Bottom Polystyrene Test Tube	5.0	Polystyrene

A 60 µg/mL DOX/PBS solution was freshly prepared in borosilicate glass vials and added to each type of tube in triplicate, maintaining a constant volume-to-surface area (*V/SA*) ratio of 0.67. Due to limited availability of non-polypropene tubes, different microtube sizes were used for polyethylene and polystyrene materials. To ensure comparability across materials, the fixed V/SA ratio of 0.67– corresponding to 1 mL of DOX solution in a 1.5 mL tube– was consistently applied across all tube sizes by adjusting the sample volume for each tube accordingly. Table 13 details the specific volumes used for each microtube type, ranging from 1.5 – 5 mL.

Table 13. Sample volumes added to different sized microtubes with a fixed volume to surface area ratio of 0.67.

	Sample Volumes (mL)		
Volume/Surface Area Ratio	*1.5 mL Microtubes*	*2 mL Microtubes*	*5 mL Microtubes*
0.67	1.00	1.33	3.33

Sample tubes were incubated at 37 °C for 24 hours at 20 RPM on a Benchmark® rotating mixer. Initial and final DOX concentrations were quantified for each microtube material using the UPLC-TUV method described in Section 4.4.1, and validated in Chapter 2, Section 2.3.

4.4.8 Effect of media composition on DOX adsorption

To evaluate the effect of media composition on DOX adsorption, six media conditions were tested: Doxil® formulation buffer, methanol (100%), acetonitrile (100%), and PBS (1X, pH 7.4) solutions with 5% α-cyclodextrin, 5% hydroxypropyl-β-cyclodextrin, or 5% γ-cyclodextrin. A 60 µg/mL DOX solution was prepared from a 1 mg/mL stock solution in PBS (1X, pH 7.4) in borosilicate glass vials. For each media condition, 1 mL of the 60 µg/mL DOX solution was added to 1.5 mL Eppendorf Natural Tubes in triplicate. Sample tubes were incubated at 37 °C for 24 hours on a Benchmark® rotating mixer set to 20 RPM. Initial and final DOX concentration was quantified for each media condition using a previously validated UPLC-TUV method with freshly prepared calibration standards (20-100 µg/mL) in PBS (1X, pH 7.4) described in Section 4.4.1, and validated in Chapter 2, Section 2.3.

4.4.9 Adsorption Kinetics of DOX

To investigate the time-dependent kinetics of DOX adsorption to microtubes, 1 mL of 60 μg/mL DOX/PBS solution was freshly prepared in glass vials and transferred to 1.5 mL Eppendorf Natural Tubes in triplicate. The tubes were incubated at 37 ℃ on the rotating mixer at 20 rpm. Sample aliquots (20 μL) were taken from each solution at 0, 1, 2, 4, 8, 12, and 24 hours, and replaced with an equal amount of phosphate buffered saline (1X, pH 7.4). All samples were analyzed by UPLC immediately after collection using the UPLC-TUV method described in Section 4.4.1, and validated in Chapter 2, Section 2.3 to calculate the percentage of DOX adsorbed over time.

4.5 Results

4.5.1 Solubility determination for DOX in various solvents and dissolution media

Solubility of doxorubicin hydrochloride was determined in different buffers, solvents, and surfactants to select the appropriate test concentration for DOX below solubility limits. Using the shake-flask solubility method described in USP <1236>, we tested the solubility of doxorubicin hydrochloride in the buffer used to develop to the Doxil® formulation at pH 6.5, dissolution media consisting of phosphate buffered saline (PBS, 1X, pH 7.4), and two organic solvents – methanol and ethanol. The Doxil® formulation buffer consists of 9.4% sucrose and 1.55 mg/mL L-histidine at pH 6.5. Solubility of DOX was also estimated in the dissolution media containing PBS and 5% *w/v* of α-cyclodextrin, 2-hydroxypropyl-β-cyclodextrin, or γ-cyclodextrin.

In Table 14, saturation solubility for doxorubicin hydrochloride dissolved in the formulation buffer was 5.79 mg/mL and was used as a baseline for solubility comparison. Doxorubicin hydrochloride is most insoluble in 100% ethanol at 85.22 μg/mL, but soluble in 100% methanol at 3.07 mg/mL. This is likely due to the effect of short-chain alcohols on lipid bilayers which increase bilayer fluidity and permeability [113]. Ethanol has a stronger effect than methanol due to rapid membrane penetration related to hydrogen bonding to lipid molecules [113]. In dissolution media with cyclodextrins, lower solubility was observed with the addition of 2-hydroxypropyl-β-cyclodextrin when compared to α-cyclodextrin in PBS due to an increase in hydrophobicity from its hydroxyalkyl groups [115].

Table 14. Solubility of DOX in various solvents.

	DOX Solubility	
PBS (1X, pH 7.4) + 5% w/v γ-CD	9.13	mg/ml
PBS (1X, pH 7.4) + 5% w/v α-CD	9.01	mg/ml
PBS (1X, pH 7.4) + 5% w/v HP-β-CD	8.20	mg/ml
PBS (1X, pH 7.4) + 5% w/v dextrose	7.93	mg/ml
PBS (1X, pH 7.4)	6.05	mg/ml
9.4% sucrose + 1.55 mg/mL L-histidine, pH 6.5	5.79	mg/ml
Methanol (100%)	3.07	mg/ml
Ethanol (100%)	85.22	μg/ml

Cyclodextrins are known for solubilizing organic compounds, such as doxorubicin hydrochloride, by forming inclusion complexes in its inner cavity [114, 115]. Cyclodextrin addition to phosphate buffered saline (PBS, 1X, pH 7.4) increases DOX solubility in PBS with a relative increase in cyclodextrin size. Each solution was evaluated for doxorubicin solubility for a subsequent study on the impact of media composition on drug adsorption to microtubes.

Based on the solubility data for the PBS, a test concentration was selected for doxorubicin hydrochloride that was approximately 100-fold beneath the solubility limit for subsequent investigations at 60 μg/mL. The assay conditions used for this drug adsorption investigation mirrored the optimized conditions established for the *in vitro* dissolution assay described in Chapter 3 excluding the use of the Bio-bead resin. Initial assay conditions include the dissolution media as phosphate buffered saline (PBS, 1X, pH 7.4), agitation speed as 20 RPM, and assay temperature as 37°C.

4.5.2 Selecting a model microtube for investigations of DOX adsorption

To begin our investigation, a model tube for adsorption must be identified based on its high propensity to absorb doxorubicin. In Fig. 46A, doxorubicin adsorption to microtubes of various brands and types was measured. Fig. 46B shows doxorubicin adsorption as a function of concentration at time zero and after 24 hours under agitation at 20 RPM and incubation at 37°C on a rotating mixer (Benchmark®, Sayreville, NJ, USA). Statistical analysis was performed using an ordinary one-way ANOVA. A statistical difference exists among means for the treatment

group: microtube brand/type (F (8,18) = 94.01; $p = 0.001$).

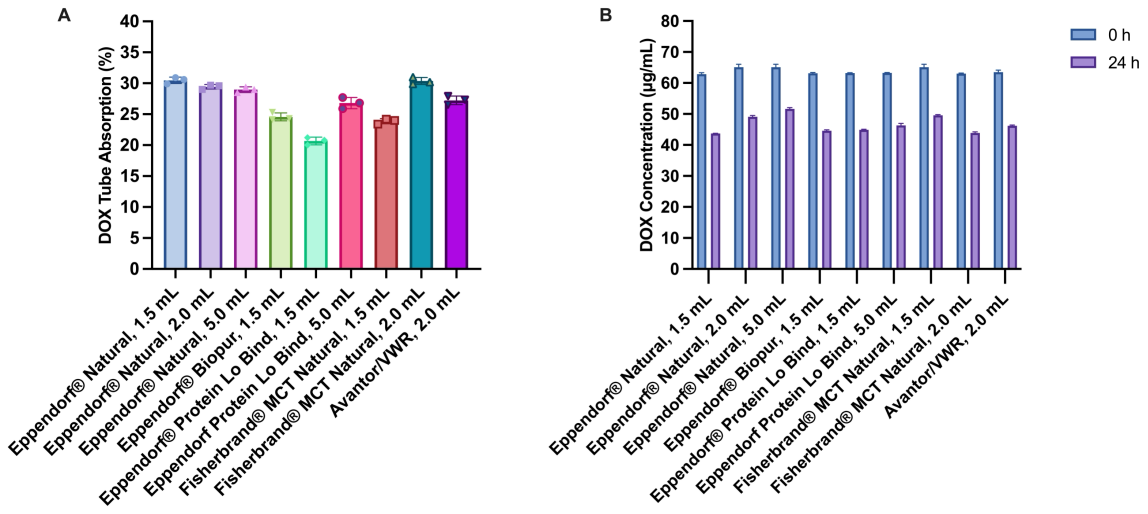

Figure 46. DOX adsorption to different brands of microtubes for the identification of a model tube for DOX adsorption in phosphate buffered saline (1X, pH 7.4) under mild agitation at 20 RPM and 37°C, reported as A) percentage, and B) initial and final concentration at 0 and 24 hours (mean ± SD, n = 3).

DOX adsorption to Eppendorf® Natural microtubes of varying sizes is statistically different than all microtubes except for the 2 mL Fisherbrand® MCT Natural tubes. Non-significant differences in DOX adsorption are observed between 1.5 mL Eppendorf® Biopur tubes and Fisherbrand® MCT Natural tubes in addition to 5 mL Eppendorf® Protein Lo Bind tubes and 2 mL Avantor/VWR microtubes. In Fig. 46, the greatest amount of DOX adsorption was to 1.5 mL Eppendorf® Natural and Fisherbrand® Natural microtubes at 30.5 ± 0.5% and 30.4 ± 0.6%, respectively. Pairwise comparisons for each pair in Fig. 46B are all statistically significant between initial and final concentrations across microtube brand and type. The least amount of DOX adsorption was observed at 20.7 ± 0.6% using 1.5 mL Eppendorf® Protein Lo Bind microtubes. Eppendorf® Natural, 1.5 mL microtubes were selected as the model tube for subsequent adsorption studies.

4.5.3 Effect of doxorubicin concentration on adsorption

Fig. 47 reveals the concentration-dependent nature of DOX adsorption to microtubes under normal dissolution conditions. Using 1.5 mL Eppendorf® Natural microtubes, the influence of concentration on the extent of drug adsorption was observed for doxorubicin hydrochloride at 20 RPM and 37°C. In a study conducted by Palmgren *et al* on drug adsorption

to plastic containers and well plates during cell culture, the effect of drug concentration on adsorption revealed that higher drug concentrations in solution corresponded to a reduced proportion of drug loss due to adsorption of drug to polystyrene tube materials.

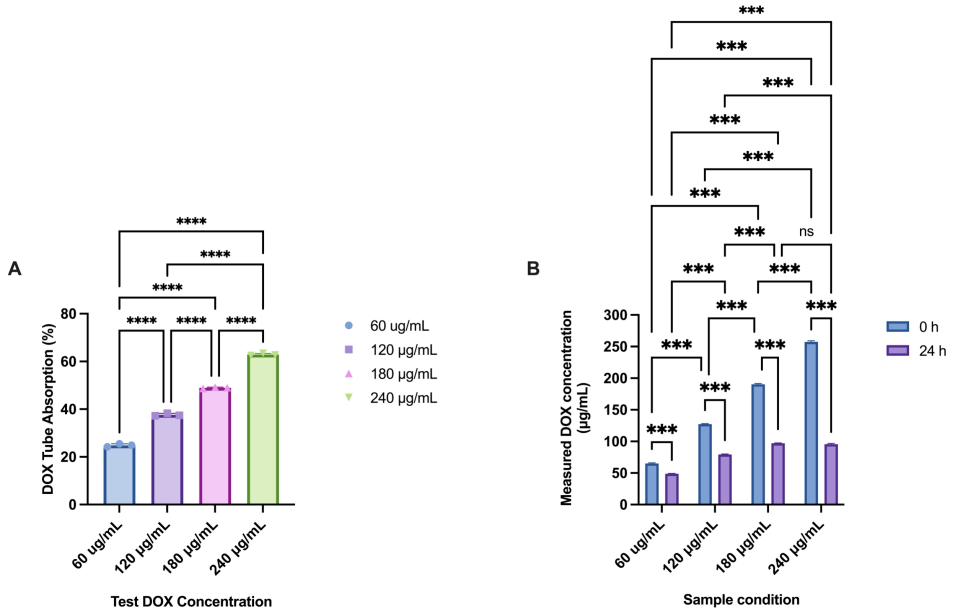

Figure 47. Concentration dependence of DOX adsorption to standard, natural polypropylene Eppendorf® microtubes at a fixed volume to surface area ratio of 1 mL to 1.5 mL in phosphate buffered saline (1X, pH 7.4) at 20 RPM and 37°C, reported as A) percentage, and B) initial and final concentration at 0 and 24 hours (mean ± SD, n = 3).

Our working hypothesis for this study was that the higher the drug concentration, the lower the proportional amount of drug loss until full saturation of the adsorption binding sites is reached for a 1 mL drug solution at 37°C. Our testing concentrations were 120, 180 and 240 µg/mL, 2 to 4 times the original test concentration of 60 µg/mL which was included for comparison. The results shown in Fig. 47A and 47B confirm our hypothesis as drug saturation of adsorptive binding sites was reached at 180 µg/mL indicated by a non-significant difference in final concentration for sample solutions prepared at 180 and 240 µg/mL. Fig. 47A shows a linear, proportional increase in DOX adsorption with increasing drug concentration in media for a fixed volume and surface area.

4.5.4 Effect of temperature on doxorubicin adsorption

Fig. 48 shows the temperature dependent adsorption of doxorubicin to Eppendorf® Natural microtubes using a fixed solution volume, surface area and agitation speed under normal dissolution conditions. Our working hypothesis was that as the test temperature increases, DOX

adsorption to standard, untreated polypropylene microtubes will increase. The data illustrated in Fig. 48A and B confirms our hypothesis with statistical significance ($F(2, 6) = 426.6$, $p < 0.0001$). At 25°C, 6.03 ± 1.16 % DOX was adsorbed by the polypropylene microtube compared to 23.7 ± 1.41 % at 37°C and 50.2 ± 2.67 % at 45°C.

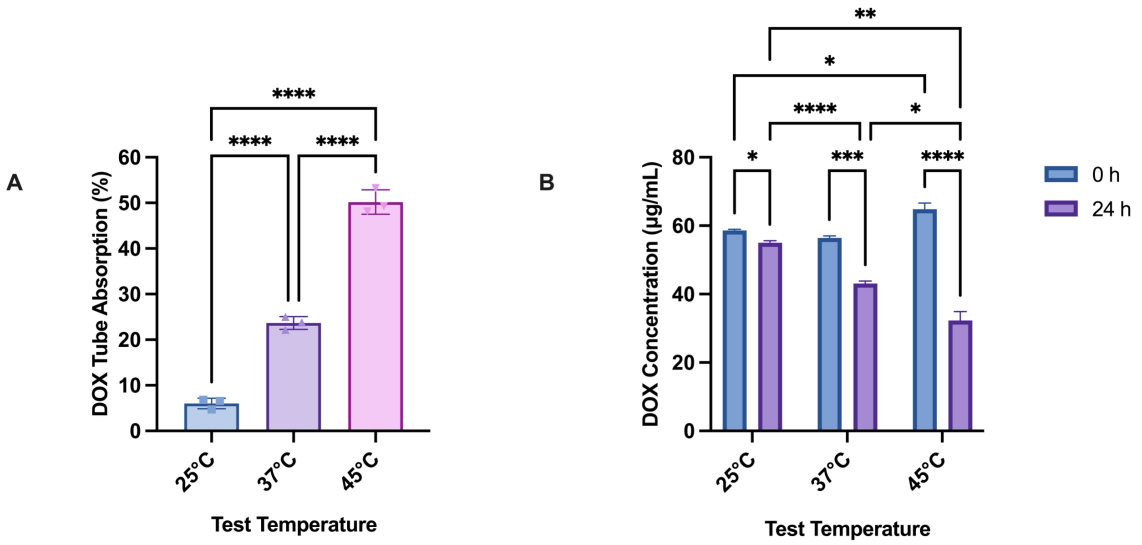

Figure 48. Temperature dependence of DOX adsorption to standard, natural polypropylene Eppendorf® microtubes at a fixed volume to surface area ratio of 1 mL to 1.5 mL in phosphate buffered saline (1X, pH 7.4) at 20 RPM, reported as A) percentage, and B) initial and final concentration at 0 and 24 hours (mean ± SD, n = 3).

Increasing temperature will increase the rate of molecular interactions due to an increase in kinetic energy of the molecules in solution leading to more frequent collisions between molecules and surfaces in the physical system. As temperature increases, an increase in DOX adsorption was observed which is due to the increased molecular interactions between free doxorubicin and polypropylene comprising the chemical nature of the Eppendorf® Natural microtube.

4.5.5 Effect of agitation speed on doxorubicin adsorption

Fig. 49 illustrates the effect of agitation speed on DOX adsorption to untreated, polypropylene Eppendorf® Natural microtubes at 37°C. DOX adsorption to polypropylene, Eppendorf® Natural microtubes is only statistically significant for comparisons with the agitation speed set to 40 RPM, in which DOX adsorption was significantly lower ($F(2, 6) = 118.9$; $p < 0.001$). At 10 RPM, 23.1 ± 1.35 % DOX was adsorbed by the polypropylene microtube compared to 24.9 ± 0.49 % at 20 RPM and 14.6 ± 0.49 % at 40 RPM.

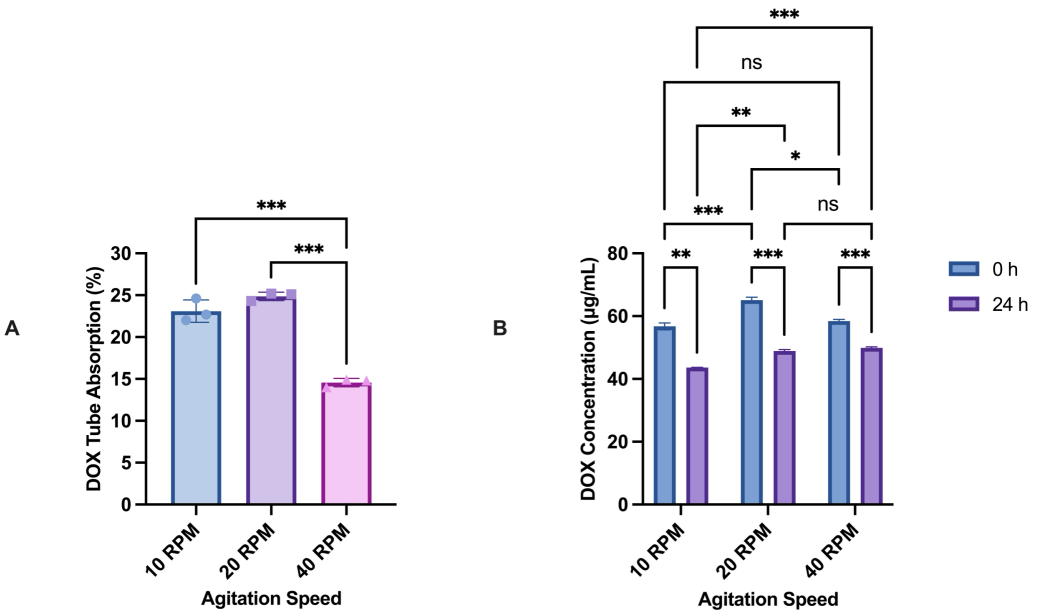

Figure 49. Speed dependence of DOX adsorption to standard, natural polypropylene Eppendorf® microtubes at a fixed volume to surface area ratio of 1 mL to 1.5 mL in phosphate buffered saline (1X, pH 7.4) at 37°C, reported as A) percentage, and B) initial and final concentration at 0 and 24 hours (mean ± SD, n = 3).

A plausible explanation for the reduction in DOX adsorption at higher agitation speeds may be due to the reduced contact time and shear force between the drug molecules in solution with the polypropylene molecules of the microtube due to the extent of physical agitation. The source of agitation was rotational using a Benchmark® rotating mixer for thorough mixing, reducing the prevalence of any dead zones for air pockets to form during mixing. It may be likely that the rapid speed of mixing could limit the extent of molecular interactions between free doxorubicin and polypropylene, but further investigation is warranted.

4.5.6 Effect of inner surface area per unit volume ratio on doxorubicin adsorption

To evaluate DOX adsorption to the inner surface area of microtubes with different nominal capacities (1.5 mL, 2.0 mL, and 5.0 mL), we conducted a study varying the solution volume to test a range of volume-to-inner surface area (V/SA) ratios from 0.1 to 1.0 to quantify the extent of drug adsorption to polypropylene, Eppendorf® Natural microtubes under otherwise identical conditions. Statistical analysis was performed within each tube group to determine whether differences in *V/SA* ratio significantly impacted drug adsorption using an ordinary one-way ANOVA and Tukey's multiple comparisons test. Our working hypothesis was that as the

ratio of solution volume to inner surface area of the microtube increased, DOX adsorption to the polypropylene tube would decrease.

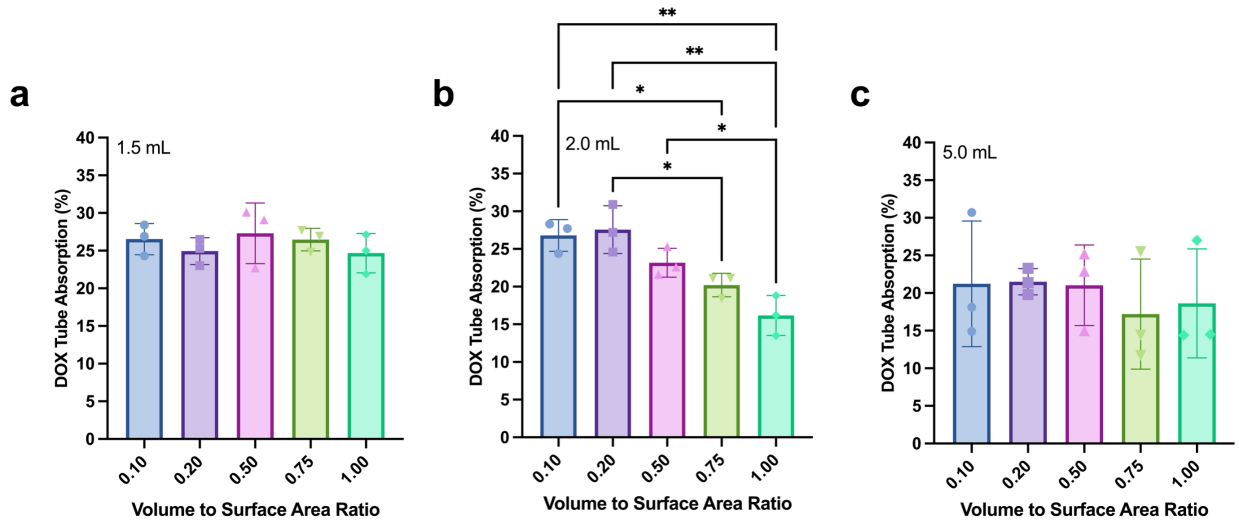

Figure 50. The influence of volume to inner surface area ratio on DOX adsorption in standard, natural polypropylene Eppendorf® microtubes of varying sizes in phosphate buffered saline (1X, pH 7.4) at 20 RPM and 37ºC for 24 hours as a percentage (mean ± SD, n = 3).

Non-significant differences in DOX adsorption were observed for increasing *V/SA* ratios for 1.5 mL and 5 mL polypropylene, Eppendorf® Natural microtubes. Interestingly, only the 2.0 mL microtube group exhibited statistically significant differences across *V/SA* ratios ($F(4, 10) = 12.20$; $p < 0.001$). Within this group, drug adsorption consistently decreased as the *V/SA* ratio increased, suggesting that a greater proportion of the drug remained in solution when the surface area per unit volume was reduced. This trend aligns with reports in literature, as lower *V/SA* ratios correspond to a higher plastic surface area relative to the solution volume, thereby increasing the likelihood of nonspecific binding [131, 132]. As the *V/SA* ratio increased, the available binding surface area per unit volume decreased, resulting in less drug loss due to adsorption.

The absence of statistically significant trends in the 1.5 mL and 5.0 mL microtube groups may be explained by the different surface area-to-volume dynamics related to their tube geometry. Due to their small size, 1.5 mL microtubes have a relatively high surface area-to-volume ratio by default which means that small volumes are exposed to a large amount of plastic surface relative to the solution volume [132]. This can result in consistently high adsorption across all *V/SA* ratios tested, making changes in *V/SA* ratio imperceptible if adsorption was

already at its maximum. Conversely, although the inner surface area is larger in 5 mL tubes, the larger size of the tube leads to a lower overall surface area per unit volume. This lower *V/SA* ratio may have make the tubes less sensitive to changes in solution volume affecting DOX adsorption to the surface within the tested range.

4.5.7 Effect of microtube material on DOX adsorption

Drug adsorption to microtubes comprised of treated and untreated polypropylene, polyethylene and polystyrene was investigated to identify the material compositions that are prone to surface binding and adsorption of DOX, particularly for use in *in vitro* dissolution testing. Fig. 51 shows the extent of DOX adsorption to the different material microtube compositions. Statistical differences in DOX adsorption are observed between polyethylene versus all polypropylene tube types and polyethylene versus polystyrene microtubes ($F(5, 12) = 31.40$; $p < 0.001$). Only polypropylene copolymer tubes show statistical differences in DOX adsorption from polystyrene microtubes compared with the other polypropylene treated types. Statistical differences within treated and untreated polypropylene types were between medical-grade polypropylene and gamma-resistant polypropylene in comparison with the polypropylene copolymer tube.

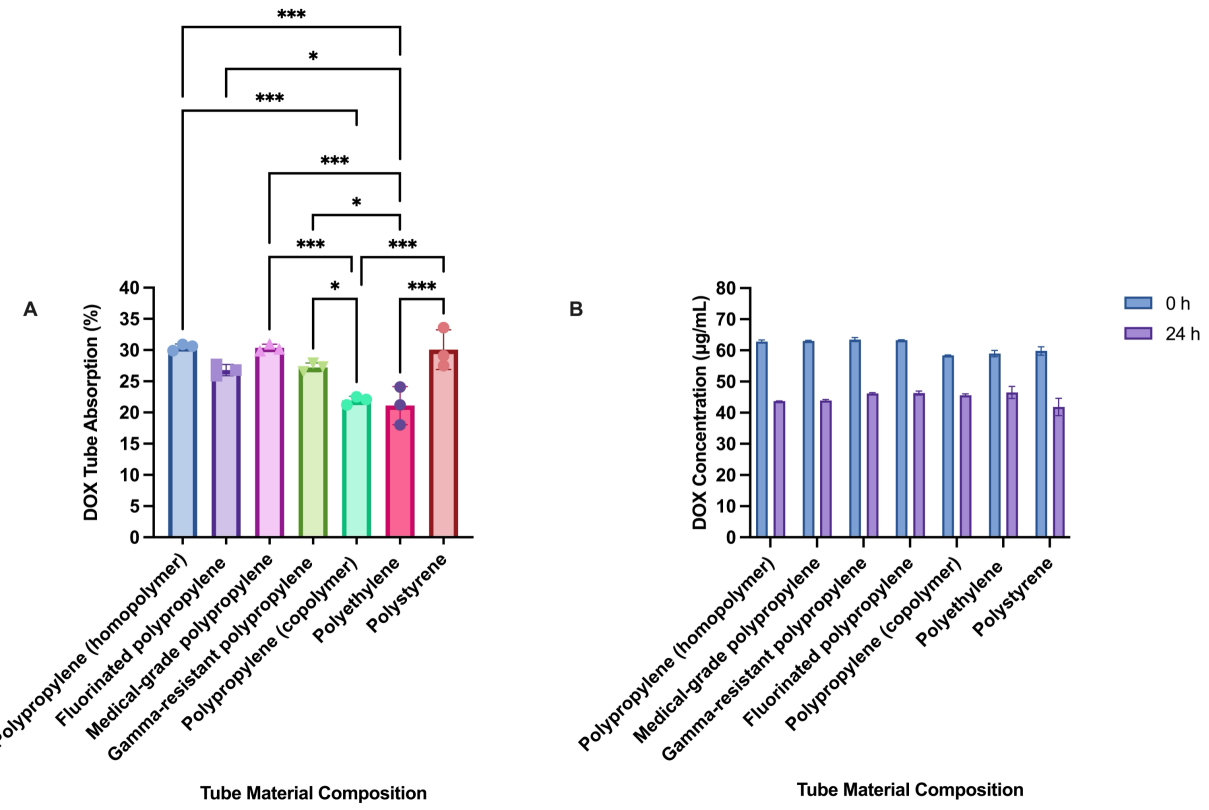

Figure 51. Microtube material composition on the extent of DOX adsorption to 1.5 mL standard, natural polypropylene Eppendorf® microtubes in phosphate buffered saline (1X, pH 7.4) at 20 RPM and 37ºC as A) percentage, and B) initial and final concentration at 0 and 24 hours (mean ± SD, n = 3).

Microtube composition corresponded to the microtube brands previously listed in Table 3. In Fig. 51A, polyethylene and polypropylene copolymer showed the lowest extent of DOX adsorption over 24 hours under dissolution conditions at 20 RPM and 37°C at 21.1 ± 3.05 % and 21.9 ± 0.67 %, respectively. Polypropylene homopolymer and polystyrene showed the greatest levels of DOX adsorption which were comparable at 30.5 ± 0.51 % and 30.1 ± 3.16 %, respectively. Fluorinated polypropylene as in the Protein Lo Bind Technology reduced the extent of DOX adsorption when compared with standard, untreated polypropylene but is found to demonstrate higher levels of adsorption than polyethylene.

4.5.8 Effect of media composition on DOX adsorption

Fig. 52 shows the influence of different solutions and solvents as the dissolution media on the extent of DOX adsorption to 1.5 mL polypropylene, Eppendorf® Natural microtubes. It has been previously reported that certain formulation additives, such as surfactants, can exhibit preferential binding to adsorptive sites on microtube surfaces, potentially displacing drug

molecules or altering the extent of drug loss due to nonspecific adsorption [133]. Other studies have shown that low polarity organic solvents are able to extract materials from plastic containers and may reduce the extent of non-specific adsorption of hydrophobic and amphiphilic drugs [134, 135]. Cyclodextrins, organic solvents and aqueous buffer solutions resembling the formulation buffer of Doxil® were tested in this media composition study for their impact on DOX adsorption.

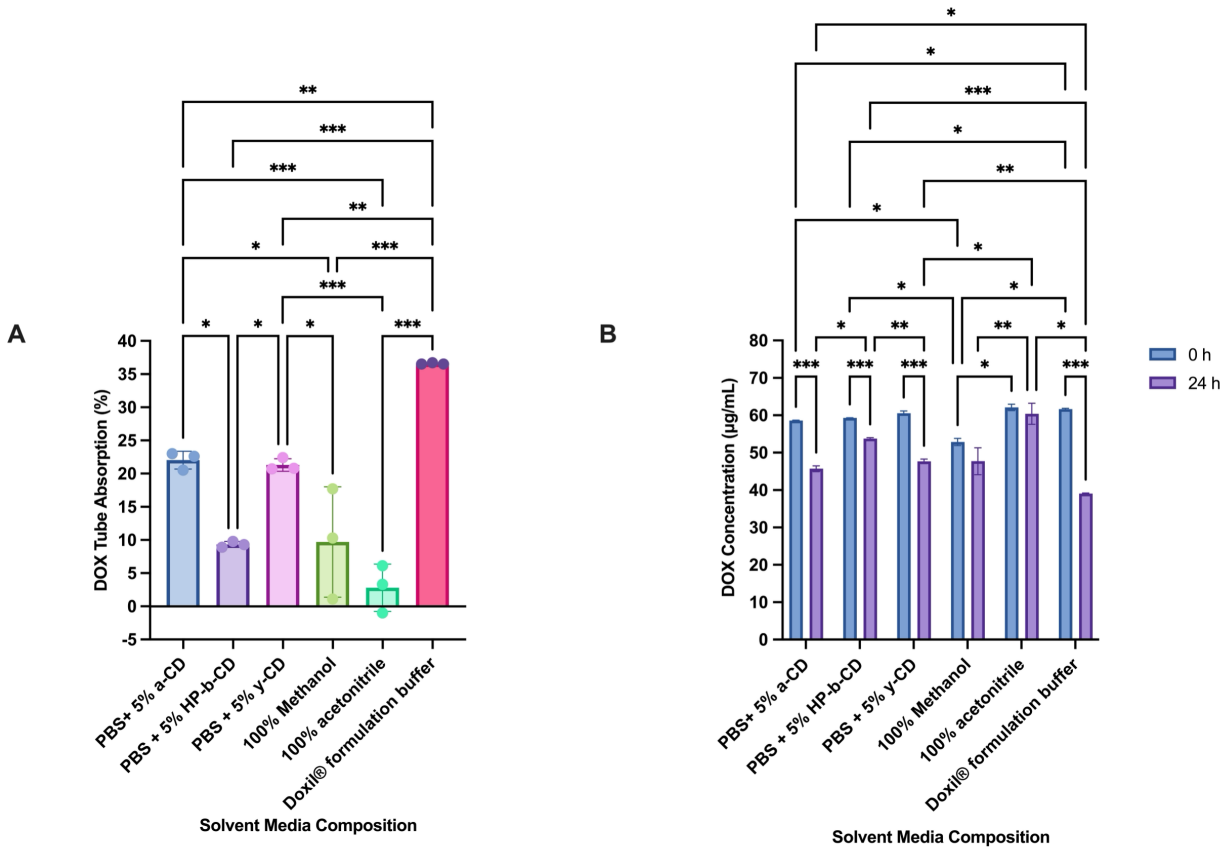

Figure 52. Effect of media composition on DOX adsorption in various solvent media conditions to standard, natural 1.5 mL polypropylene Eppendorf® microtubes under mild agitation at 20 RPM and 37ºC, as A) percentage, and B) initial and final concentration (mean ± SD, n = 3).

DOX adsorption is greatest to the 1.5 mL polypropylene, Eppendorf® Natural microtube in aqueous Doxil® formulation buffer consisting of 9.4% sucrose, 1.55 mg/mL L-histidine at pH 6.5 at 36.6 ± 0.12% and lowest in 100% acetonitrile at 2.80 ± 3.58 %. Statistical differences among means exist across all groups using an ordinary one-way ANOVA and Tukey's multiple comparisons test ($F(5, 12) = 31.4$; $p < 0.001$). While DOX adsorption is confirmed to be significantly reduced in organic solutions from literature claims, addition of hydroxypropyl-β-cyclodextrin to PBS has comparable effects to 100% methanol on reduced DOX adsorption in

respect to the formulation buffer. Competitive complexation with the addition of cyclodextrins to the dissolution media is a likely cause for reduced adsorption to polypropylene microtubes in respect to doxorubicin hydrochloride dissolved in Doxil® formulation buffer.

4.5.9 Adsorption Kinetics of DOX

The kinetics of DOX adsorption was evaluated under the dissolution conditions employed in each investigation of the factors and conditions influencing drug adsorption to the polypropylene, Eppendorf® Natural microtube. At 20 RPM and 37°C, samples were withdrawn and replaced with a fresh PBS and doxorubicin concentration in samples at each time point were quantified using the previously validated UPLC-UV doxorubicin quantitation method described in Chapter 2 Section 2.3 against calibration standards prepared from 20-100 µg/mL in PBS.

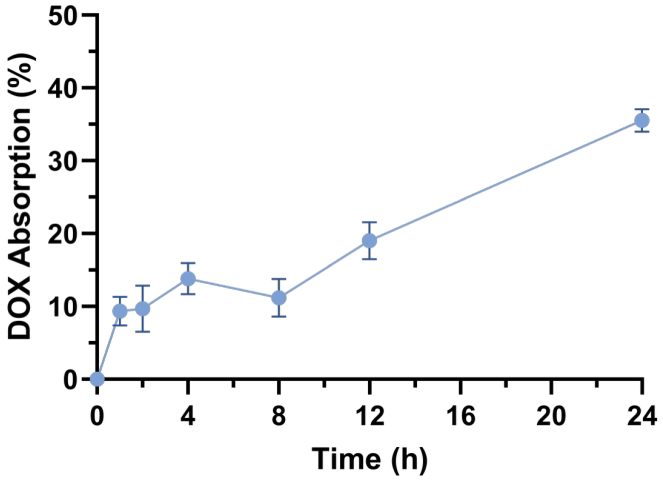

Figure 53. Rate of adsorption of doxorubicin hydrochloride to standard, polypropylene Eppendorf® microtubes in phosphate buffered saline at 20 RPM and 37C for 24 hrs (mean ± SD; n = 3).

The cumulative adsorption profile of doxorubicin hydrochloride binding to the polypropylene surface of 1.5 mL Eppendorf® Natural microtubes shows drug loss increasing steadily to 35.5 ± 1.56 % within 24 hrs in the absence of any sink material in Fig. 53. The data suggests that despite the popularity and widespread use of standard, untreated polypropylene tubes for everyday lab practices, polypropylene tubes should not be used for accelerated dissolution testing for doxorubicin hydrochloride and similar drug products due to the high prevalence of drug adsorption to the physicochemical nature of the microtube material. Furthermore, strategies for microtube selection should be included alongside recommendations

for proper filter selection in available USP guidelines and regulations for dissolution assay development [112].

4.6 Conclusion

Significant doxorubicin adsorption to polypropylene, polystyrene, and polyethylene microtubes was observed under specific dissolution conditions, with polypropylene microtubes—commonly used in laboratory workflows—serving as the primary focus of this investigation. Saturation of the adsorptive binding sites in polypropylene occurred at 180 µg/mL, beyond which further increases in drug concentration had minimal effect on adsorption. DOX adsorption increased with higher temperatures and decreased under faster rotational mixing. Additionally, the internal surface area-to-volume ratio strongly influenced drug loss, with statistically significant differences observed in 2.0 mL tubes compared to 1.5 mL and 5.0 mL tubes of the same brand, where differences were not significant. Media modifications using organic solvents or cyclodextrins reduce nonspecific binding through competitive interactions or altered surface affinity.

These findings emphasize the importance of strategic microtube selection and assay optimization when evaluating drug release from complex drug formulations. The extent of doxorubicin loss due to adsorption can substantially affect mass balance and compromise the reliability of dissolution data, particularly for liposomal formulations where accurate quantification of free and encapsulated drug is essential. Identifying low-binding tube materials and using appropriate dissolution media additives, such as cyclodextrins or organic solvents, may mitigate adsorption effects and improve data integrity. This work provides a practical framework for improving the reproducibility and reliability of *in vitro* release testing for amphiphilic drug products like doxorubicin hydrochloride and is highly applicable to other novel, hydrophobic drug products. This work also highlights key assay design considerations for regulatory evaluation and quality control of complex liposomal generics.

Chapter 5 Conclusions and Future Directions

Liposomes present a unique and versatile strategy for safe and efficacious drug delivery of poorly soluble, cytotoxic drugs often used in chemotherapy and a variety of other indications. The research described in this dissertation extends our understanding of the implications influencing the critical quality attributes of Doxil® and their impact on *in vitro* and predictive *in vivo* drug performance to support complex, liposomal generic development.

Chapter 2 discussed the development and application of methodologies established for doxorubicin liposome characterization including particle size analysis, zeta potential, quantification of doxorubicin and lipid content and purity, free non-encapsulated doxorubicin content in liposomal formulations, morphology and nanostructure on reference Doxil® products and each approved, generic version at the time of analysis. A comparative study of the physicochemical profiles of liposomal doxorubicin hydrochloride formulations revealed batch-to-batch variation across attributes within and between manufacturers. Morphology and nanostructure analysis utilized cryo-TEM and SAXS techniques to identify direct similarities and differences in shape, lamellarity and size between individual batches from each reference and generic manufacturer. Standard characterization data for particle size, zeta potential, drug and lipid content all agreed with label claim and literature, and a comparison of *in vitro* drug performance between products was conducted using a conventional dialysis-based *in vitro* release (IVR) assay. Results of the IVR assay demonstrated that despite minor differences in certain physicochemical attributes, a high degree of similarity in *in vitro* release is observed suggesting physicochemical similarity for bioequivalence assessment.

Chapter 3 described the development of an accelerated, rotator-based single-vial IVR assay using Bio-beads SM-2 resin as a novel sink agent to evaluate doxorubicin liposomes. Over 90% of the encapsulated drug was released from liposomes within 24 hours under optimized conditions for drug concentration in the dissolution media, resin weight, temperature, agitation speed, and media composition. The suitability of Bio-bead SM-2 resin as a sink agent was validated at the select resin weight for sink conditions in the non-compendial microtube system,

and the discriminative capacity of the assay was evaluated for formulation stress. While the developed assay was incapable of distinguishing between liposomal formulations with intrinsic differences due to varying free drug content, the assay could detect changes in the formulation due to extreme process or storage related variations induced by freeze thaw stress. Further optimization is warranted to increase the sensitivity of the assay to detect intrinsic differences in liposomal drug formulations to further study the impact of CQAs on drug performance.

Chapter 4 discussed a complimentary study for the dissolution assessment of liposomal drug products that evaluated the propensity of doxorubicin adsorption to microtubes used in dissolution testing. Accuracy in mass balance is critical to retain the integrity of dissolution results used to evaluate the formulation performance, quality and comparability to reference drug products for generic drug approvals. Incomplete drug recovery in dissolution due to non-specific drug adsorption was investigated under dissolution conditions using free doxorubicin hydrochloride solutions to identify the critical assay parameters that significantly influence the rate and extent of drug adsorption. Concentration, temperature, surface area and media composition significantly influenced the extent of doxorubicin adsorption, and the results of the study highlight the importance of integrating strategic microtube selection and drug adsorption investigations into regulatory considerations for dissolution assay development. From a clinical perspective, future work for Chapter 4 defining the clinical significance of drug adsorption to plastic surfaces used in treatment protocols to elucidate its impact on the actual dose delivered to patients could prove useful. Exploring the link between the experimental findings and clinical implications may reveal whether dose adjustments or modified dosing parameters are warranted in specific patient populations (e.g. neonates, infants, children, elderly).

Ultimately, this dissertation deepens our understanding of which CQAs have a significant effect on *in vitro* drug performance for predictive insights on *in vivo* drug performance using Doxil® as a model drug for investigation. The primary CQAs identified for *in vitro* drug performance included drug/lipid content, non-encapsulated drug content, particle size and polydispersity. Secondary CQAs for liposomal products included drug/lipid purity, zeta potential, and morphology. These attributes were ranked based on literature study on their implications on *in vivo* safety and performance following experimental investigation in Chapters 2-4. Future directions for this thesis work should involve targeted investigations to determine the actual relevance for which CQAs most significantly impact the *in vivo* performance and safety of

approved, liposomal doxorubicin formulations. This could include *in vitro–in vivo* correlation (IVIVC) studies, comparative pharmacokinetic and toxicity studies across formulations with different CQA profiles or applying design of experiments to systematically evaluate the relationship between specific CQAs and *in vivo* outcomes.

Several amphiphilic and hydrophobic drug products – such as antifungals, hormonal contraceptives, antibiotics, nuclear receptor modulators, small-molecule kinase inhibitors, and novel chemotherapeutics – are currently marketed as brand formulations. Many of these drugs have patents or exclusivities that recently expired within the last year or are approaching expiration within the next 1-5 years, making them attractive candidates for generic development [136–138]. This developed framework employing physicochemical characterization, IVR assay development and adsorption propensity presents a rigorous, adaptable approach for generic companies seeking to develop high-quality, low-cost alternative versions across the globe. Particularly in low-income countries where access to imported drug products is limited, this framework can be applied in research facilities within those countries to drive generic drug development in-house to help treat disease and ultimately save more lives. Additionally, elements of this framework may be used to improve standard research practices and optimize existing workflows for drug development and clinical treatment globally.

Appendix

Chapter 2 Supplementary Information[1] [2]

Supplementary Method Descriptions

Section S1. Doxorubicin Content - Standard Curve Generation

Stock solutions of doxorubicin hydrochloride (1 mg/mL) were prepared in methanol, and working standards were prepared by further diluting the stock solutions 10-fold in methanol. Calibration standards for doxorubicin (10-50 μg/mL) were also prepared in methanol to generate a standard curve to calculate the doxorubicin concentration in each formulation. Standard curves were generated by quantifying the peak area of the doxorubicin peak at 254 nm at each calibrant concentration and performing linear regression analysis. The slope, intercept, and coefficient of regression (R^2) were calculated using GraphPad Prism. The R^2 values greater than 0.990 indicated the linear response of area concerning concentration. Doxorubicin concentration was calculated using the equation obtained from the linear regression curve. Three individual sets of calibration standards were measured using UPLC and data was analyzed using GraphPad Prism.

Validation results for the doxorubicin quantitation method according to the ICH Harmonised Tripartite Guideline Q2(R1) Validation of Analytical Procedures (https://database.ich.org/sites/default/files/Q2%28R1%29%20Guideline.pdf) are included below.

[1] Author information: Adaeze Eneli, Kaikai Wang, Jingyao Gan, Rimpy Diwan, Ziyi Lu, Minzhi Yu, Rose Ackermann, Brian Shay, Anna Schwendeman

[2] Author affiliation: College of Pharmacy and Biointerfaces Institute, University of Michigan, 2800 Plymouth Rd Ann Arbor, MI 48109

Doxorubicin

ICH Q2(R1) validation results for the doxorubicin quantitation method.

Appendix Table 1. ICH Q2(R1) validation results for the doxorubicin quantitation method.

Sensitivity	LOD = 1.68 µg/mL LOQ = 5.10 µg/mL
Linearity	y = 12686x+4306.8 0-50 µg/mL R^2 = 0.999
Accuracy (n=9)	LQC, % Recovery = 105 ± 4% MQC, % Recovery = 106 ± 3% HQC, % Recovery = 103 ± 2%
Precision (n=6)	LQC, RSD = 3.74% MQC, RSD = 2.93% HQC, RSD = 2.09%

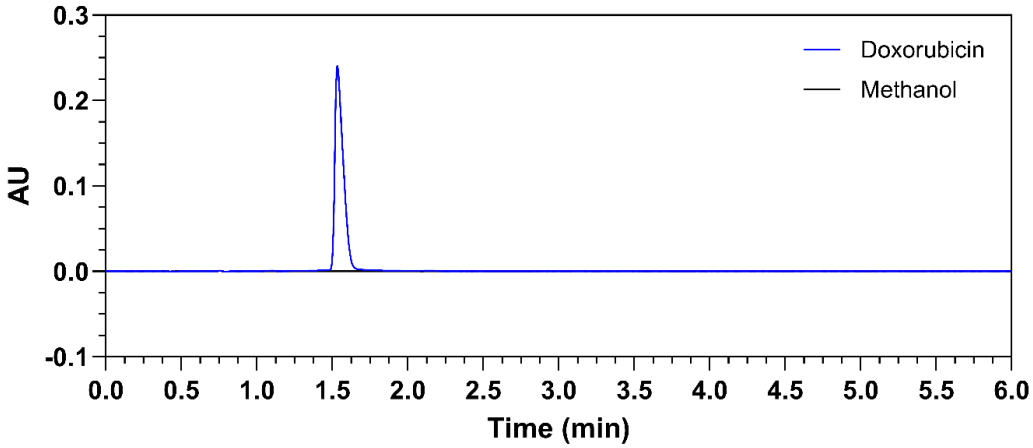

Appendix Figure 1. Specificity of doxorubicin quantification assay. Blank is in black, doxorubicin in blue.

Section S2. Lipid Content - Standard Curve Generation

Stock standards (1 mg/mL) for HSPC, DSPE-PEG (Mw 2000), and cholesterol were prepared in methanol. Solutions were vortexed and incubated in a water bath at 35 °C for 5 minutes to dissolve the lipids completely in methanol. Working standards were prepared by diluting the stock standards 2-fold in methanol. Calibration standards (50-250 µg/mL for HSPC and 25-125 µg/mL for cholesterol and DSPE-PEG2000) were prepared in methanol for standard curve generation. Standard curves were generated by quantifying the peak area of each lipid for each calibrant concentration and linear regression analysis was conducted. The slope, intercept and

coefficient of regression (R^2) were calculated using GraphPad Prism. The R^2 values were found to be greater than 0.990 indicating the linear response of area with respect to concentration. The unknown concentrations of the lipids were calculated using the linear equation obtained from the standard curve. Data was generated in triplicates and GraphPad Prism was used for analysis.

Appendix Table 2. Gradient mobile phase for the UPLC-ELSD assay for lipid quantification.

Time (minute)	**Flow Rate (mL/min)**	**Solvent A (%)**	**Solvent B (%)**
0	0.3	100	0
1	0.3	100	0
3	0.3	20	80
3.5	0.3	20	80
5	0.3	0	100
10	0.3	0	100
11	0.3	100	0
15	0.3	100	0

Validation results for the lipid quantitation method according to the ICH Harmonised Tripartite Guideline Q2(R1) Validation of Analytical Procedures (https://database.ich.org/sites/default/files/Q2%28R1%29%20Guideline.pdf) are included below.

HSPC

Appendix Table 3. ICH Q2(R1) validation results for the lipid quantitation method for HSPC.

Sensitivity	LOD = 20.52 µg/mL LOQ = 62.17 µg/mL
Linearity	y = 53340.4x-1939931.9 50-250 µg/mL R^2 = 0.994
Accuracy	LQC, % Recovery = 113 $\pm$ 1% MQC, % Recovery = 91 $\pm$ 4% HQC, % Recovery = 104 $\pm$ 3%
Precision (n=6)	LQC, RSD = 0.81% MQC, RSD = 4.17% HQC, RSD = 2.88%

Cholesterol

Appendix Table 4. ICH Q2(R1) validation results for the lipid quantitation method for cholesterol.

Sensitivity	LOD = 10.48 μg/mL LOQ = 31.77 μg/mL
Linearity	y = 87285.2x-1823519.3 25-125 μg/mL R^2 = 0.995
Accuracy	LQC, % Recovery = 112 $\pm$ 2% MQC, % Recovery = 97 $\pm$ 3% HQC, % Recovery = 102 $\pm$ 2%
Precision (n=6)	LQC, RSD = 1.93% MQC, RSD = 2.87% HQC, RSD = 2.42%

DSPE-PEG 2000

Appendix Table 5. ICH Q2(R1) validation results for the lipid quantitation method for DSPE-PEG 2000.

Sensitivity	LOD = 2.51 μg/mL LOQ = 7.61 μg/mL
Linearity	y = 24271x-511889 25-125 μg/mL R^2 = 0.995
Accuracy (%Recovery)	LQC, % Recovery = 100 $\pm$ 1% MQC, % Recovery = 98 $\pm$ 3% HQC, % Recovery = 89 $\pm$ 3%
Precision (n=6)	LQC, RSD = 1.15% MQC, RSD = 3.48% HQC, RSD = 3.48%

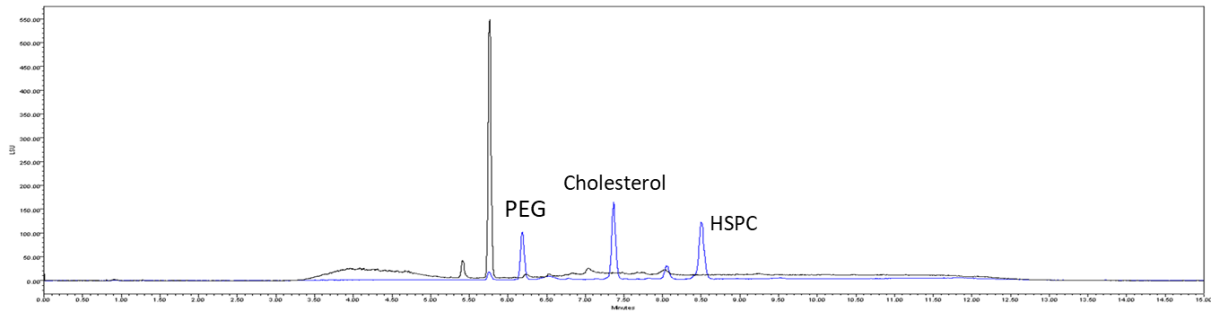

Appendix Figure 2. Specificity of the lipid quantification assay. Blank is in black, lipids in blue.

Section S3. Doxorubicin Purity – Standard Curve Generation

Stock solutions (1 mg/mL) for doxorubicin and each USP-designated impurity (daunorubicin, doxorubicinone, and daunorubicinone) were prepared in methanol. The standards were incubated in a water bath at 35 °C for 5 minutes to dissolve the solids completely in methanol. Working solutions for doxorubicin and each impurity were prepared by performing a 10-fold dilution in methanol. Calibration standards for pure doxorubicin were prepared at concentrations from 0.01 - 0.15 µg/mL in methanol. Calibration standards for each USP impurity were prepared at concentrations 10-fold lower than that of doxorubicin (0.001 - 0.015 µg/mL). The gradient mobile phase used for this assay is described in **Appendix Table 6**.

Appendix Table 6. Gradient mobile phase for the UPLC-TUV assay for DOX and impurity quantification in formulations.

Time (minute)	Solvent A (%)	Solvent B (%)
0	90	10
8	50	50
9	25	75
9.1	90	10
10	90	10

Standard curves were generated using linear regression analysis of the impurity and doxorubicin peak AUC versus calibrant concentration at 220 and 254 nm, respectively. The slope, intercept, and coefficient of regression (R^2) were calculated using GraphPad Prism. R^2 values found to be greater than 0.990 indicated the linear response of area with respect to concentration. Data was generated in triplicates and GraphPad Prism was used for analysis.

Supplementary Data

Appendix Table 7. Size distribution, polydispersity index and zeta potential measurements of different liposomal doxorubicin formulations analyzed by DLS ($n \geq 3$, mean ± SD).

	Batch No.	Size (nm)	Polydispersity Index	Zeta Potential (mV)
Doxil®	KGZTG01	89.1 ± 0.71	0.050 ± 0.011	-23.2 ± 3.34
	KIZTI00	89.3 ± 0.64	0.049 ± 0.019	-24.7 ± 1.53
	KJZU901	89.9 ± 2.19	0.046 ± 0.002	-27.1 ± 0.53
	LJZTS00	95.4 ± 0.73	0.065 ± 0.015	-25.9 ± 3.39
	MDZT300	86.9 ± 1.28	0.082 ± 0.035	-27.9 ± 2.72
Dr. Reddy's Laboratories	501451	87.0 ± 0.85	0.047 ± 0.011	-27.4 ± 2.18
	501630	87.4 ± 1.00	0.051 ± 0.014	-27.3 ± 1.54
	501635	87.5 ± 1.04	0.052 ± 0.005	-29.0 ± 0.90
	501693	90.2 ± 0.99	0.052 ± 0.014	-25.8 ± 2.20
Sun Pharmaceuticals	JKX5514A	86.6 ± 0.51	0.065 ± 0.005	-31.5 ± 2.55
	HAC1612A	84.3 ± 0.62	0.082 ± 0.015	-30.9 ± 4.02
Zydus Pharmaceuticals	P100084	84.0 ± 0.85	0.045 ± 0.007	-29.5 ± 2.65

Appendix Table 8. Quantification of doxorubicin and lipid content within liposomal doxorubicin formulations by different manufacturers (mean ± SD; n = 3).

	Batch No.	Doxorubicin (mg/ml)	HSPC (mg/ml)	DSPE-PEG 2000 (mg/ml)	Cholesterol (mg/ml)
	Label Claim	*2.00 ± 0.10*	*9.58 ± 0.48*	*3.19 ± 0.16*	*3.19 ± 0.16*
Doxil®	KGZTG01	2.03 ± 0.06	9.44 ± 0.03	3.19 ± 0.02	3.05 ± 0.02
	KIZTI00	1.95 ± 0.06	9.44 ± 0.33	3.26 ± 0.09	3.24 ± 0.08
	KJZU901	2.00 ± 0.01	9.72 ± 0.04	3.17 ± 0.04	3.29 ± 0.03
	LJZTS00	1.94 ± 0.02	9.85 ± 0.04	3.20 ± 0.11	3.09 ± 0.01
	MDZT300	2.01 ± 0.02	9.64 ± 0.26	3.22 ± 0.10	3.15 ± 0.08
Dr. Reddy's Laboratories	501451	1.97 ± 0.03	9.64 ± 0.04	3.23 ± 0.04	3.05 ± 0.03
	501630	2.01 ± 0.01	9.83 ± 0.09	3.24 ± 0.07	3.13 ± 0.09
	501635	2.09 ± 0.06	9.63 ± 0.21	3.28 ± 0.06	3.28 ± 0.03
	501693	2.07 ± 0.01	9.70 ± 0.24	3.12 ± 0.02	3.13 ± 0.13
Sun Pharmaceuticals	JKX5514A	1.90 ± 0.04	9.85 ± 0.02	3.20 ± 0.05	3.36 ± 0.02
	HAC1612A	1.91 ± 0.03	9.58 ± 0.02	3.21 ± 0.06	3.24 ± 0.01
Zydus Pharmaceuticals	P100084	2.09 ± 0.06	9.25 ± 0.03	3.27 ± 0.05	3.19 ± 0.07

Appendix Table 9. Quantification of doxorubicin purity and identification of USP impurities within liposomal doxorubicin formulations by different manufacturers (mean ± SD; n = 3).

	Batch No.	Doxorubicin (%)	Doxorubicinone (%)	Daunorubicin (%)	Daunorubicinone (%)	Other/Unspecified (%)
Doxil®	KGZTG01	99.3 ± 0.38	0.33 ± 0.06	0.06 ± 0.07	0.31 ± 0.27	0.00 ± 0.00
	KIZTI00	99.1 ± 0.26	0.22 ± 0.19	0.18 ± 0.24	0.00 ± 0.00	0.47 ± 0.21
	KJZU901	99.2 ± 0.15	0.27 ± 0.08	0.00 ± 0.00	0.50 ± 0.07	0.00 ± 0.00
	LJZTS00	98.9 ± 0.11	0.25 ± 0.22	0.17 ± 0.17	0.50 ± 0.04	0.24 ± 0.11
	MDZT300	99.1 ± 0.07	0.11 ± 0.20	0.16 ± 0.14	0.39 ± 0.01	0.26 ± 0.10
Dr. Reddy's Laboratories	501451	99.8 ± 0.04	0.20 ± 0.03	0.00 ± 0.00	0.01 ± 0.02	0.00 ± 0.00
	501630	99.8 ± 0.04	0.13 ± 0.03	0.00 ± 0.00	0.02 ± 0.02	0.00 ± 0.00
	501635	99.7 ± 0.15	0.14 ± 0.03	0.00 ± 0.00	0.12 ± 0.19	0.00 ± 0.00
	501693	99.3 ± 0.05	0.06 ± 0.10	0.19 ± 0.02	0.39 ± 0.03	0.11 ± 0.10
Sun Pharmaceuticals	JKX5514A	99.2 ± 0.36	0.67 ± 0.43	0.06 ± 0.11	0.02 ± 0.04	0.02 ± 0.03
	HAC1612A	99.4 ± 0.14	0.40 ± 0.35	0.18 ± 0.25	0.00 ± 0.00	0.04 ± 0.04
Zydus Pharmaceuticals	P100084	99.5 ± 0.20	0.42 ± 0.24	0.04 ± 0.08	0.03 ± 0.03	0.01 ± 0.01

Appendix Table 10. Quantification of free doxorubicin present in liposomal doxorubicin formulations by different manufacturers (n > 2).

	Batch No.	Free Doxorubicin (%)
Doxil®	KGZTG01	1.03 ± 0.35
	KIZTI00	1.93 ± 1.01
	KJZU901	0.95 ± 0.67
	LJZTS00	1.20 ± 0.02
	MDZT300	1.04 ± 0.33
Dr. Reddy's Laboratories	501451	1.99 ± 0.03
	501630	0.57 ± 0.32
	501635	0.61 ± 0.39
	501693	0.92 ± 0.27
Sun Pharmaceuticals	JKX5514A	0.37 ± 0.04
	HAC1612A	0.41 ± 0.01
Zydus Pharmaceuticals	P100084	1.32 ± 0.92

Appendix Table 11. Measured size dimensions and membrane thickness of doxorubicin liposomes in different liposomal doxorubicin hydrochloride formulations imaged by cryo-TEM (mean ± SD, n ≥ 500).

	Batch No.	Length (nm)	Width (nm)	Membrane Thickness (nm)
Doxil®	MDZT300	73.3 ± 13.1	66.0 ± 13.0	4.80 ± 0.60
Dr. Reddy's Laboratories	501635	69.1 ± 9.60	61.5 ± 10.3	5.00 ± 0.40
Sun Pharmaceuticals	JKX5514A	60.9 ± 15.1	57.6 ± 14.8	4.80 ± 0.90
Zydus Pharmaceuticals	P100084	67.9 ± 16.3	61.8 ± 17.0	4.50 ± 0.70

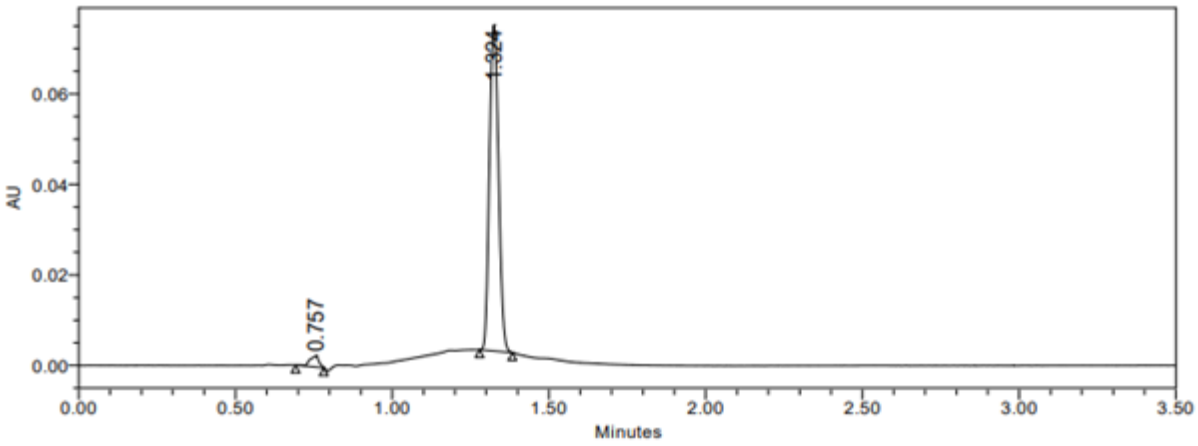

Appendix Figure 3. Chromatographic identification of doxorubicin in a Doxil® formulation using an isocratic mobile phase of deionized water and methanol with 0.1% formic acid (Baxter Healthcare, batch no. MDZT300).

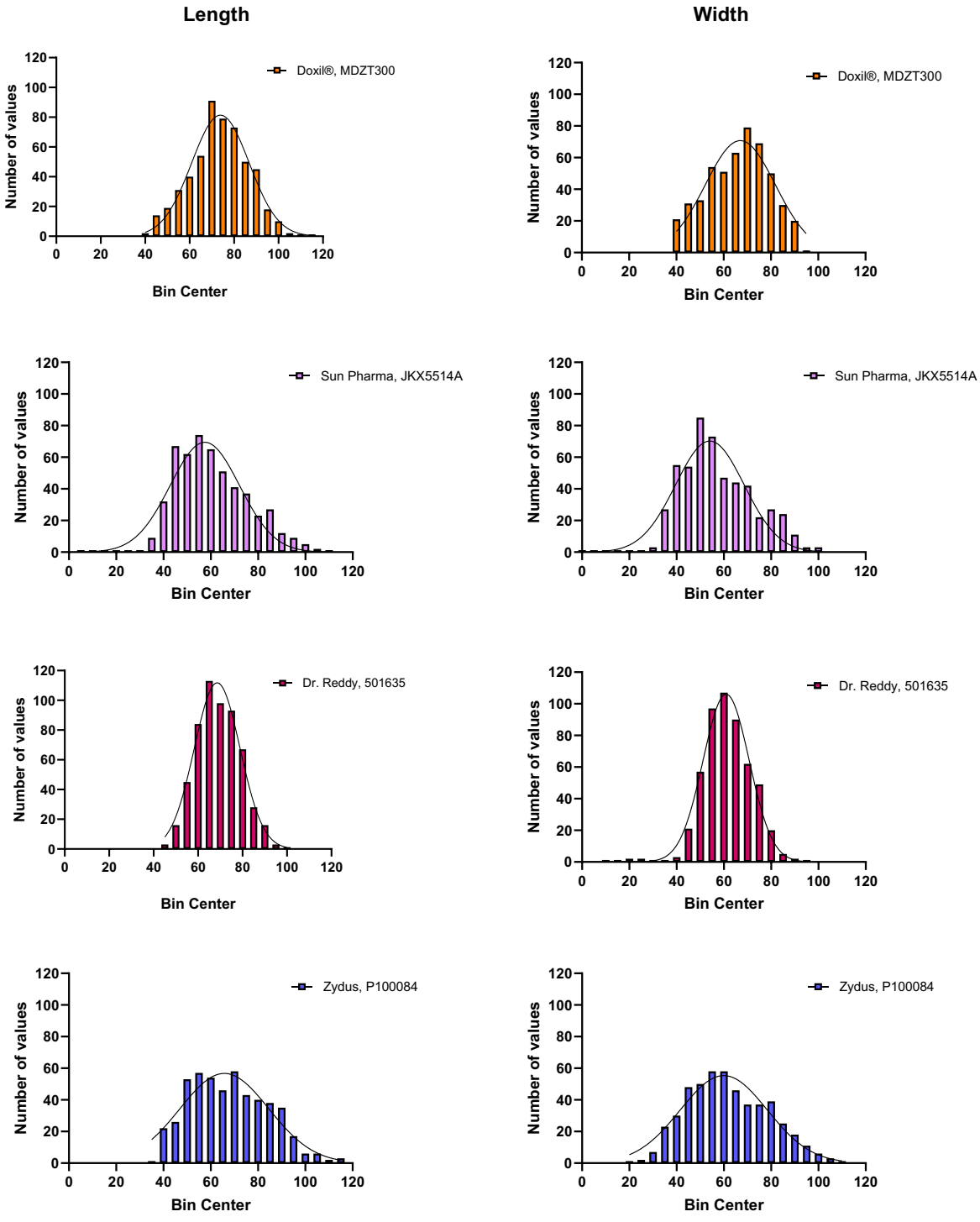

Appendix Figure 4. Size distribution histograms for liposome length and width measured in images generated by cryo-TEM.

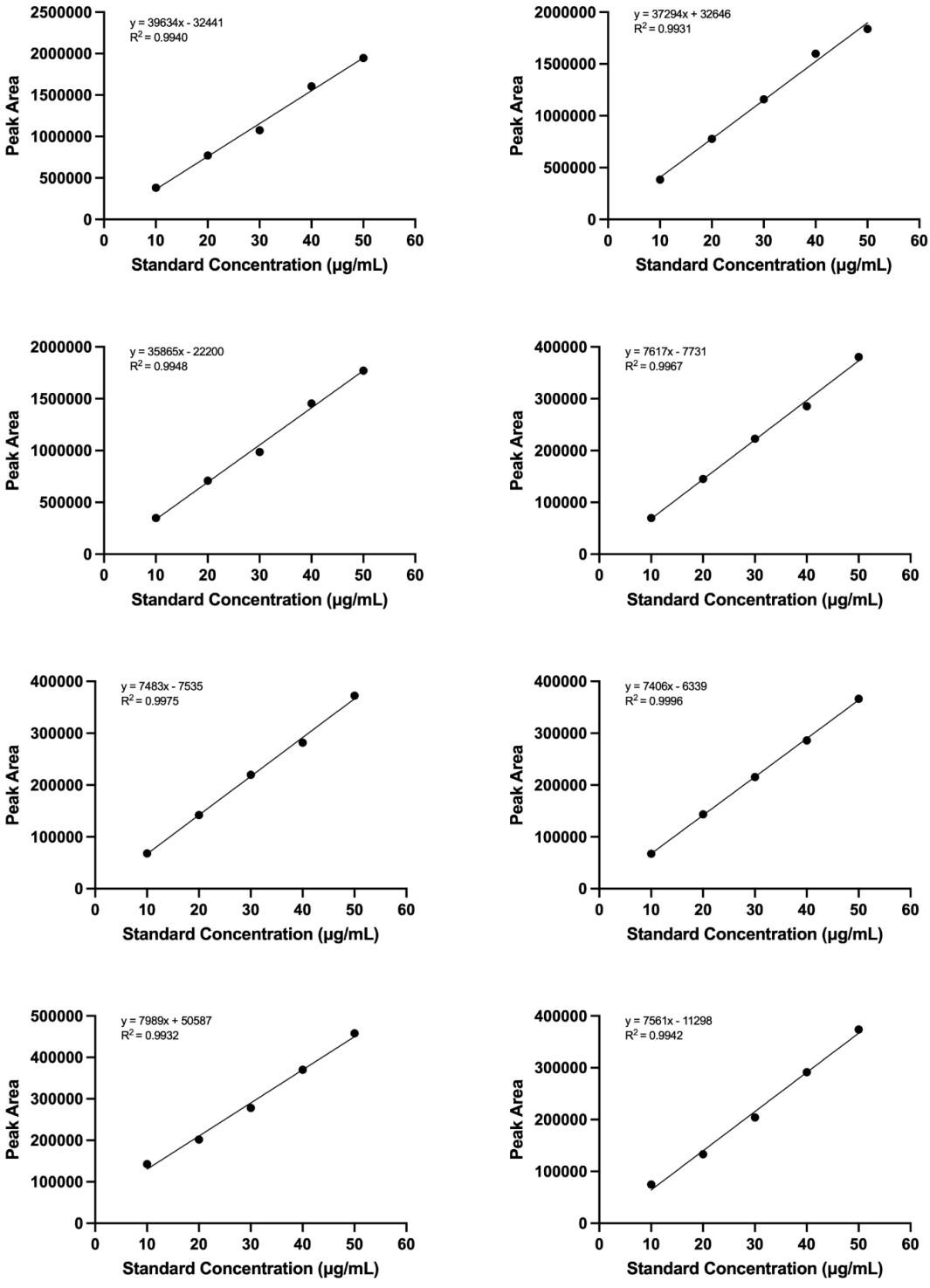

Appendix Figure 5. Calibration curves for doxorubicin quantification assay.

Bibliography

1. Nsairat, H., Khater, D., Sayed, U., Odeh, F., Al Bawab, A., & Alshaer, W. (2022). Liposomes: structure, composition, types, and clinical applications. *Heliyon*, *8*(5), e09394. https://doi.org/10.1016/j.heliyon.2022.e09394

2. Wang, S., Chen, Y., Guo, J., & Huang, Q. (2023). Liposomes for Tumor Targeted Therapy: A Review. *International Journal of Molecular Sciences*, *24*(3), 2643. https://doi.org/10.3390/ijms24032643

3. Pande, S. (2023). Liposomes for drug delivery: review of vesicular composition, factors affecting drug release and drug loading in liposomes. *Artificial Cells, Nanomedicine, and Biotechnology*, *51*(1), 428–440. https://doi.org/10.1080/21691401.2023.2247036

4. Mall, J., Naseem, N., Haider, M. F., Rahman, M. A., Khan, S., & Siddiqui, S. N. (2024). Nanostructured lipid carriers as a drug delivery system: A comprehensive review with therapeutic applications. *Intelligent Pharmacy*. https://doi.org/10.1016/j.ipha.2024.09.005

5. Sercombe, L., Veerati, T., Moheimani, F., Wu, S. Y., Sood, A. K., & Hua, S. (2015). Advances and Challenges of Liposome Assisted Drug Delivery. *Frontiers in Pharmacology*, *6*. https://doi.org/10.3389/fphar.2015.00286

6. U.S. Food & Drug Administration & Ramesh Raghavachari. (2022, May 6). Doxil Label. Retrieved June 25, 2025, from https://www.accessdata.fda.gov/drugsatfda_docs/label/2022/050718Orig1s060lbl.pdf

7. Ghosh, S. (2024, January 1). Liposomal Doxorubicin Market Outlook for 2024-2034. Retrieved June 25, 2024, from https://www.futuremarketinsights.com/reports/liposomal-doxorubicin-market

8. Yu, Y., & Gupta, S. (2014). Pioneering advantage in generic drug competition. *International Journal of Pharmaceutical and Healthcare Marketing*, *8*(2), 126–150. https://doi.org/10.1108/IJPHM-11-2013-0063

9. U.S. Food & Drug Administration. (2018, April 1). Liposome Drug Products Chemistry, Manufacturing, and Controls; Human Pharmacokinetics and Bioavailability; and Labeling Documentation Guidance for Industry. Retrieved from https://www.fda.gov/media/70837/download

10. FDA CDER, & Mahadevan, C. (2018). Draft Guidance on Doxorubicin hydrochloride. Retrieved from

https://www.accessdata.fda.gov/drugsatfda_docs/psg/Doxorubicin%20Hydrochloride_draft_Injection%20injec%20lipo_RLD%2050718_RC09-18.pdf

11. Food and Drug Administration. (2002, December 19). 21 CFR 320.22 Criteria for waiver of evidence of *in vivo* bioavailability or bioequivalence. Retrieved from https://www.ecfr.gov/current/title-21/chapter-I/subchapter-D/part-320/subpart-B/section-320.22

12. Food and Drug Administration, D. of H. and H. S. (2002, December 19). 21 CFR 320.24 -- Types of evidence to measure bioavailability or establish bioequivalence. Retrieved from https://www.ecfr.gov/current/title-21/part-320/section-320.24

13. Onakpoya, I. J., Heneghan, C. J., & Aronson, J. K. (2016). Post-marketing withdrawal of 462 medicinal products because of adverse drug reactions: a systematic review of the world literature. *BMC Medicine*, *14*, 10. https://doi.org/10.1186/s12916-016-0553-2

14. Liu, P., Chen, G., & Zhang, J. (2022). A Review of Liposomes as a Drug Delivery System: Current Status of Approved Products, Regulatory Environments, and Future Perspectives. *Molecules*, *27*(4), 1372. https://doi.org/10.3390/molecules27041372

15. Lin, Z., Deng, T., Liu, Y., Zheng, S., Wang, G., He, H., & Zhang, J. (2023). Comprehensive analysis of the influence of physicochemical properties and tumor-associated environments on liposome intratumoral penetration. *Journal of Controlled Release*, *359*, 33–51. https://doi.org/10.1016/j.jconrel.2023.05.027

16. Barenholz, Y. (Chezy). (2012). Doxil® — The first FDA-approved nano-drug: Lessons learned. *Journal of Controlled Release*, *160*(2), 117–134. https://doi.org/10.1016/j.jconrel.2012.03.020

17. Immordino, M. L., Dosio, F., & Cattel, L. (2006). Stealth liposomes: review of the basic science, rationale, and clinical applications, existing and potential. *International Journal of Nanomedicine*, *1*(3), 297–315.

18. Cˇeh, B., Winterhalter, M., Frederik, P. M., Vallner, J. J., & Lasic, D. D. (1997). Stealth® liposomes: from theory to product. *Advanced Drug Delivery Reviews*, *24*(2–3), 165–177. https://doi.org/10.1016/S0169-409X(96)00456-5

19. Lasic, D. D., & Needham, D. (1995). The “Stealth” Liposome: A Prototypical Biomaterial. *Chemical Reviews*, *95*(8), 2601–2628. https://doi.org/10.1021/cr00040a001

20. Buzdar, A. U., Marcus, C., Blumenschein, G. R., & Smith, T. L. (1985). Early and delayed clinical cardiotoxicity of doxorubicin. *Cancer*, *55*(12), 2761–2765. https://doi.org/10.1002/1097-0142(19850615)55:12<2761::AID-CNCR2820551206>3.0.CO;2-P

21. Lipshultz, S. E., Cohen ,Harvey, Colan ,Steven D., & and Herman, E. H. (2006). The relevance of information generated by *in vitro* experimental models to clinical doxorubicin

cardiotoxicity. *Leukemia & Lymphoma*, *47*(8), 1454–1458. https://doi.org/10.1080/10428190600800231

22. Sheibani, M., Azizi, Y., Shayan, M., Nezamoleslami, S., Eslami, F., Farjoo, M. H., & Dehpour, A. R. (2022). Doxorubicin-Induced Cardiotoxicity: An Overview on Pre-clinical Therapeutic Approaches. *Cardiovascular Toxicology*, *22*(4), 292–310. https://doi.org/10.1007/s12012-022-09721-1

23. Jiang, W., Lionberger, R., & Yu, L. X. (2011). *In vitro* and *in vivo* characterizations of PEGylated liposomal doxorubicin. *Bioanalysis*, *3*(3), 333–344. https://doi.org/10.4155/bio.10.204

24. Bulbake, U., Doppalapudi, S., Kommineni, N., & Khan, W. (2017). Liposomal Formulations in Clinical Use: An Updated Review. *Pharmaceutics*, *9*(4), 12. https://doi.org/10.3390/pharmaceutics9020012

25. Chen, J., Cheng, D., Li, J., Wang, Y., Guo, J., Chen, Z., … Yang, T. (2013). Influence of lipid composition on the phase transition temperature of liposomes composed of both DPPC and HSPC. *Drug Development and Industrial Pharmacy*, *39*(2), 197–204. https://doi.org/10.3109/03639045.2012.668912

26. Kaddah, S., Khreich, N., Kaddah, F., Charcosset, C., & Greige-Gerges, H. (2018). Cholesterol modulates the liposome membrane fluidity and permeability for a hydrophilic molecule. *Food and Chemical Toxicology*, *113*, 40–48. https://doi.org/10.1016/j.fct.2018.01.017

27. Orange Book: Approved Drug Products with Therapeutic Equivalence Evaluations. (n.d.). Retrieved June 27, 2025, from https://www.accessdata.fda.gov/scripts/cder/ob/patent_info.cfm?Product_No=001&Appl_No=207793&Appl_type=N

28. Palmer, E. (2012, August 3). Johnson & Johnson releases some Doxil for trials. *Fierce Pharma*. Retrieved from https://www.fiercepharma.com/sales-and-marketing/johnson-johnson-releases-some-doxil-for-trials

29. Walsh, S. (2013, February 4). FDA approval of generic version of cancer drug Doxil is expected to help resolve shortage. *Fierce Pharma*. Retrieved from https://www.fiercepharma.com/pharma/fda-approval-of-generic-version-of-cancer-drug-doxil-expected-to-help-resolve-shortage

30. U.S. Department of Health and Human Services, & FDA CDER. (2020, October 1). Referencing Approved Drug Products in ANDA Submissions Guidance for Industry. FDA. Retrieved from https://www.fda.gov/media/102360/download

31. Bioequivalence for Liposomal Drug Products. (2014). In *AAPS Advances in the Pharmaceutical Sciences Series* (pp. 275–296). New York, NY: Springer New York. https://doi.org/10.1007/978-1-4939-1252-0_11

32. Dimov, N., Kastner, E., Hussain, M., Perrie, Y., & Szita, N. (2017). Formation and purification of tailored liposomes for drug delivery using a module-based micro continuous-flow system. *Scientific Reports*, *7*(1). https://doi.org/10.1038/s41598-017-11533-1

33. Sheikholeslami, B., Lam, N. W., Dua, K., & Haghi, M. (2022). Exploring the impact of physicochemical properties of liposomal formulations on their *in vivo* fate. *Life Sciences*, *300*, 120574. https://doi.org/10.1016/j.lfs.2022.120574

34. Basak, S., & Das, T. K. (2025). Liposome-Based Drug Delivery Systems: From Laboratory Research to Industrial Production—Instruments and Challenges. *ChemEngineering*, *9*(3), 56. https://doi.org/10.3390/chemengineering9030056

35. Haran, G., Cohen, R., Bar, L. K., & Barenholz, Y. (1993). Transmembrane ammonium sulfate gradients in liposomes produce efficient and stable entrapment of amphipathic weak bases. *Biochimica et Biophysica Acta (BBA) - Biomembranes*, *1151*(2), 201–215. https://doi.org/10.1016/0005-2736(93)90105-9

36. Jiang, W., Lionberger, R., & Yu, L. X. (2011). *In vitro* and *in vivo* characterizations of PEGylated liposomal doxorubicin. *Bioanalysis*, *3*(3), 333–344. https://doi.org/10.4155/bio.10.204

37. Clerc, S., & Barenholz, Y. (1998). A Quantitative Model for Using Acridine Orange as a Transmembrane pH Gradient Probe. *Analytical Biochemistry*, *259*(1), 104–111. https://doi.org/10.1006/abio.1998.2639

38. Grabielle-Madelmont, C., Lesieur, S., & Ollivon, M. (2003). Characterization of loaded liposomes by size exclusion chromatography. *Journal of Biochemical and Biophysical Methods*, *56*(1–3), 189–217. https://doi.org/10.1016/S0165-022X(03)00059-9

39. Hupfeld, S., Holsæter, A. M., Skar, M., Frantzen, C. B., & Brandl, M. (2006). Liposome Size Analysis by Dynamic/Static Light Scattering upon Size Exclusion-/Field Flow-Fractionation. *Journal of Nanoscience and Nanotechnology*, *6*(9), 3025–3031. https://doi.org/10.1166/jnn.2006.454

40. Gabizon, A., Catane, R., Uziely, B., Kaufman, B., Safra, T., Cohen, R., … Barenholz, Y. (1994). Prolonged Circulation Time and Enhanced Accumulation in Malignant Exudates of Doxorubicin Encapsulated in Polyethylene-glycol Coated Liposomes.

41. Jiang, W., Lionberger, R., & Yu, L. X. (2011). *In Vitro* and *In vivo* Characterizations of Pegylated Liposomal Doxorubicin. *Bioanalysis*, *3*(3), 333–344. https://doi.org/10.4155/bio.10.204

42. National Library of Medicine. (2022, March 10). Bioequivalence Study of Doxorubicin Hydrochloride Liposome Injection (Lipodox®) in Chinese Patients. *ClinicalTrials.gov*. Retrieved from https://clinicaltrials.gov/study/NCT05273944?intr=Lipodox&rank=20

43. Li, Y., Qi, L., Wang, Y., Li, Y., Lei, C., Zhang, Y., … Wang, X. (2022). A multicenter randomized trials to compare the bioequivalence and safety of a generic doxorubicin hydrochloride liposome injection with Caelyx® in advanced breast cancer. *Frontiers in Oncology*, *12*. https://doi.org/10.3389/fonc.2022.1070001

44. U.S. Food & Drug Administration. (2012, March 1). Ambisome Package Insert. Retrieved December 19, 2023, from https://www.accessdata.fda.gov/drugsatfda_docs/label/2012/050740s021lbl.pdf

45. Taro Pharmaceuticals Inc. (2024, December 20). Product Monograph: Taro-Amphotericin B Liposomal. Retrieved from https://pdf.hres.ca/dpd_pm/00078103.PDF

46. U.S. Food & Drug Administration. (2020, August 1). Draft Guidance on Amphotericin B.

47. Adler-Moore, J., & Proffitt, R. T. (2002). AmBisome: liposomal formulation, structure, mechanism of action and pre-clinical experience. *Journal of Antimicrobial Chemotherapy*, *49*(suppl_1), 21–30. https://doi.org/10.1093/jac/49.suppl_1.21

48. Faustino, C., & Pinheiro, L. (2020). Lipid Systems for the Delivery of Amphotericin B in Antifungal Therapy. *Pharmaceutics*, *12*(1), 29. https://doi.org/10.3390/pharmaceutics12010029

49. Liu, Y., Mei, Z., Mei, L., Tang, J., Yuan, W., Srinivasan, S., … Schwendeman, A. S. (2020). Analytical method development and comparability study for AmBisome® and generic Amphotericin B liposomal products. *European Journal of Pharmaceutics and Biopharmaceutics*, *157*, 241–249. https://doi.org/10.1016/j.ejpb.2020.09.008

50. Olson, J. A., Schwartz, J. A., Hahka, D., Nguyen, N., Bunch, T., Jensen, G. M., & Adler-Moore, J. P. (2015). Toxicity and efficacy differences between liposomal amphotericin B formulations in uninfected and Aspergillus fumigatus infected mice. *Medical Mycology*, *53*(2), 107–118. https://doi.org/10.1093/mmy/myu070

51. Adler-Moore, J. P., Gangneux, J.-P., & Pappas, P. G. (2016). Comparison between liposomal formulations of amphotericin B. *Medical Mycology*, *54*(3), 223–231. https://doi.org/10.1093/mmy/myv111

52. Tang, J., Srinivasan, S., Yuan, W., Ming, R., Liu, Y., Dai, Z., … Schwendeman, A. (2019). Development of a flow-through USP 4 apparatus drug release assay for the evaluation of amphotericin B liposome. *European Journal of Pharmaceutics and Biopharmaceutics*, *134*, 107–116. https://doi.org/10.1016/j.ejpb.2018.11.010

53. Yuan, W., Kuai, R., Dai, Z., Yuan, Y., Zheng, N., Jiang, W., … Schwendeman, A. (2017). Development of a Flow-Through USP-4 Apparatus Drug Release Assay to Evaluate Doxorubicin Liposomes. *The AAPS Journal*, *19*(1), 150–160. https://doi.org/10.1208/s12248-016-9958-2

54. Olson, J. A., Adler-Moore, J. P., Jensen, G. M., Schwartz, J., Dignani, M. C., & Proffitt, R. T. (2008). Comparison of the physicochemical, antifungal, and toxic properties of two

liposomal amphotericin B products. *Antimicrobial Agents and Chemotherapy*, *52*(1), 259–268. https://doi.org/10.1128/AAC.00870-07

55. Jensen, G. M., Skenes, C. R., Bunch, T. H., Weissman, C. A., Amirghahari, N., Satorius, A., … Eley, C. G. S. (1999). Determination of the Relative Toxicity of Amphotericin B Formulations: A Red Blood Cell Potassium Release Assay. *Drug Delivery*, *6*(2), 81–88. https://doi.org/10.1080/107175499266995

56. Midez, J. A., Hopfer, R. L., Lopez-Berestein, G., & Mehta, R. T. (1989). Effects of free and liposomal amphotericin B and gramicidin S alone and in combination on potassium leakage from human erythrocytes and Candida albicans. *Antimicrobial Agents and Chemotherapy*, *33*(2), 152–155. https://doi.org/10.1128/aac.33.2.152

57. Stone, N. R., Bicanic, T., Salim, R., & Hope, W. (2016). Liposomal Amphotericin B (AmBisome®): A review of the pharmacokinetics, pharmacodynamics, clinical experience and future directions. *Drugs*, *76*(4), 485–500. https://doi.org/10.1007/s40265-016-0538-7

58. Leenders, A. C. A. P., Daenen, S., Jansen, R. L. H., Hop, W. C. J., Lowenberg, B., Wijermans, P. W., … Marie, S. D. (1998). Liposomal amphotericin B compared with amphotericin B deoxycholate in the treatment of documented and suspected neutropenia-associated invasive fungal infections. *British Journal of Haematology*, *103*(1), 205–212. https://doi.org/10.1046/j.1365-2141.1998.00944.x

59. Penack, O., Schwartz, S., Martus, P., Reinwald, M., Schmidt-Hieber, M., Thiel, E., & Blau, I. W. (2006). Low-dose liposomal amphotericin B in the prevention of invasive fungal infections in patients with prolonged neutropenia: results from a randomized, single-center trial. *Annals of Oncology*, *17*(8), 1306–1312. https://doi.org/10.1093/annonc/mdl128

60. Cornely, O. A., Maertens, J., Bresnik, M., Ebrahimi, R., Ullmann, A. J., Bouza, E., … AmBiLoad Trial Study Group. (2007). Liposomal Amphotericin B as Initial Therapy for Invasive Mold Infection: A Randomized Trial Comparing a High-Loading Dose Regimen with Standard Dosing (AmBiLoad Trial). *Clinical Infectious Diseases*, *44*(10), 1289–1297. https://doi.org/10.1086/514341

61. U.S. Food & Drug Administration. (2023, November 1). EXPAREL Package Insert.

62. U.S. Food & Drug Administration. (2022, May 1). Draft Guidance on Bupivacaine.

63. Mantripragada, S. (2002). A lipid based depot (DepoFoam® technology) for sustained release drug delivery. *Progress in Lipid Research*, *41*(5), 392–406. https://doi.org/10.1016/S0163-7827(02)00004-8

64. Ye, Q., Asherman, J., Stevenson, M., & Brownson, E. (1999). DepoFoamE technology: a vehicle for controlled delivery of protein and peptide drugs.

65. Yu, M., Yuan, W., Xia, Z., Liu, Y., Wang, Y., Xu, X., … Schwendeman, A. (2023). Characterization of exparel bupivacaine multivesicular liposomes. *International Journal of Pharmaceutics*, *639*, 122952. https://doi.org/10.1016/j.ijpharm.2023.122952

66. Yılmaz, H. O., & Turan, A. (2022). Liposomal bupivacaine, pain relief and adverse events. In *Treatments, Mechanisms, and Adverse Reactions of Anesthetics and Analgesics* (pp. 291–307). Elsevier. https://doi.org/10.1016/B978-0-12-820237-1.00027-2

67. Chahar, P., & Cummings, K. C. (2012). Liposomal bupivacaine: a review of a new bupivacaine formulation. *Journal of Pain Research*, *5*, 257–264. https://doi.org/10.2147/JPR.S27894

68. Manna, S., Wu, Y., Wang, Y., Koo, B., Chen, L., Petrochenko, P., … Zheng, J. (2019). Probing the mechanism of bupivacaine drug release from multivesicular liposomes. *Journal of Controlled Release*, *294*, 279–287. https://doi.org/10.1016/j.jconrel.2018.12.029

69. Xia, Z., Liu, Y., Lu, Z., Gan, J., Yu, M., Olsen, K., … Schwendeman, A. (2025). The impact of product quality attributes on *in vivo* performance of bupivacaine multivesicular liposomes. *Drug Delivery and Translational Research*. https://doi.org/10.1007/s13346-025-01806-y

70. Golf, M., Daniels, S. E., & Onel, E. (2011). A phase 3, randomized, placebo-controlled trial of DepoFoam® bupivacaine (extended-release bupivacaine local analgesic) in bunionectomy. *Advances in Therapy*, *28*(9), 776–788. https://doi.org/10.1007/s12325-011-0052-y

71. National Library of Medicine. (2025, June 12). A Study of Bupivacaine Liposome Injection in Local Analgesia of Pediatric Patients. *ClinicalTrials.gov*. Retrieved June 27, 2025, from https://clinicaltrials.gov/study/NCT06344091?viewType=Table&limit=100&spons=Jiangsu%20HengRui%20Medicine%20Co.,%20Ltd.&intr=Bupivacaine%20liposome&rank=1

72. Jiangsu HengRui Medicine Co., Ltd. (2024). *Efficacy, Safety and Pharmacokinetics of Bupivacaine Liposome Injection for Paravertebral Nerve Block in the Treatment of Postoperative Pain After Thoracoscopic Surgery: a Multicenter, Randomized, Double-blind, Dose-finding, Positive Control, Phase II Clinical Trial* (Clinical trial registration No. NCT06529432). clinicaltrials.gov. Retrieved from https://clinicaltrials.gov/study/NCT06529432

73. U.S. Food & Drug Administration. (2024, December 1). Onivyde Package Insert. Retrieved June 25, 2025, from https://www.accessdata.fda.gov/drugsatfda_docs/label/2024/207793s018lbl.pdf

74. Gan, J., Juang, V., Wang, K., Xia, Z., Ackermann, R., Yu, M., … Schwendeman, A. (2025). Reverse engineering of Onivyde® – Irinotecan liposome injection. *International Journal of Pharmaceutics*, *669*, 125000. https://doi.org/10.1016/j.ijpharm.2024.125000

75. Meyers, W. (2016, January 18). Merrimack Pharmaceuticals Should Drive Higher In 2016 On Onivyde And Pipeline. *Seeking Alpha*. Retrieved from https://seekingalpha.com/article/3816696-merrimack-pharmaceuticals-should-drive-higher-in-2016-on-onivyde-and-pipeline

76. U.S. Food & Drug Administration. (2022, February 1). Draft Guidance on Irinotecan Hydrochloride. Retrieved June 25, 2025, from https://www.accessdata.fda.gov/drugsatfda_docs/psg/PSG_207793.pdf

77. Lombardo, D., & Kiselev, M. A. (2022). Methods of Liposomes Preparation: Formation and Control Factors of Versatile Nanocarriers for Biomedical and Nanomedicine Application. *Pharmaceutics*, *14*(3), 543. https://doi.org/10.3390/pharmaceutics14030543

78. Jiang, W., Lionberger, R., & Yu, L. X. (2011). *In Vitro* and *In vivo* Characterizations of Pegylated Liposomal Doxorubicin. *Bioanalysis*, *3*(3), 333–344. https://doi.org/10.4155/bio.10.204

79. Papi, M., Caputo, D., Palmieri, V., Coppola, R., Palchetti, S., Bugli, F., … Caracciolo, G. (2017). Clinically approved PEGylated nanoparticles are covered by a protein corona that boosts the uptake by cancer cells. *Nanoscale*, *9*(29), 10327–10334. https://doi.org/10.1039/C7NR03042H

80. Yang, W., Yang, Z., Liu, J., Liu, D., & Wang, Y. (2019). Development of a method to quantify total and free irinotecan and 7-ethyl-10-hydroxycamptothecin (SN-38) for pharmacokinetic and bio-distribution studies after administration of irinotecan liposomal formulation. *Asian Journal of Pharmaceutical Sciences*, *14*(6), 687–697. https://doi.org/10.1016/j.ajps.2018.08.003

81. Juang, V., Gan, J., Xia, Z., Wang, Y., & Schwendeman, A. (2024). Development and optimization of an *in vitro* release assay for evaluation of liposomal irinotecan formulation. *International Journal of Pharmaceutics*, *667*, 124854. https://doi.org/10.1016/j.ijpharm.2024.124854

82. U.S. Food & Drug Administration. (2023, February 1). Arikayce Label. Retrieved June 26, 2025, from https://www.accessdata.fda.gov/drugsatfda_docs/label/2023/207356s012lbl.pdf

83. BioSpace. (2021, March 24). LAMIRA®, an eFlow® Technology nebulizer, expected to launch in Japan as a medical device for exclusive administration of ARIKAYCE® (amikacin liposome inhalation suspension). *BioSpace*. Retrieved June 27, 2025, from https://www.biospace.com/lamira-an-eflow-technology-nebulizer-expected-to-launch-in-japan-as-a-medical-device-for-exclusive-administration-of-arikayce-amikacin-liposome-inhalation-suspension

84. Maxwell, A., Chaudhari, B. B., Chaudhari, P., Ananthamurthy, K., Aranjani, J., Moorkoth, S., … Lewis, S. (2022). *In vitro* antibacterial activity and *in vivo* pharmacokinetics of intravenously administered Amikacin-loaded Liposomes for the management of bacterial septicaemia, *220*. https://doi.org/10.1016/j.colsurfb.2022.112892

85. Maxwell, A., Mary, E., Ghate, V., Aranjani, J., & Lewis, S. (2022). A novel high throughput 96-well-based fluorimetric method to measure amikacin in pharmaceutical formulations: development using response surface methodology. *Luminescence*, *37*(6), 930–943. https://doi.org/10.1002/bio.4238

86. Fielding, R. M., Moon-Mcdermott, L., Lewis, R. O., & Horner, M. J. (1999). Pharmacokinetics and Urinary Excretion of Amikacin in Low-Clearance Unilamellar Liposomes after a Single or Repeated Intravenous Administration in the Rhesus Monkey. *Antimicrobial Agents and Chemotherapy*, *43*(3), 503–509. https://doi.org/10.1128/aac.43.3.503

87. Leitzke, S., Bucke, W., Borner, K., Müller, R., Hahn, H., & Ehlers, S. (1998). Rationale for and Efficacy of Prolonged-Interval Treatment Using Liposome-Encapsulated Amikacin in Experimental Mycobacterium avium Infection. *Antimicrobial Agents and Chemotherapy*, *42*(2), 459–461. https://doi.org/10.1128/aac.42.2.459

88. Gabizon, A. A., Gabizon-Peretz, S., Modaresahmadi, S., & La-Beck, N. M. (2025). Thirty years from FDA approval of pegylated liposomal doxorubicin (Doxil/Caelyx): an updated analysis and future perspective. *BMJ Oncology*, *4*(1), e000573. https://doi.org/10.1136/bmjonc-2024-000573

89. Global Doxorubicin Market Trajectory & Analytics Report 2022-2026: Rising Incidence of Cancers & Development of Technologically Advanced Systems for Drug Delivery Driving Growth. (2022, May 25). *GlobeNewswire News Room*. Retrieved June 25, 2024, from https://www.globenewswire.com/en/news-release/2022/05/25/2450132/28124/en/Global-Doxorubicin-Market-Trajectory-Analytics-Report-2022-2026-Rising-Incidence-of-Cancers-Development-of-Technologically-Advanced-Systems-for-Drug-Delivery-Driving-Growth.html

90. Alshaer, W., Nsairat, H., Lafi, Z., Hourani, O. M., Al-Kadash, A., Esawi, E., & Alkilany, A. M. (2022). Quality by Design Approach in Liposomal Formulations: Robust Product Development. *Molecules*, *28*(1), 10. https://doi.org/10.3390/molecules28010010

91. Food and Drug Administration. (n.d.). Orange Book: Approved Drug Products with Therapeutic Equivalence Evaluations. Retrieved June 25, 2024, from https://www.accessdata.fda.gov/scripts/cder/ob/search_product.cfm

92. Schindelin, J., Arganda-Carreras, I., Frise, E., Kaynig, V., Longair, M., Pietzsch, T., … Cardona, A. (2012). Fiji: an open-source platform for biological-image analysis. *Nature Methods*, *9*(7), 676–682. https://doi.org/10.1038/nmeth.2019

93. SIBYLS MailinSAXS HT-SAXS Instructions. (2010, 2024). Retrieved June 4, 2024, from https://sibyls.als.lbl.gov/htsaxs/instructions/htsaxs

94. U.S. Food & Drug Administration. (2024). Compilation of FDA Guidance and Resources for *in vitro* Dissolution Testing of Immediate Release Solid Oral Dosage Forms. *FDA*. Retrieved from https://www.fda.gov/animal-veterinary/new-animal-drug-applications/compilation-fda-guidance-and-resources-in-vitro-dissolution-testing-immediate-release-solid-oral-dosage

95. Wu, Y., Petrochenko, P., Szoka, F. C., Manna, S., Koo, B., Zheng, N., … Zheng, J. (2017). Cryogenic Transmission Electron Microscopy (Cryo-TEM) Reveals Morphological

Changes of Liposomal Doxorubicin during *In Vitro* Release. *Microscopy and Microanalysis*, *23*(S1), 1216–1217. https://doi.org/10.1017/S1431927617006742

96. Murray, D. T., Shin, D. S., Classen, S., Brosey, C. A., & Hura, G. L. (2023). Visualizing and accessing correlated SAXS data sets with Similarity Maps and Simple Scattering web resources. *Methods in enzymology*, *678*, 411–440. https://doi.org/10.1016/bs.mie.2022.09.024

97. Maiti, K., Bhowmick, S., Jain, P., Zope, M., Doshi, K., & Rajamannar, T. (2018). Comparison of Physicochemical Properties of Generic Doxorubicin HCl Liposome Injection with the Reference Listed Drug. *Anti-Cancer Agents in Medicinal Chemistry*, *18*(4), 597–609. https://doi.org/10.2174/1871520617666171121124610

98. Souza, I. D. L., Saez, V., & Mansur, C. R. E. (2023). Lipid nanoparticles containing coenzyme Q10 for topical applications: An overview of their characterization. *Colloids and Surfaces B: Biointerfaces*, *230*, 113491. https://doi.org/10.1016/j.colsurfb.2023.113491

99. Bhattacharjee, S. (2016). DLS and zeta potential – What they are and what they are not? *Journal of Controlled Release*, *235*, 337–351. https://doi.org/10.1016/j.jconrel.2016.06.017

100. Smith, M. C., Crist, R. M., Clogston, J. D., & McNeil, S. E. (2017). Zeta potential: a case study of cationic, anionic, and neutral liposomes. *Analytical and Bioanalytical Chemistry*, *409*(24), 5779–5787. https://doi.org/10.1007/s00216-017-0527-z

101. Outomuro, D., Grana, D. R., Azzato, F., & Milei, J. (2007). Adriamycin-induced myocardial toxicity: New solutions for an old problem? *International Journal of Cardiology*, *117*(1), 6–15. https://doi.org/10.1016/j.ijcard.2006.05.005

102. Gómez-Lázaro, L., Martín-Sabroso, C., Aparicio-Blanco, J., & Torres-Suárez, A. I. (2024). Assessment of *In Vitro* Release Testing Methods for Colloidal Drug Carriers: The Lack of Standardized Protocols. *Pharmaceutics*, *16*(1), 103. https://doi.org/10.3390/pharmaceutics16010103

103. Yu, M., Yuan, W., Li, D., Schwendeman, A., & Schwendeman, S. P. (2019). Predicting drug release kinetics from nanocarriers inside dialysis bags. *Journal of Controlled Release*, *315*, 23–30. https://doi.org/10.1016/j.jconrel.2019.09.016

104. Yu, M., Yuan, W., Li, D., Schwendeman, A., & Schwendeman, S. P. (2019). Predicting drug release kinetics from nanocarriers inside dialysis bags. *Journal of Controlled Release*, *315*, 23–30. https://doi.org/10.1016/j.jconrel.2019.09.016

105. Wallace, S. J., Li, J., Nation, R. L., & Boyd, B. J. (2012). Drug release from nanomedicines: selection of appropriate encapsulation and release methodology. *Drug Delivery and Translational Research*, *2*(4), 284–292. https://doi.org/10.1007/s13346-012-0064-4

106. Moreno-Bautista, G., & Tam, K. C. (2011). Evaluation of dialysis membrane process for quantifying the *in vitro* drug-release from colloidal drug carriers. *Colloids and Surfaces A: Physicochemical and Engineering Aspects*, *389*(1–3), 299–303. https://doi.org/10.1016/j.colsurfa.2011.07.032

107. Magalhaes, N. S. S., Fessi, H., Puisieux, F., Benita, S., & Seiller, M. (1995). An *in vitro* release kinetic examination and comparative evaluation between submicron emulsion and polylactic acid nanocapsules of clofibride. *Journal of Microencapsulation*, *12*(2), 195–205. https://doi.org/10.3109/02652049509015290

108. Levy, M. Y., & Benita, S. (1990). Drug release from submicronized o/w emulsion: a new *in vitro* kinetic evaluation model. *International Journal of Pharmaceutics*, *66*(1–3), 29–37. https://doi.org/10.1016/0378-5173(90)90381-d

109. Abouelmagd, S. A., Sun, B., Chang, A. C., Ku, Y. J., & Yeo, Y. (2015). Release Kinetics Study of Poorly Water-Soluble Drugs from Nanoparticles: Are We Doing It Right? *Molecular Pharmaceutics*, *12*(3), 997–1003. https://doi.org/10.1021/mp500817h

110. Bio-Rad. (n.d.). Bio-Beads SM Hydrophobic and Polar Interaction Adsorbents Instruction Manual. Bio-Rad Laboratories. Retrieved from https://www.bio-rad.com/webroot/web/pdf/lsr/literature/Lit195.pdf

111. Bio-Rad. (n.d.). Introduction to Hydrophobic Interaction Chromatography. *Bio-Rad Laboratories Inc.* Retrieved July 2, 2025, from https://www.bio-rad.com/en-us/applications-technologies/introduction-hydrophobic-interaction-chromatography?ID=LUSN8F4VY

112. Marques, M. (2020, December 1). USP <1092> The Dissolution Procedure: Development and Validation. *USP-NF/PF*. Retrieved July 1, 2025, from https://online.uspnf.com/uspnf/document/1_GUID-CE0902BA-77AC-422D-8BF0-A221B5DE6012_5_en-US?source=Activity#C1092S59

113. Patra, M., Salonen, E., Terama, E., Vattulainen, I., Faller, R., Lee, B. W., … Karttunen, M. (2006). Under the Influence of Alcohol: The Effect of Ethanol and Methanol on Lipid Bilayers. *Biophysical Journal*, *90*(4), 1121–1135. https://doi.org/10.1529/biophysj.105.062364

114. Peng, M., Liu, Y., Zhang, H., Cui, Y., Zhai, G., & Chen, C. (2010). Photostability Study of Doxorubicin Aqueous Solution Enhanced by Inclusion Interaction between Doxorubicin and Hydroxypropyl-β-cyclodextrin. *Chinese Journal of Chemistry*, *28*(7), 1291–1295. https://doi.org/10.1002/cjoc.201090223

115. Saokham, P., Muankaew, C., Jansook, P., & Loftsson, T. (2018). Solubility of Cyclodextrins and Drug/Cyclodextrin Complexes. *Molecules : A Journal of Synthetic Chemistry and Natural Product Chemistry*, *23*(5), 1161. https://doi.org/10.3390/molecules23051161

116. Liu, P., De Wulf, O., Laru, J., Heikkilä, T., van Veen, B., Kiesvaara, J., … Laaksonen, T. (2013). Dissolution Studies of Poorly Soluble Drug Nanosuspensions in Non-sink Conditions. *AAPS PharmSciTech*, *14*(2), 748–756. https://doi.org/10.1208/s12249-013-9960-2

117. Marques, M. (2020, December 1). 〈1092〉 The Dissolution Procedure: Development and Validation. https://doi.org/10.31003/USPNF_M643_05_01

118. Yuksel, N. (2000). Comparison of *in vitro* dissolution profiles by ANOVA-based, model-dependent and -independent methods. *International Journal of Pharmaceutics*, *209*(1–2), 57–67. https://doi.org/10.1016/S0378-5173(00)00554-8

119. Medicine, C. for V. (2025). Compilation of FDA Guidance and Resources for *in vitro* Dissolution Testing of Immediate Release Solid Oral Dosage Forms. *FDA*. Retrieved from https://www.fda.gov/animal-veterinary/new-animal-drug-applications/compilation-fda-guidance-and-resources-in-vitro-dissolution-testing-immediate-release-solid-oral-dosage

120. Raghavan, L., Brown, M., Michniak-Kohn, B., Ng, S., & Sammeta, S. (2019). *In Vitro* Release Tests as a Critical Quality Attribute in Topical Product Development. In N. Langley, B. Michniak-Kohn, & D. W. Osborne (Eds.), *The Role of Microstructure in Topical Drug Product Development* (Vol. 36, pp. 47–87). Cham: Springer International Publishing. https://doi.org/10.1007/978-3-030-17355-5_2

121. U.S. Food & Drug Administration. (1997, August 1). Dissolution Testing of Immediate Release Solid Oral Dosage Forms: Guidance for Industry. U.S. Food & Drug Administration. Retrieved from https://www.fda.gov/media/70936/download

122. Yamada, Y. (2020). Dimerization of Doxorubicin Causes Its Precipitation. *ACS Omega*, *5*(51), 33235–33241. https://doi.org/10.1021/acsomega.0c04925

123. Jambhekar, S. S., & Breen, P. J. (2013). Drug dissolution: significance of physicochemical properties and physiological conditions. *Drug Discovery Today*, *18*(23–24), 1173–1184. https://doi.org/10.1016/j.drudis.2013.08.013

124. Fülöp, Z., Gref, R., & Loftsson, T. (2013). A permeation method for detection of self-aggregation of doxorubicin in aqueous environment. *International Journal of Pharmaceutics*, *454*(1), 559–561. https://doi.org/10.1016/j.ijpharm.2013.06.058

125. Kaushik, D., & Bansal, G. (2015). Four new degradation products of doxorubicin: An application of forced degradation study and hyphenated chromatographic techniques. *Journal of Pharmaceutical Analysis*, *5*(5), 285–295. https://doi.org/10.1016/j.jpha.2015.05.003

126. Loftsson, T. (2010). Aqueous solubility and true soutions, (6), 404–407. https://doi.org/10.1691/ph.2010.0034R

127. Schreier, S., Malheiros, S. V. P., & De Paula, E. (2000). Surface active drugs: self-association and interaction with membranes and surfactants. Physicochemical and

biological aspects. *Biochimica et Biophysica Acta (BBA) - Biomembranes*, *1508*(1–2), 210–234. https://doi.org/10.1016/s0304-4157(00)00012-5

128. Loftsson, T., & Brewster, M. E. (2008). Physicochemical properties of water and its effect on drug delivery. *International Journal of Pharmaceutics*, *354*(1–2), 248–254. https://doi.org/10.1016/j.ijpharm.2007.08.049

129. Fukazawa, T., Yamazaki, Y., & Miyamoto, Y. (2010). Reduction of non-specific adsorption of drugs to plastic containers used in bioassays or analyses. *Journal of Pharmacological and Toxicological Methods*, *61*(3), 329–333. https://doi.org/10.1016/j.vascn.2009.12.005

130. Geary, T. G., Akood, M. A., & Jensen, J. B. (1983). Characteristics of Chloroquine Binding to Glass and Plastic. *The American Journal of Tropical Medicine and Hygiene*, *32*(1), 19–23. https://doi.org/10.4269/ajtmh.1983.32.19

131. Palmgren, J., Monkkonen, J., Korjamo, T., Hassinen, A., & Auriola, S. (2006). Drug adsorption to plastic containers and retention of drugs in cultured cells under *in vitro* conditions. *European Journal of Pharmaceutics and Biopharmaceutics*, *64*(3), 369–378. https://doi.org/10.1016/j.ejpb.2006.06.005

132. Esser, P. (2015). The Surface/Volume Ratio in Solid Phase Assays. Retrieved from https://assets.fishersci.com/TFS-Assets/LCD/Product-Bulletins/D19566.pdf?utm_source=chatgpt.com

133. Angelikopoulos, P., & Bock, H. (2010). The Differences in Surfactant Adsorption on Carbon Nanotubes and Their Bundles. *Langmuir*, *26*(2), 899–907. https://doi.org/10.1021/la902376b

134. Ahmad, I., Sabah, A., Anwar, Z., Arif, A., Arsalan, A., & Qadeer, K. (2017). Effect of solvent polarity on the extraction of components of pharmaceutical plastic containers. *Pak. J. Pharm. Sci.*

135. Zhang, X., Yang, L., Zhang, C., Liu, D., Meng, S., Zhang, W., & Meng, S. (2019). Effect of Polymer Permeability and Solvent Removal Rate on In Situ Forming Implants: Drug Burst Release and Microstructure. *Pharmaceutics*, *11*(10), 520. https://doi.org/10.3390/pharmaceutics11100520

136. Venkatesan, S., Lamfers, M., Leenstra, S., & Vulto, A. G. (2017). Overview of the patent expiry of (non-)tyrosine kinase inhibitors approved for clinical use in the EU and the US. *Generics and Biosimilars Initiative Journal*, *6*(2), 89–96. https://doi.org/10.5639/gabij.2017.0602.016

137. Kolia, S. (2025, April 18). A Pharmacist's Guide to Blockbuster Patent Expirations: 2025 and Beyond. *Pharmacy Times*. Retrieved July 27, 2025, from https://www.pharmacytimes.com/view/a-pharmacist-s-guide-to-blockbuster-patent-expirations-2025-and-beyond?utm_source=chatgpt.com

138. U.S. Food & Drug Administration. (2025, July 2). List of Off-Patent, Off-Exclusivity Drugs without an Approved Generic. *U.S. Food & Drug Administration*. Retrieved July 27, 2025, from https://www.fda.gov/drugs/abbreviated-new-drug-application-anda/list-patent-exclusivity-drugs-without-approved-generic?utm_source=chatgpt.com